THE UNIVERSITY OF CALGARY

Blueschist Metamorphism within the Bridge River Complex, Goldbridge, British Columbia

by

David J. Hozjan (Hons. B.Sc.)

A THESIS SUBMITTED TO THE FACULTY OF GRADUATE STUDIES IN PARTIAL FULFILLMENT OF THE REQUIREMENTS FOR THE DEGREE OF MASTER OF SCIENCE.

DEPARTMENT OF GEOLOGY AND GEOPHYSICS

CALGARY, ALBERTA
July 1999

ABSTRACT

The Bridge River Terrane, within the Coast Belt of the Canadian Cordillera near Goldbridge, B.C. (50^{O} 51'N, 122^{O} 50'W), hosts 5 fault-bounded, 230 Ma blocks of blueschist facies rocks. The characteristic lithology is a dark blue, fine-grained phyllite to schist. Also present in the blocks are the massive to weakly foliated Bridge River greenstones, which contain lenses and foliae of blueschist minerals as well as relict igneous minerals and textures. These lenses and foliae reflect original protolith heterogeneities enhanced by metamorphic segregation. Protoliths for these rocks are inferred to be basaltic flows, volcanic tuffs, and possibly argillites with a significant tuffaceous component. Epidote blueschist and lawsonite blueschist assemblages occur in various parts of the study area possibly demonstrating variations in a_{H_2O} among the blocks. Inferred P-T conditions are between 8 to 10 kbar at 250 to 300°C. These metamorphic conditions were attained in an accretion-subduction complex.

ACKNOWLEDGMENTS

First, I would like to extend my sincerest gratitude to Dr. E.D. Ghent for suggesting this research topic. He has been supportive and enthusiastic throughout the duration of the project.

P.S. Simony generously assisted me with a detailed and conscientious review of my writing. A.A. Levinson has been a source of support and insight and broadened my view of geology. I am grateful to them both.

I am no less indebted to Dr. J.W. Nicholls and M.Z. Stout for their assistance with microprobe analysis and to Dr. R.J. Spencer for his help with the fluid inclusion study. Further thanks go out to G. Gibbs for his assistance in the field. I would also like to thank S. Resultay and M. Horvath for thin section preparation as well as M.E. Back, M. Raudsepp and F.J. Wicks for their analytical assistance.

Several graduate students at the University of Calgary provided excellent forums for scientific discussion, friendship and necessary distractions throughout the course of my work. For this, I would like to thank C. Ardic, C. Augereau, C. Debuhr, P. McNeil, S. Rose, D. Thomas and B. Urlwin.

I would also like to thank my family. Without their support and inspiration, I would not have been able to accomplish this study. Finally, I would like to acknowledge L. Connell for being a constant source of love and encouragement from the day we met through the completion of my thesis.

TABLE OF CONTENTS

LIST OF FIGURES

LIST OF TABLES

1. INTRODUCTION

1.1 BLUESCHIST METAMORPHISM

Since its definition by Eskola (1920), the blueschist facies (originally named 'glaucophane schist facies') has intrigued petrologists. Eskola (1920) described this facies as forming under conditions of moderate temperatures and high pressures, an idea based on the widespread occurrence of very dense phases and the high specific gravities of these rocks compared to the greenschist facies. The facies is generally defined on the basis of the presence of glaucophane + lawsonite (or another hydrous Ca-Al phase such as epidote) or some combination of jadeitic pyroxene with quartz and metamorphic aragonite. This facies apparently requires a history of rapid, deep burial of relatively cool rocks followed by rapid uplift. Initially, the notion of such conditions challenged the concepts of Earth dynamics. The recognition of the global distribution of blueschists in association with Phanerozoic convergent plate junctions, (e.g. Blake et al., 1969), as well as thermal models proposed by numerous researchers (e.g. Oxburgh and Turcotte, 1971; Platt, 1987; Peacock, 1993), indicate that the conditions required for blueschist formation and preservation exist at subduction zones.

Although the spatial distribution of blueschists is well known, the exact mechanisms by which these rocks are generated and subsequently exhumed remain unclear. Therefore, in undertaking any study of blueschist metamorphism, it is of utmost importance to attempt to understand how such well preserved examples of high pressure rocks are found at the Earth's surface. First, studies should attempt to explain or devise mechanisms whereby blueschists are preserved under relatively cool, dry conditions so that there is no extensive reaction that would produce lower pressure and/or higher temperature overprints. Second, blueschists are believed to have been uplifted from depths corresponding to the base of the crust to a position at the surface. The question that must be answered then is "what is the driving force behind such an uplift scenario?"

A further complication with these rocks is the apparent coexistence of blueschist and greenschist assemblages reported in several areas. (e.g. Garver et al., 1989; Schiarizza et al., 1990; Baltatzis, 1996). Such interlayered sequences can easily be explained by bulk chemical differences between the layers (e.g. Evans, 1990). Barrientos and Selverstone (1993) in studying blueschists at Ile de Groix, France proposed a model of fluid infiltration to account for the coexistence of the two assemblages. The basis of the Barrientos and Selverstone (1993) theory is that all reactions that relate chloritic greenschist to blueschists requires the addition of $H_2O \pm CO_2$ (e.g. Evans, 1990). Therefore, the apparent coexistence of these two assemblages can be accomplished by the local introduction of fluids into the blueschist assemblage which then reacts to form a greenschist assemblage. Similar examples of blueschists apparently coexisting with other assemblages have been reported in the Bridge River Terrane (Garver et al., 1989; Schiarizza et al., 1990).

1.2 BLUESCHIST OCCURRENCES IN THE CANADIAN CORDILLERA

Blueschist metamorphism most frequently occurs along continental margins where oceanic crust is underthrust or subducted beneath the edge of a continental block (Miyashiro, 1961). Discontinuous belts of blueschists that reflect relatively high pressure, prograde, metamorphic trajectories, mark these regions. (Blake et al., 1969, Ernst, 1988). In the Canadian Cordillera, several blueschist localities have been recognized. These are found within the Slide Mountain Terrane in the Omineca Belt; within the Cache Creek Terrane of the Intermontane Belt; in the Bridge River Terrane of the Coast Belt; and in the San Juan Islands of the Pacific Rim Terrane of the Insular Belt (Greenwood et al., 1991) (see Figure 1-1).

Blueschist and eclogite lenses have been reported by Erdmer and Helmstaedt (1983), and by Erdmer (1987) in the Anvil Allochthon of the Slide Mountain Terrane. K-Ar and Rb-Sr dating of blueschist minerals in these rocks yield a Late Permian age (e.g. Greenwood et al., 1991). Therefore, these rocks are petrologically very interesting but do not provide any direct information about Mesozoic Cordilleran tectonics (Simony, pers.

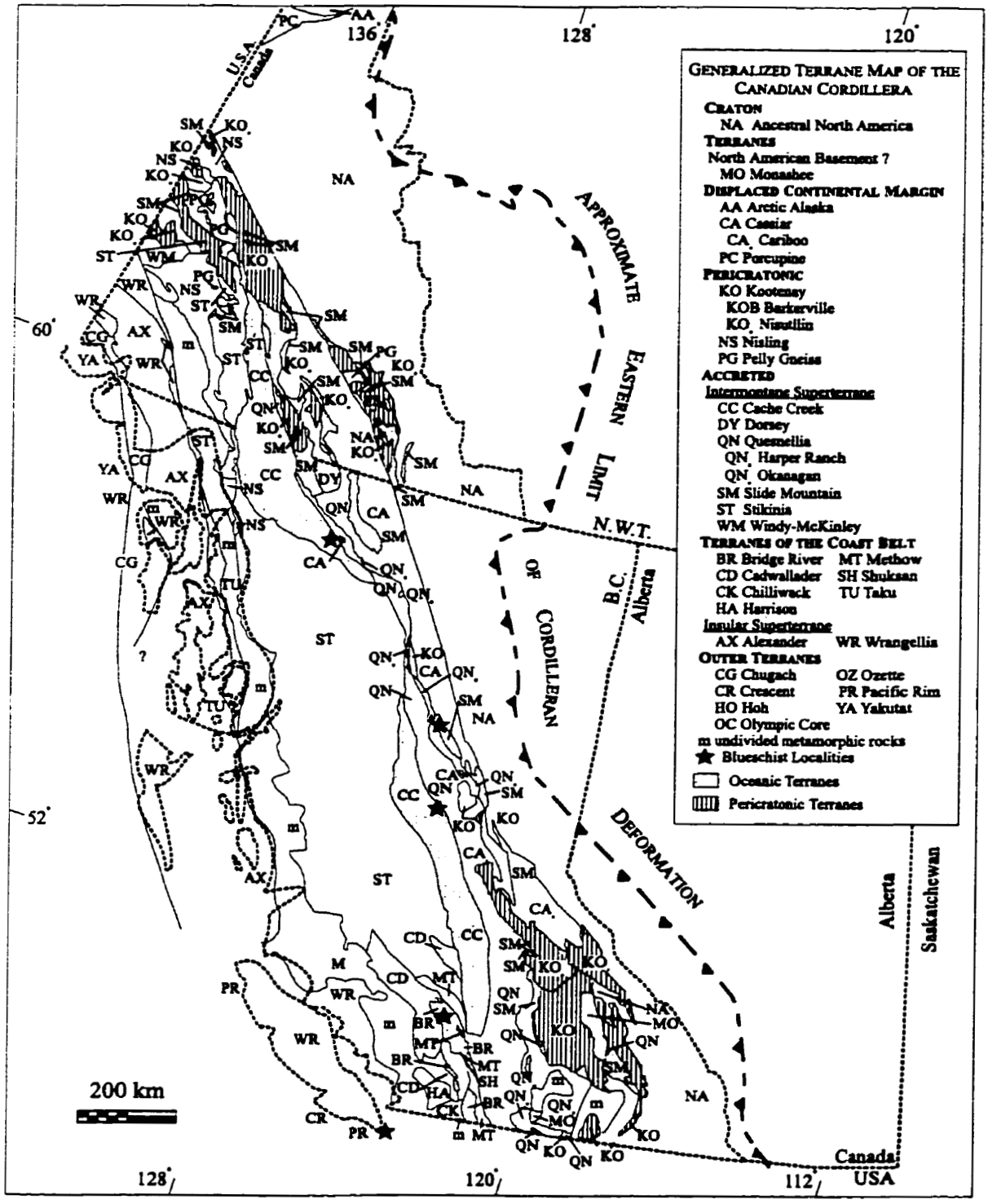

Figure 1-1. Terrane map of the Canadian Cordillera showing blueschist occurrences. (From Gabrielse et al., 1991.)

comm., 1999). According to these studies, these blueschists and eclogites were believed to have formed in a subduction complex at pressures of 10-15 kbars between 470 and 750°C.

Within the Cache Creek Terrane, Greenwood et al., (1991) report the presence of a variably developed blueschist assemblages of Late Triassic age. Much of the Dease Lake region of the terrane, has been metamorphosed to prehnite-pumpellyite facies; locally blue amphibole and lawsonite are present indicating lawsonite blueschist metamorphism (Ghent pers. comm., 1998). High pressure assemblages also occur in the Vital Range area of the Cache Creek Terrane reflecting widespread distribution of high-pressure, subduction-related assemblages in the Cache Creek Terrane (e.g. Greenwood et al., 1991). Blueschist and eclogite facies rocks have also been studied in the Pinchi Lake region of the terrane (e.g. Ghent et al, 1990; 1993; and 1996). The assemblages include lawsonite, jadeite, glaucophane, aragonite, calcite, chlorite quartz, phengitic white mica (e.g. Greenwood et al., 1991; Ghent et al., 1996) and the first reported occurrence of howieite in Canada (Ghent et al., 1990). Ghent et al. (1996) report Triassic ages in the range of 221.8±1.9 Ma to 223.5 ±1.7 Ma for blueschists and eclogites in the area. Ghent et al., (1996) report minimum pressures of 8 to 10 kbars at temperatures of 200 to 300°C for the Pinchi Lake blueschists.

Within the Insular Belt evidence of high pressure metamorphism is found in the southwest portion of Vancouver Island and on the San Juan Islands which are underlain by the Jura-Cretaceous Pacific Rim Terrane and the Eocene, Crescent Terrane (e.g. Greenwood et al., 1991). The Pacific Rim Terrane contains two distinctive assemblages: a high-pressure, low temperature assemblage consisting of lawsonite + quartz + calcite/aragonite ± prehnite ± pumpellyite ± epidote (Vance, 1968, Brandon, 1980). In this region Wrangellia is underthrust by the Pacific Rim Terrane which itself is underthrust by the Crescent Terrane. Thus, the high pressure parts of the Pacific Rim Terrane result from the extreme tectonic thickening during plate collision in the Late Cretaceous (Greenwood et al., 1991).

1.3 PURPOSE AND SCOPE OF THIS STUDY

The purpose of this study is to investigate the blueschist facies metamorphism of rocks associated with the Bridge River Complex in southwestern British Columbia. The mode of occurrence, mineralogy, chemical compositions and the physical conditions of metamorphism are discussed. These rocks were investigated through field study as well as through laboratory study.

The fieldwork was aimed primarily at mapping and collecting of the blueschists and related rocks within the areas delineated by previous workers (e.g. Schiarizza and Gaba, 1993) in order to refine the tracing of the contacts of the blueschists with the adjacent rocks, to collect meaningful structural data whenever possible and to improve our understanding of the nature of these contacts.

Laboratory work concentrated on petrographic and microprobe analyses. Due to the fine grained nature of these rocks, X-ray diffraction (XRD) techniques were used to aid in mineral identification. In addition, several metavolcanic samples (collected by E.D. Ghent prior to the start of my study) were analyzed by X-ray fluorescence (XRF) to determine whole rock chemistry.

1.4 LOCATION AND ACCESS

The study area is located northeast of the village of Goldbridge, British Columbia (50°51'N, 122°50'W), approximately 300 kilometres north of Vancouver and 100 kilometres west of the town of Lillooet (see Figure 1-2).

The area is accessible from Lillooet by travelling west on Carpenter Lake Road (Road #40), a well-maintained gravel road. The rocks examined in this study were collected to the north of Carpenter Lake and in the watershed of North Cinnabar Creek (see Figure 1-3). Schiarizza and Gaba (1993) compiled the geologic base-map from which the blueschist contacts were taken. The rock outcrops to the north of Carpenter Lake are

readily accessible by an abandoned logging road that intersects Carpenter Lake Road. Outcrops in the North Cinnabar Creek area can be accessed via an abandoned trail that intersects Tyaughton Lake Road. All-terrain vehicles are a necessity on this trail. Outcrops in the Tyaughton Creek valley are also accessible from Tyaughton Lake Road.

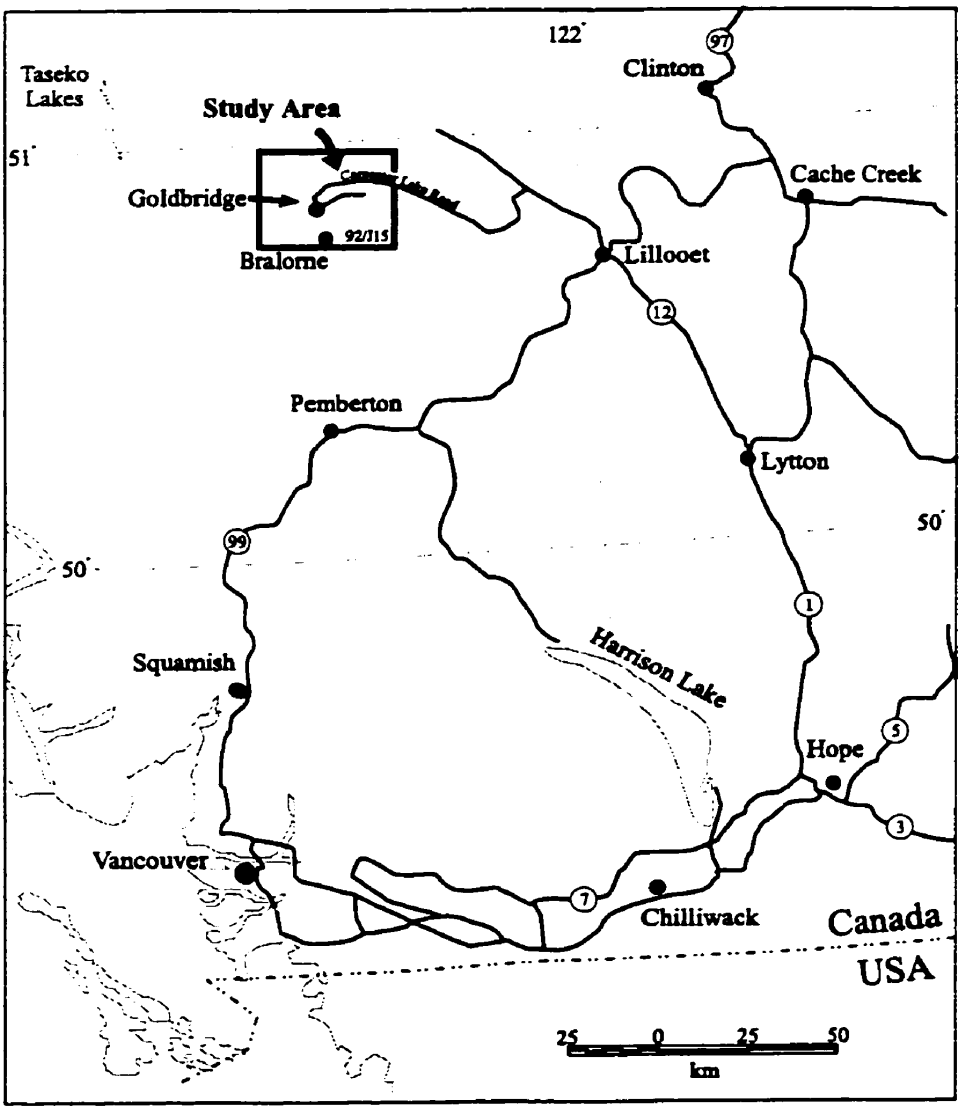

Figure 1-2. General location map of southwestern British Columbia (modified from Schiarizza et al., 1995)

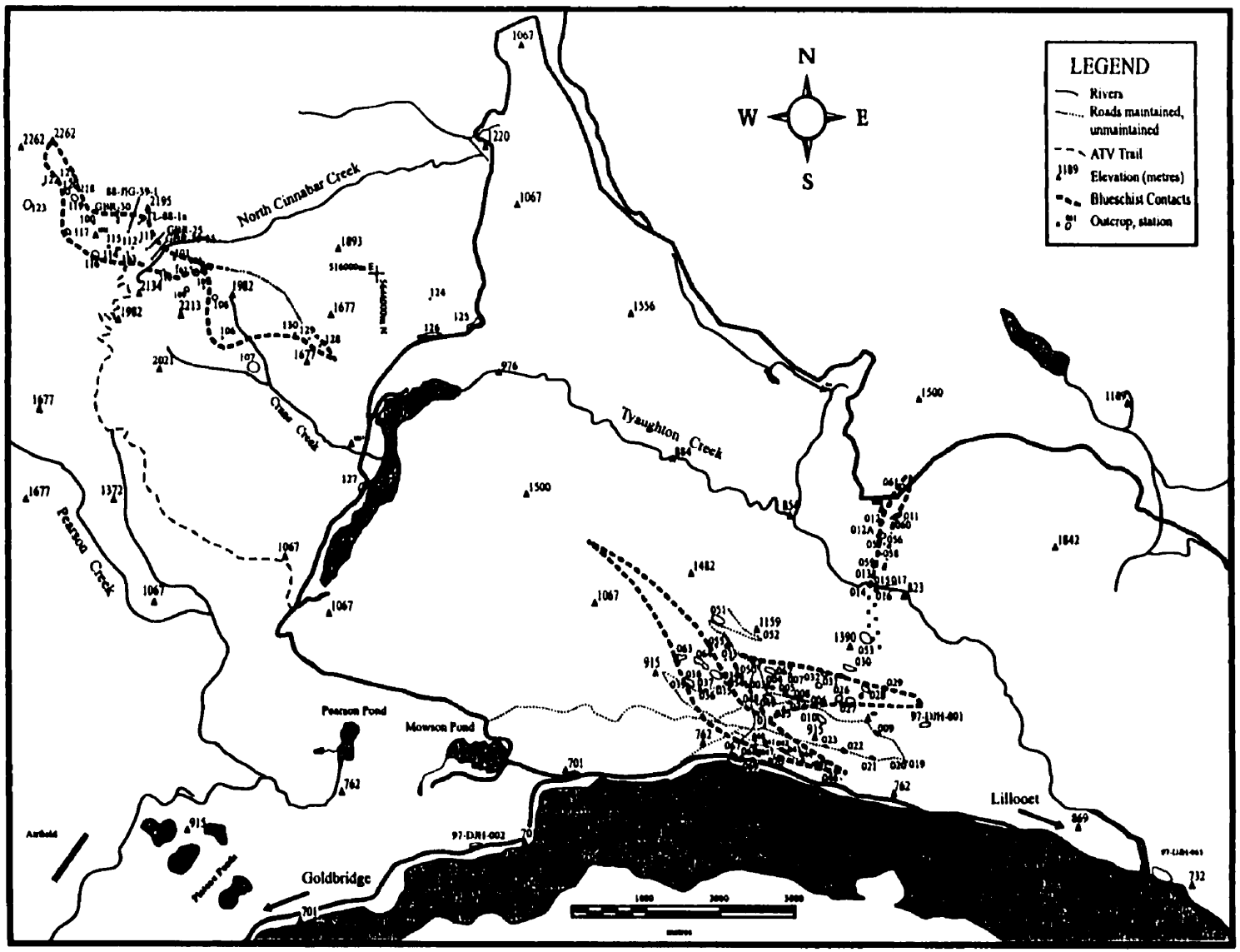

Figure 1-3. Location of the Bridge River blueschists and related rocks from this study. Numbers refer to outcrop stations and sample locations referred to in the text. GBR refers to samples provided by E.D. Ghent; JIG refers to samples from J.Garver and TL refers to samples from D.A. Archibald.

2. PREVIOUS WORK

2.1 REGIONAL SETTING

The rocks that are the subject of this study are from the Bridge River Terrane, one of six small terranes in southwestern British Columbia that lie between the Intermontane and Insular superterranes in the southern Coast Belt. The Bridge River Terrane in the study area lies in the southeastern portion of the Coast Belt. It is one of several crustal fragments in the western part of North America that originated elsewhere and have been incorporated into North America (Potter, 1986) (see Figure 2-1).

The Bridge River Terrane in the study area consists primarily of the Bridge River Complex (after Potter, 1986). It is a unit of Mississippian to late Middle Jurassic age (approximately 340 – 160 Ma). It consists of radiolarian chert, argillite and greenstone with lesser siltstone, greywacke, tuff, limestone and clastic rocks with no coherent internal stratigraphy. The Complex also includes minor late Triassic and associated alpine-type ultramafic and mafic igneous rocks. Serpentinite is common along fault zones (Potter, 1986; Schiarizza et al., 1989). According to Schiarizza et al. (1989), the area is characterized by a high degree of internal fault disruption so that most contacts are faults with individual units traceable only over short distances. The exception to this are the contacts between chert, argillite, tuff, limestone and clastic rocks which appear to be depositional (Potter, 1986, Schiarizza et al., 1989). Figure 2-2 is a generalized geological map (after Schiarizza et al., 1989) of the Bridge River complex surrounding the study area. Potter (1986) relates the chaotic, disrupted aspect of the Complex to a primary depositional lenticularity that was modified by faulting. The faults observed in outcrop are typically discontinuous, curved and accommodate only small displacements between rock bodies.

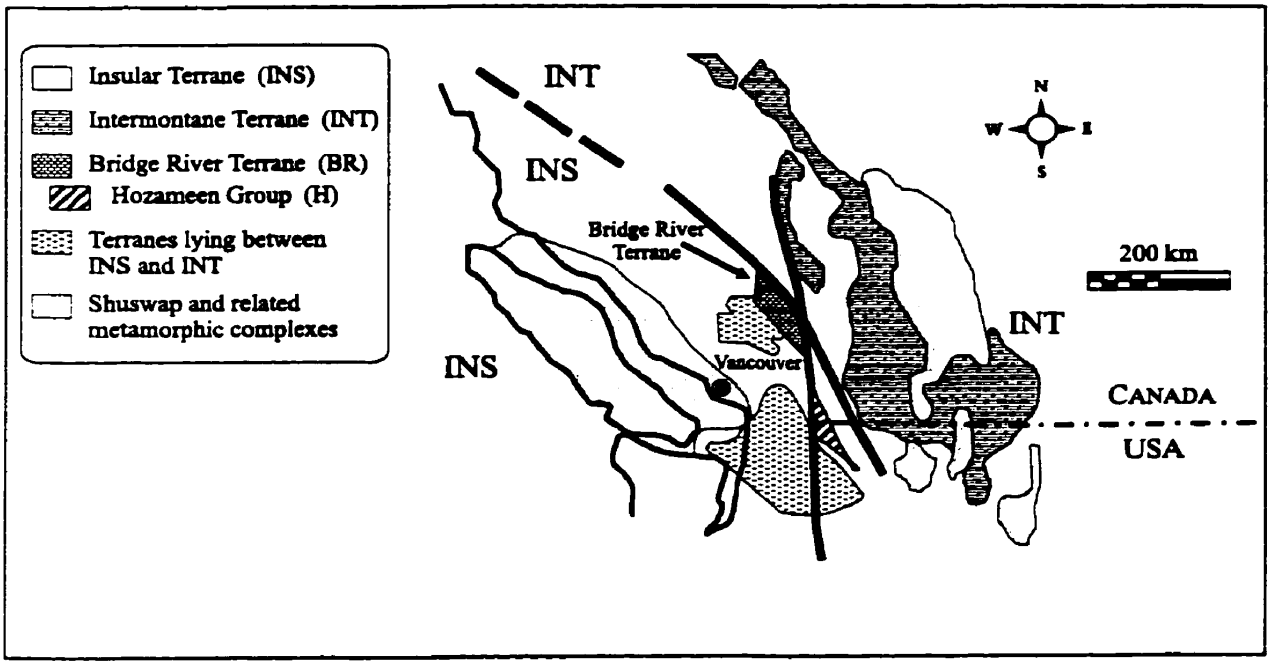

Figure 2-1. Regional setting of the Bridge River Terrane. Dark lines refer to major faults in the area (after Potter, 1986).

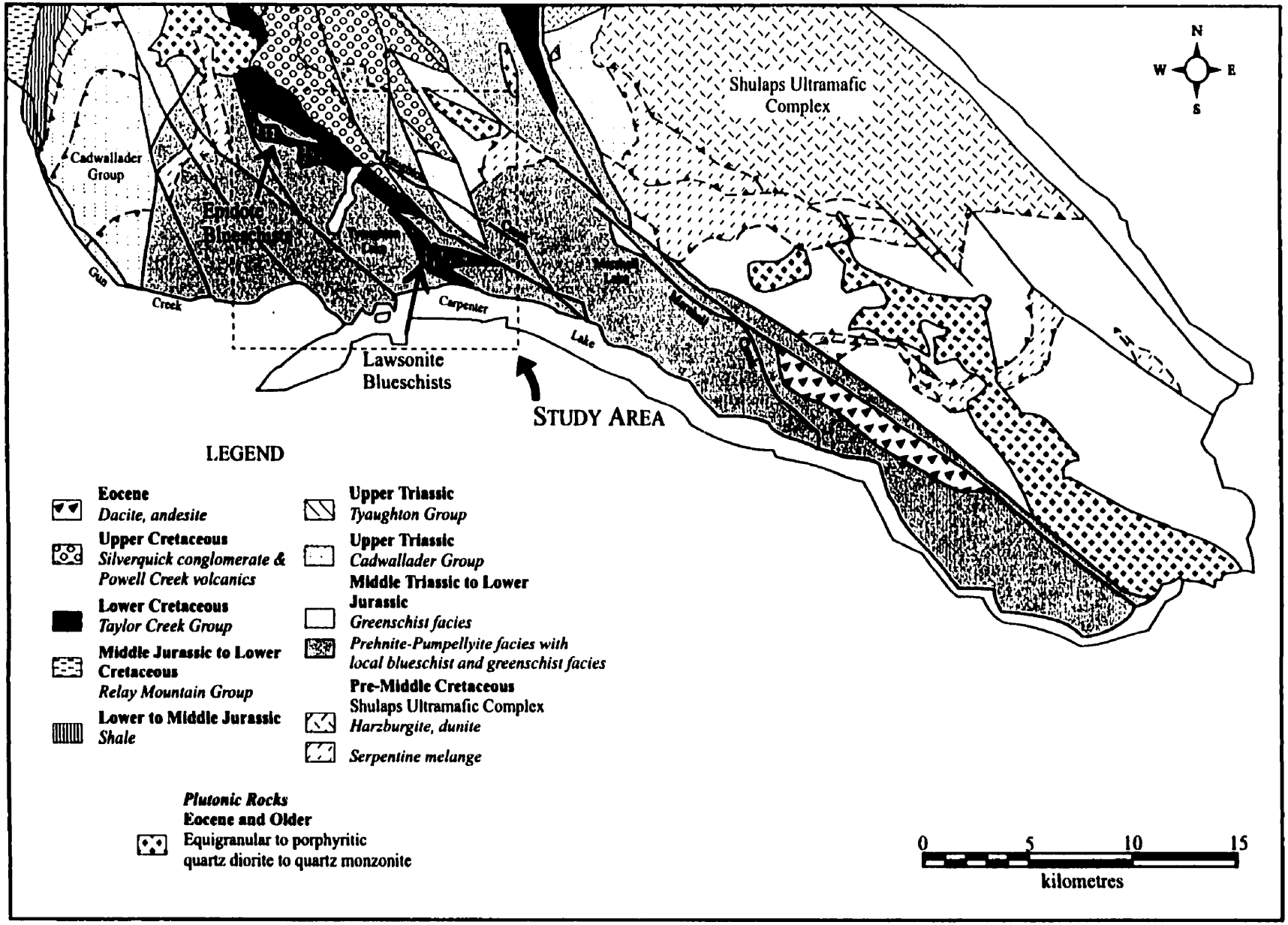

Figure 2-2. Generalized geological map of the study area (after Schiarizza et al., 1989)

2.1.1 Lithologies

According to Potter (1986), much of the Bridge River Complex in the study area consists of chert and greenstone units. The Bridge River chert occurs in beds typically 1 to 10 centimetres thick, as well as massive pods several metres thick and as narrow lenses within argillite. It consists of grey, red, brown and green varieties. Greenstone is a commonly massive grey-green to chocolate brown weathering metabasalt. It also consists of pillowed varieties and pillow breccia. It is locally amygdaloidal and contains rare phenocrysts of plagioclase and altered ferromagnesian minerals (Schiarizza et al., 1989). Potter (1983) reports that normative calculations of the pillowed and massive units indicate that these rocks were derived from tholeiites with a geochemical signature intermediate between ocean floor tholeiites and alkalic ocean-island type basalts.

Gabbroic rocks occur locally throughout the Bridge River Complex. These medium to coarse-grained rocks are typically associated with the greenstones (Potter, 1986). According to Schiarizza et al (1989) at the east end of Carpenter Lake gabbro occurs as a sequence of steeply south dipping sheeted dykes. The dykes typically display only one chilled margin.

A unit of the Bridge River Complex, to the northeast of Marshall Creek, consists of grey phyllite, quartz phyllite and biotite-bearing schists derived from argillite and chert as well as chloritic schists derived from mafic volcanic rocks. These were penetratively deformed under predominantly greenschist facies conditions. These rocks have been structurally interleaved with serpentinite melange and talc-serpentine-carbonate schists beneath the Shulaps ultramafic complex (Schiarizza et al., 1989).

The most distinctive rocks in the Bridge River complex, and the focus of this study, are the Bridge River blueschists. Studies by Garver et al., (1989) and Schiarizza et al. (1989; 1993) have documented five distinctive fault-bounded blueschist-bearing blocks in the area that occur in a belt approximately 14 km in length. These range in size from 0.2 to 1.5 km^2 and cover a total area of 6 km^2. The characteristic lithology is a dark blue, fine

grained, foliated and commonly crenulated phyllitic to schistose rock consisting of glaucophane, lawsonite ± quartz ± carbonate. These rocks also locally contain epidote, garnet, and white mica. Present in the blueschist-bearing blocks is the Bridge River greenstone, a massive to foliated unit displaying relict igneous minerals (clinopyroxene and plagioclase) and textures but commonly containing lenses and foliae of blueschist minerals.

$^{40}Ar/^{39}Ar$ dating of white mica by Archibald (1991) indicates that the blueschist metamorphic event ended at approximately 230 Ma. This poses an interesting problem since this would suggest that the metamorphism is older than some parts of the complex (e.g. Schiarizza et al., 1989). These age discrepancies allude to several stratigraphic, tectonic and metamorphic problems that perhaps suggest that the Bridge River Complex, as defined by Potter (1986), is definitely not one coherent unit.

2.1.2 Structural Setting

Regional mapping of the Bridge River complex by workers such as Schiarizza et al. (1989) and Garver et al. (1989) suggests the following relationships. Mid-Cretaceous to Tertiary, north to northwest trending contractional, strike-slip and extensional faults dominate the structural styles in the Bridge River area. The oldest map-scale structures are mid to early Late Cretaceous, southwest-vergent, thrust faults. In Late Cretaceous through Early Eocene time, the deformation history was dominated by dextral strike-slip faulting. These structures include the Castle Pass fault and the Yalakom – Marshall Creek – Relay Creek fault system. Extensional faults such as the Mission Ridge fault have been related, both spatially and temporally, to the dextral strike-slip systems (Journeay et al., 1996).

Studies in the Bridge River area recognize five distinctive deformational events: (1) lower Mesozoic (Archibald et al., 1990) blueschist deformation seen only at outcrop and thin section scale; (2) southwest-vergent thrusting which is best displayed in the Shulaps Range, and younger thrusts and reverse faults with the same vergence; (3) northeast-vergent thrusts and folds that post-date the earlier thrusting; (4) northwest striking dextral strike-slip

faulting and extension with significant movement on the Yalakom, Relay Creek and Mission Ridge faults during the Eocene; and (5) north-striking dextral strike-slip faulting that is synthetic with the Fraser fault (Garver, 1991).

Potter (1986) recognized that there was a lack of an internal stratigraphy within the Bridge River Complex. This problem is very evident in the study area and makes the recording and deciphering of map scale structures extremely difficult. This is primarily due to the relatively sparse exposure, the general complex structural relationships and the lack of marker horizons in the area, which makes the tracing of structural features beyond the outcrop extremely difficult.

The area defining the Bridge River blueschists has a distinctly chaotic and disrupted nature. Many of the structures (e.g. folds, faults) are discontinuous and cannot be traced beyond any one outcrop. The faults are commonly curved and show only minor apparent offsets. Several northwest trending, high angle faults are present and indicate dextral strike-separation as observed by offset veins. Garver (1991) suggests that these dextral faults in addition to the brittle faults he observed indicate north-northeast to south-southwest contraction and nearly east to west extension. In earlier work, Garver et al. (1989), mapped the blueschist-bearing regions as lenticular panels of rock imbricated against rocks of differing metamorphic grade along northwest trending, southwest dipping metre wide zones of high strain. They interpreted these structures to be thrust faults. Most of the principal contacts within the Bridge River complex are interpreted to be southwest-dipping thrusts (Garver, 1991). This imbrication of lithologies is interpreted to have preceded deposition of the overlying Taylor Creek group (middle Albian) which contains pebbles and boulders from the blueschist and other panels. The other contacts that the blueschist-bearing regions have with other rocks of the Bridge River complex are less obvious and lack these high strain zones (Garver et al., 1989).

Detailed studies by various workers (e.g. Potter, 1983; Garver, 1989; Garver, 1991; Schiarizza et al., 1995) have described the structural setting of the Bridge River blueschists in relation to the surrounding lithologies. Blueschists exposed in the Carpenter Lake area

are overlain to the northeast by northeast dipping imbricated rocks of the Bralorne-East Liza Complex and the Cadwallader Group of the mid-Cretaceous Liza Lake thrust belt (see Figure 2-3). In the North Cinnabar Creek area, the blueschists are overlain by Albian rocks of the Taylor Creek Group, which in turn are unconformably overlain by the Albian-Cenomanian Silverquick conglomerate. Figure 2-4 is a schematic representation of these structural relationships. The entire stratigraphic package is regarded as the overturned limb of a northeast vergent syncline, which post-dated the earlier southwest vergent thrusting. If the blueschists are a reliable marker within the Bridge River complex, three possible relationships between the Cadwallader – Bralorne-East Liza thrust stack and the mid-Cretaceous clastic succession: 1) the thrust stack was eroded away prior to deposition of the Taylor Creek Group; 2) the thrust stack ramped to the west, over the top of the Taylor Creek Group, and was then eroded away prior to deposition of the Silverquick conglomerate; 3) the Cadwallader – Bralorne-East Liza thrust stack ramped to the west over both the Taylor Creek Group and Silver quick conglomerate (Schiarizza et al., 1995).

According to Garver (1991), some fault zones in the Bridge River complex were probably produced during this northeast vergent thrusting. However, structures developed during the earlier southwest vergent thrusting were likely overturned during this later folding. Garver (1991) also noted the presence of folds and faults beneath the unconformity that may be older than the northeast vergent structures related to the syncline. These structures may be related to the subduction-accretion process within the Bridge River Complex (Schiarizza et al., 1995).

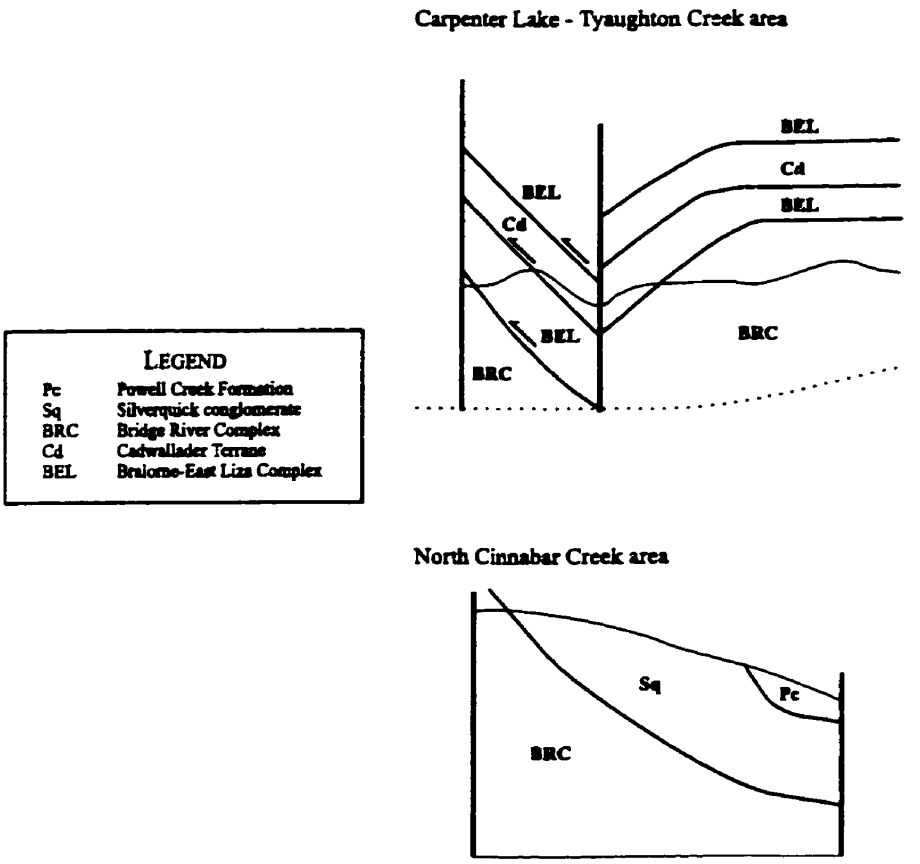

Figure 2-3. Schematic representation of the structural setting of the Bridge River blueschists in relation to surrounding lithologies. In the Carpenter Lake – Tyaughton Creek area, the blueschists are structurally overlain by the Bralorne-East Liza Complex and the Cadwallader Group. In the North Cinnabar Creek area, the blueschists are overlain by the Taylor Creek Group which in turn is overlain by the Silverquick conglomerate (modified from Schiarizza et al., 1995).

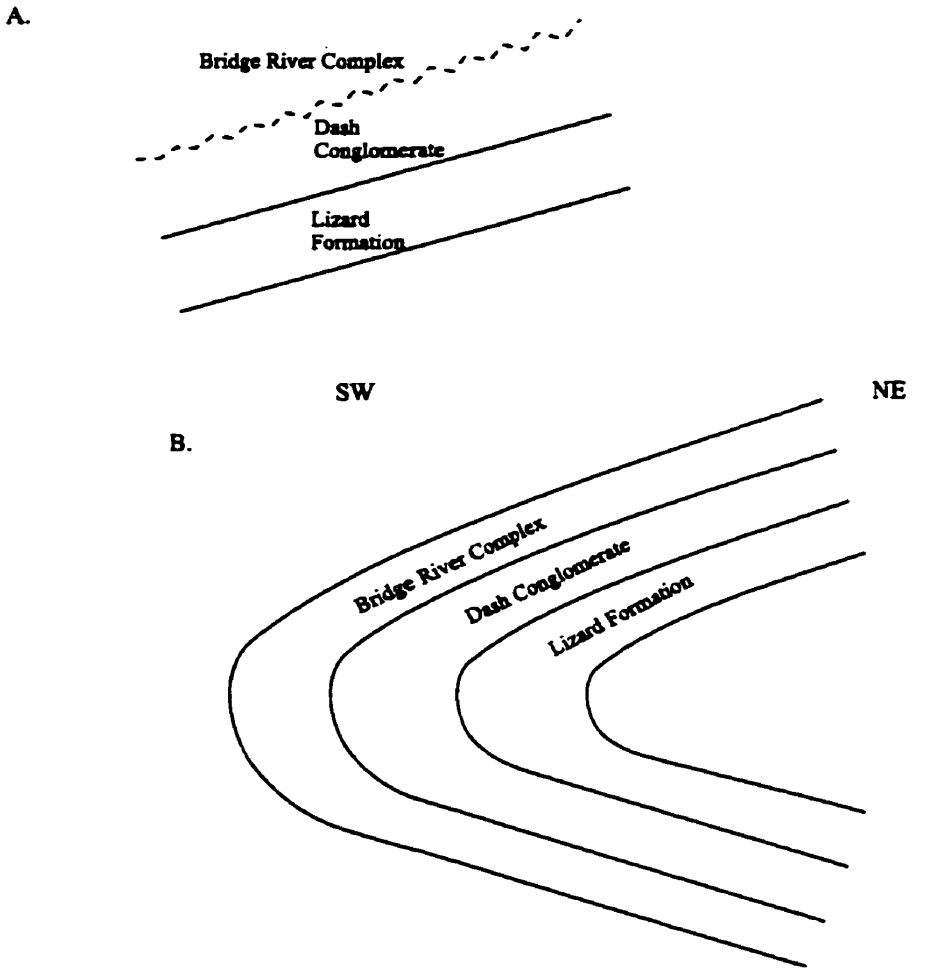

Figure 2-4. Schematic representation of stratigraphic relationships in the North Cinnabar Creek area. Figure 1-2A is a representation of the overturned unconformity with Albian Dash conglomerate depositionally overlying the Bridge River rocks. Figure 1-2B is a representation of the northeast vergent syncline (Mid-Cretaceous) that overturned earlier southwest dipping structures and which produced the current configuration of the units.

2.1.3 Metamorphism in the Bridge River Area

The Bridge River Terrane in the study area consists of two structural blocks separated by a high-angle fault. The greenstones in the southwestern block are characterized by subgreenschist facies assemblages (Potter, 1983) which are of the type thought to be stable over a wide range of metamorphic conditions (T≅ 200°C – 320°C; P_{H_2O}≅1-4 kbar) (e.g. Yardley, 1989). Metamorphism in this block was essentially static as few rocks show penetrative fabrics. This subgreenschist metamorphism is the only metamorphic event that has affected these rocks, except for one area where prehnite veining postdates an earlier hornblende-chlorite-epidote paragenesis (Potter, 1983). According to Potter (1986), this earlier hornblende-chlorite-epidote assemblage is indicative of metamorphism in an oceanic setting close to a submarine volcanic centre or intrusion. These rocks are not near any major late intrusions and are of much higher grade than rocks adjacent to such intrusions in the area.

An inverted metamorphic aureole, ranging from lower amphibolite at high structural levels to prehnite-pumpellyite facies at the structural base, is seen in the northeastern block (Greenwood et al., 1991). Based upon the assemblages in this metamorphic aureole, Potter (1986) describes the metamorphic conditions as being between 325 to 525°C at about 4 to 5 kbar. This deformation and metamorphism is interpreted as resulting from Late Jurassic overthrusting by hot rocks of the Shulaps ultramafic complex (Potter, 1983).

2.1.4 Paleotectonic Setting

Based upon its wide age range, the apparent lack of internal stratigraphy, outcrop scale tectonic disruptions and the presence of the Middle to Late Triassic blueschists the Bridge River Complex is believed to have accumulated as an accretion-subduction complex such as in a back arc basin (e.g. Potter, 1986; Schiarizza et al., 1995). This paleotectonic setting, according to Potter (1986), is consistent with (1) a high geothermal gradient, indicated by seafloor volcanism and locally developed static amphibolite facies metamorphism, (2) significant topographic gradients during deposition of both the chert-greenstone and slump facies of the assemblage, and (3) basaltic, andesitic and silicic detritus in clastic rocks.

Potter (1986) illustrates several possible scenarios for the earliest deformational history of the Bridge River Complex in the area (see Figure 2-4). Firstly, if the assemblage does in fact represent a back arc basin, the deformation could record the closing of the basin after a colliding fragment stalled forearc subduction. Alternatively, the Complex may have been deformed in a forearc setting as part of a subduction complex. In this setting volcaniclastic trench deposits would dominate the inner trench wall thrust packets. The presence of large, undeformed basaltic bodies in the Complex suggests that if these rocks were deformed in a forearc subduction setting they were peeled off as large underplated slabs at depths above which high-pressure metamorphic assemblages would be generated. Another possible scenario involves a transpressional or compressional collapse of a small ocean basin during a collision event without involving subduction of the small basin. This model would suggest that the Bridge River would represent a small sea between an arc or some other offshore landmass and the western North American margin (Potter, 1986).

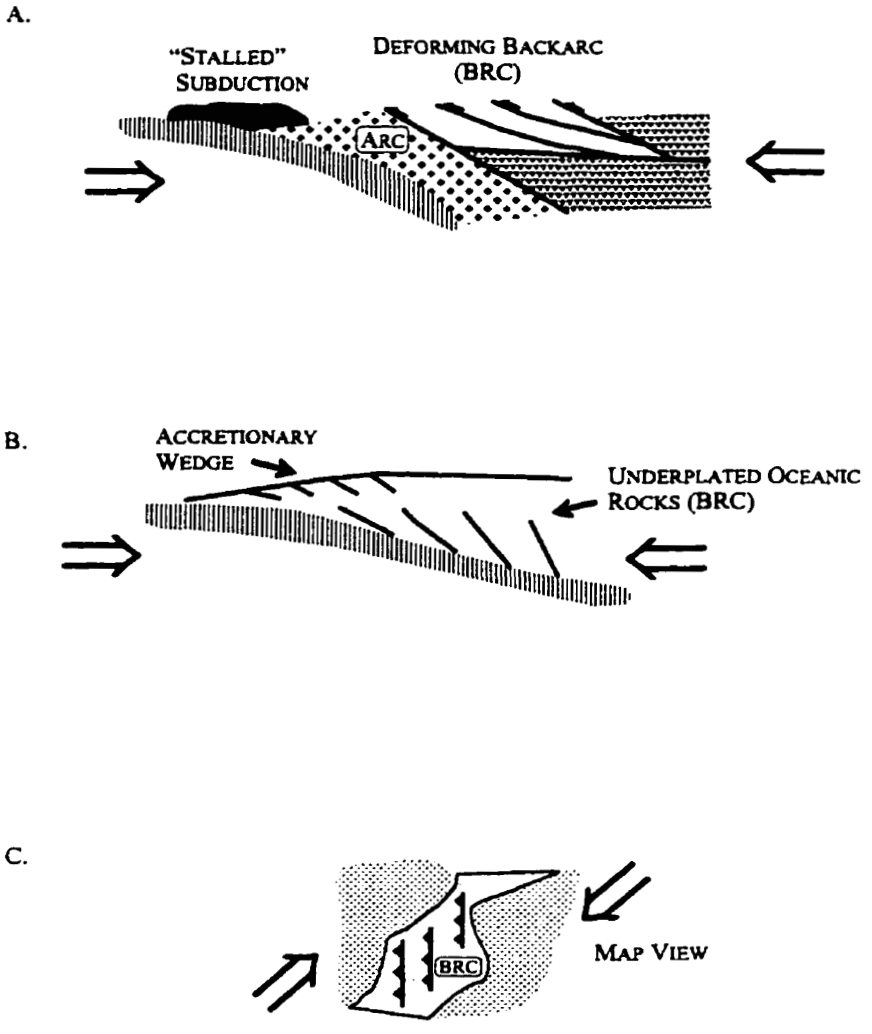

Figure 2-5. Proposed deformational setting of the Bridge River Complex (from Potter, 1986). (A) Telescoping of a back arc basin after a colliding fragment has stalled forearc subduction. (B) Underplating of undeformed slabs of oceanic rocks in a subduction complex. (C) Transpressional collapse of a small sea of unspecified origin.

3. FIELD RELATIONS

3.1 INTRODUCTION

The fieldwork for this project took place over a period of five weeks during the summers of 1996 and 1997. The purpose of this portion of the project was to sample and describe the field setting of the blueschists and related rocks in the area outlined on the base map compiled by Schiarizza and Gaba (1993). I also attempted to document the lithologic variation in the area and extract meaningful structural data by mapping, in detail, two areas used for the detailed sampling (see Figures 3-1 and 3-2)

The mapping and sampling was accomplished using 1:20 000 scale maps and airphotos. Other techniques used included pace and compass traversing as well as navigating and outcrop locating using a Global Positioning Satellite system.

3.2 FIELD UNITS AND STRUCTURAL RELATIONSHIPS

The results of mapping and sampling of the area are presented graphically in Figure 3-1 and Figure 3-2. Mapping of the area defined four distinctive units: a blueschist unit, a blueschist unit with greenstone lenses, a greenstone unit with local blueschist lenses/foliae; and a chert unit. The fine-grained nature of most of these rocks made mineralogical identification in the field next to impossible.

Figures 3-3 and 3-4 are schematic cross sections across the blueschist-bearing blocks. As concluded by Garver (1991) and discussed in Chapter 2, the contacts between the blueschists and surrounding lithologies as well as among the four different lithologies are believed to be southwest dipping thrust faults. Other southwest dipping structures within the blocks are probably related to this deformation. The abundant northeast dipping foliations observed throughout the area probably the northeast vergent thrusting during the late Cretaceous. Other structural complexities within the blocks probably resulted from the

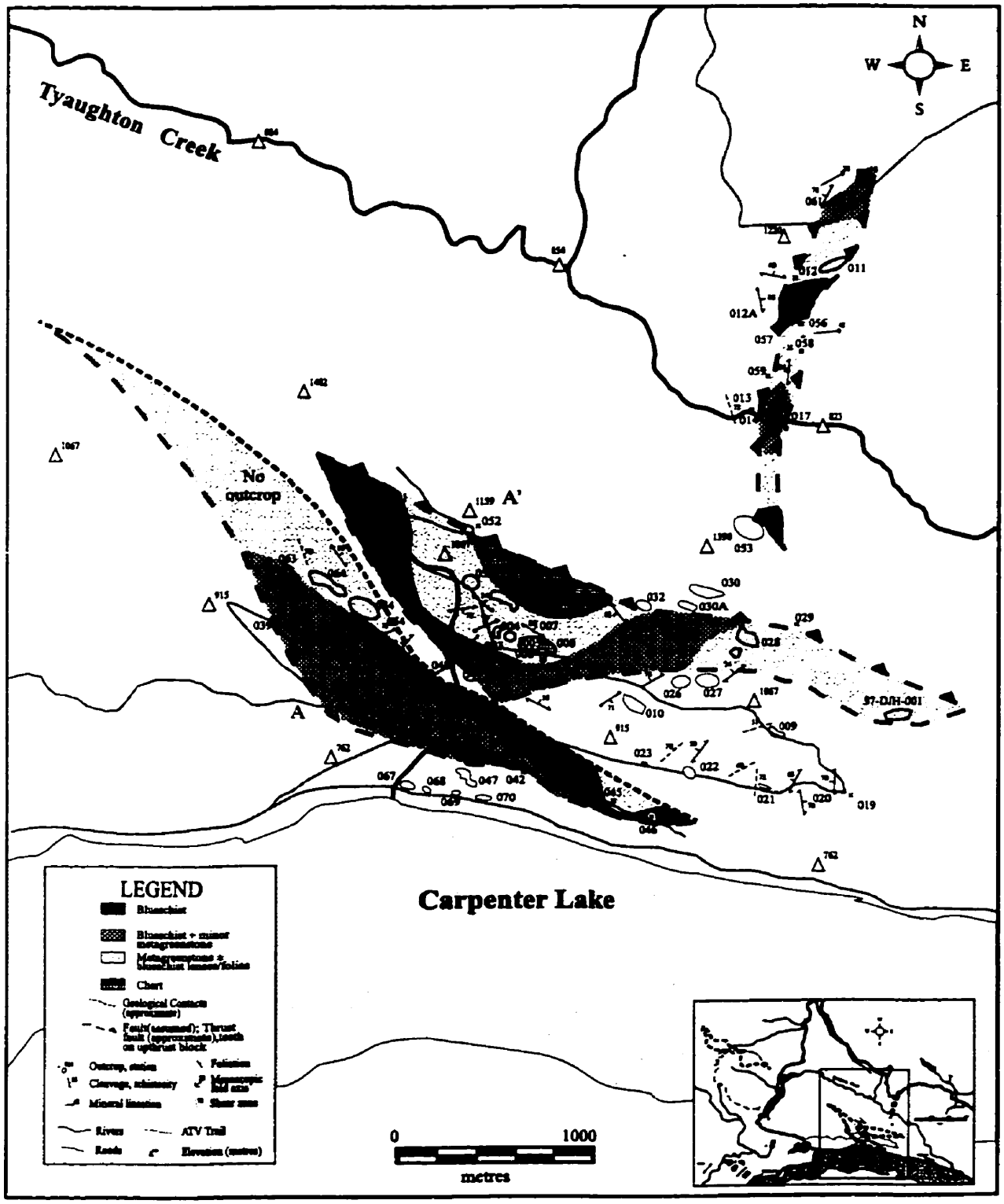

Figure 3-1. Map of station location and lithologic variation within the blueschists-bearing area in the Carpenter Lake - Tyaughton Creek region.

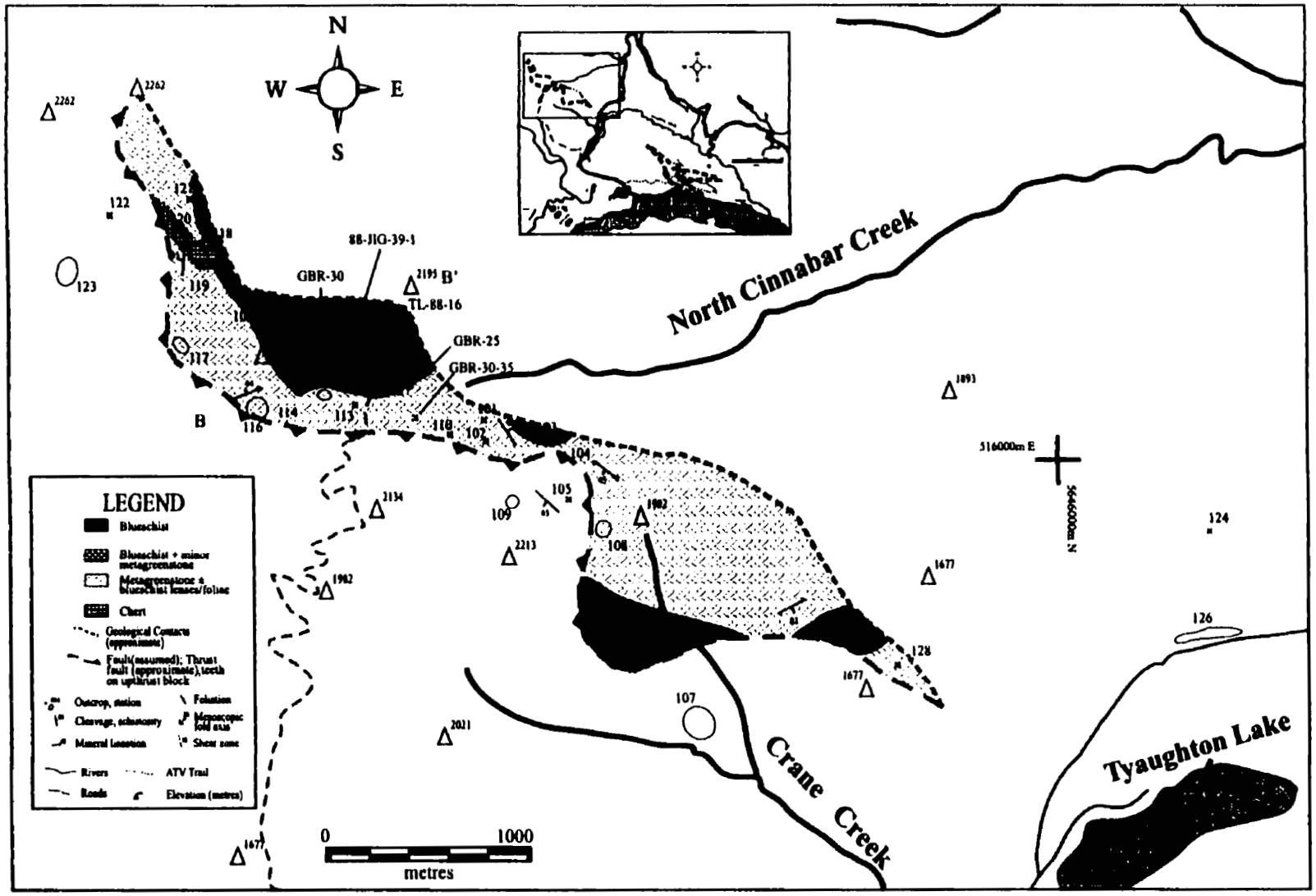

Figure 3-2. Station location and lithologic variation map within the blueschist-bearing area from the North Cinnabar Creek area

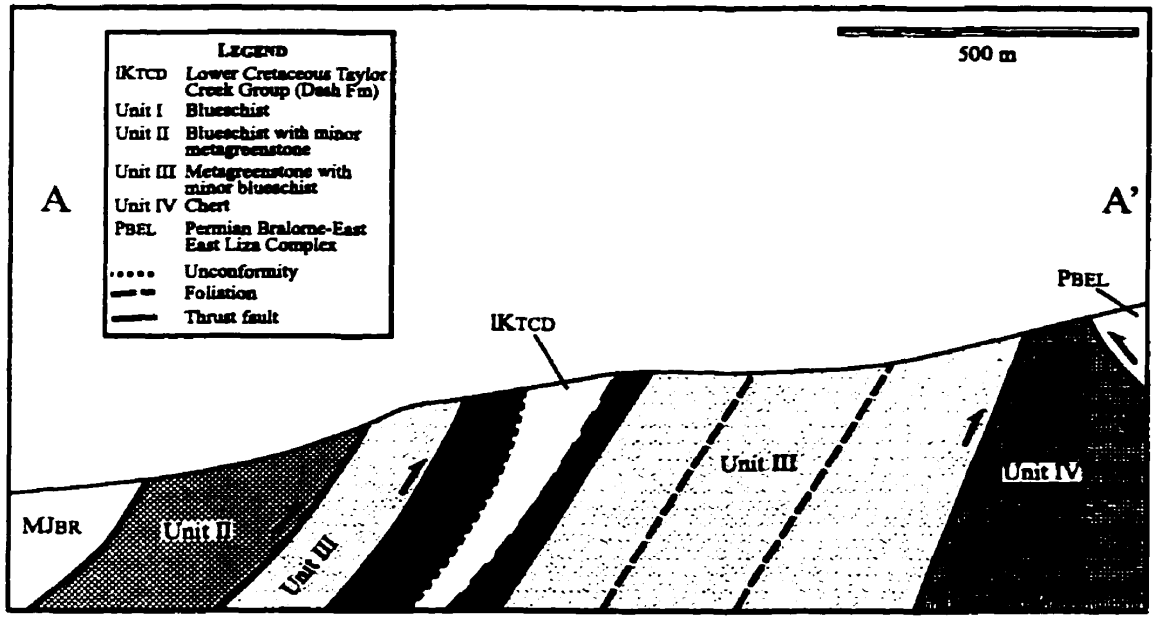

Figure 3-3. Schematic cross section across blueschist blocks in the Carpenter Lake – Tyaughton Creek area. Contacts between units are interpreted as southwest dipping thrust/reverse faults and other similarly oriented foliations being related to this deformation event. Northeast dipping structures probably formed during the late Cretaceous thrusting event in the area.

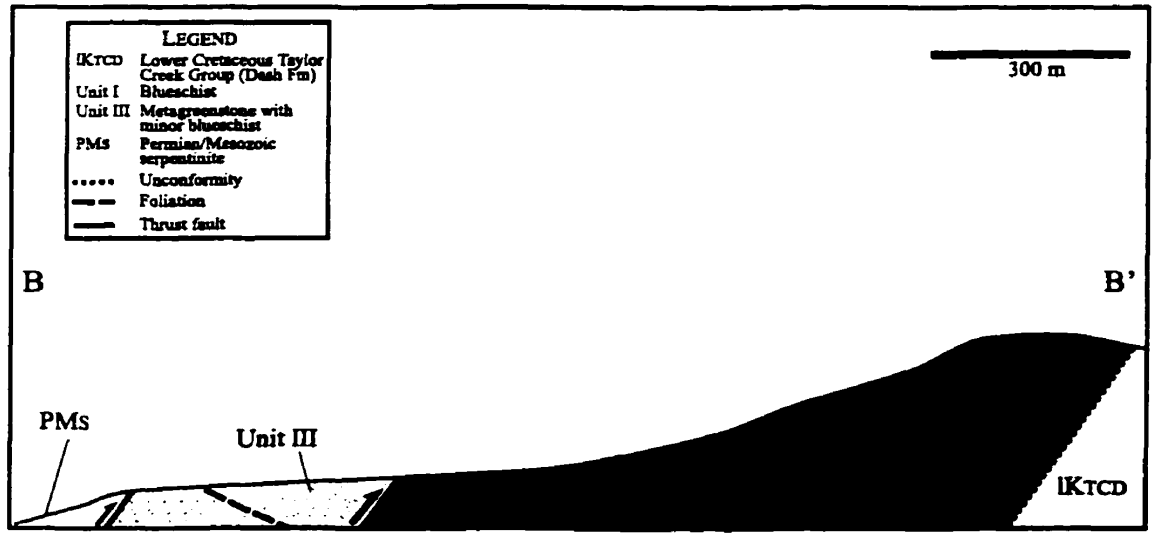

Figure 3-4. Schematic cross section across blueschist blocks in the North Cinnabar Creek area. Contacts between units are interpreted as southwest dipping thrust/reverse faults and other similarly oriented foliations being related to this deformation event. Northeast dipping structures probably formed during the late Cretaceous thrusting event in the area.

superimposing of the various stages of deformation upon one another as well as upon result of syn-kinematic blueschist metamorphism and deformation during the accretion-subduction process. These structures were probably then modified by much later folding and faulting (Schiarizza et al., 1989; Garver et al., 1989; Garver, 1991).

3.2.1 Unit I: Blueschist

The blueschist unit, the most distinctive lithology in the area, consists of dark blue fine-grained, strongly foliated and commonly crenulated schist to phyllite (see Figure 3-5). Weathered surfaces range from dark blue to tan in colour. When grain size is coarse enough, blue amphibole with characteristic amphibole cleavage, white mica, green chlorite, carbonate and quartz are evident. One sample, 88-JIG-39-1 (sample provided by J. Garver) contains abundant red garnet porphyroblasts approximately 0.5 to 1.5 mm in diameter. Locally, the unit is much more massive and consists of metamorphosed siliceous sedimentary and mafic volcanic rocks (Figure 3-6). This portion of the unit consists of complexly folded interlayered white quartzite and dark blue phyllite. These quartzite layers may have been quartz veins that were transposed parallel to the foliation during an earlier stage of deformation.

Structurally the unit is complex. The map pattern of foliations is complex and since there is no one distinctive marker horizon present, the patterns are difficult to interpret. Typically, the phyllitic to schistose rocks display a weak to moderately anastomosing foliation. The more massive rocks commonly display strong mineral lineations (defined by elongate Na-amphiboles) that have subsequently been folded. Asymmetric Z- and S-folds are present as well in these units (see Figure 3-6). The foliation, lineation and small fold patterns observed (Figures 3-1 and 3-2) are consistent with foliated and folded rocks being cut up into tectonic slices that are further deformed during faulting (Simony, 1999, pers. comm.). Garver (1991) reports that the asymmetry of these structures suggest a vergence to the northeast. In a detailed kinematic analysis of the rocks in the North Cinnabar Creek

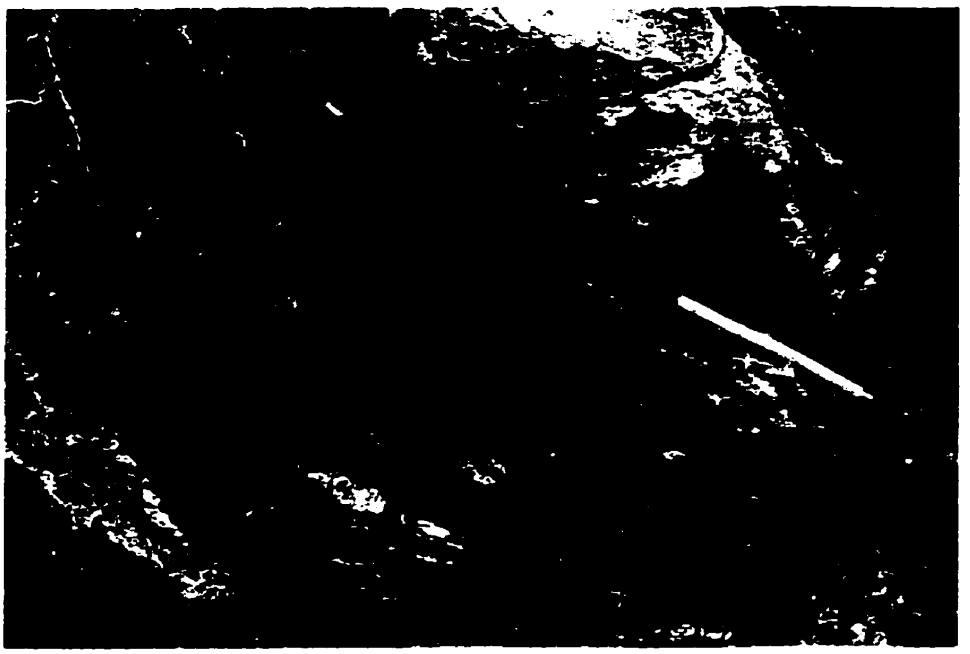

Figure 3-5. Typical well foliated blueschist outcrop with a slight anastomosing foliation (Station 97-DJH-049). Pen magnet for scale

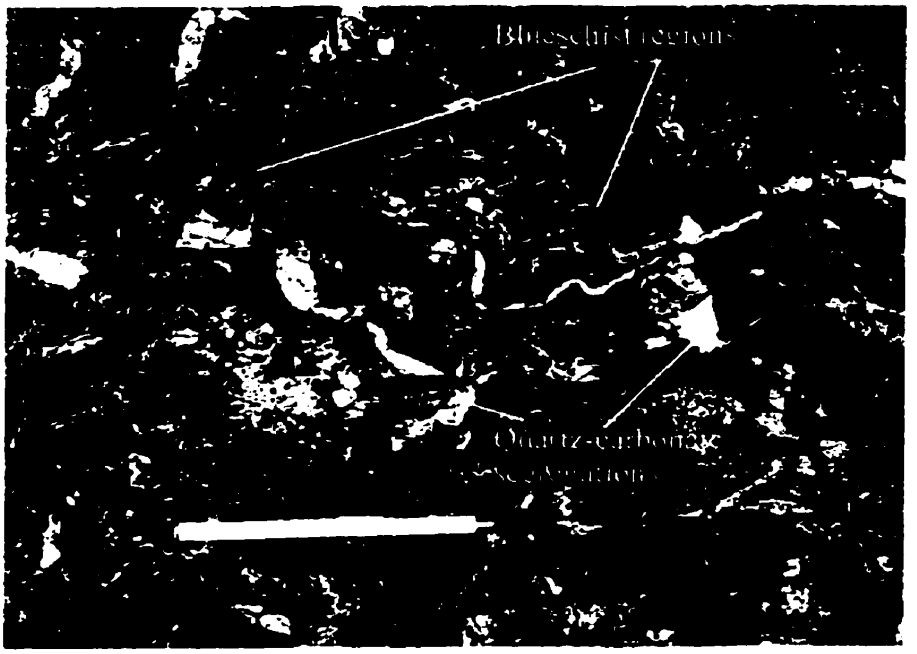

Figure 3-6. Complexly folded interlayered quartzite and phyllite in Unit I. Pen magnet is pointing towards the northeast. Station 97-DJH-049.

area, Garver (1991) first recorded the presence of brittle, high angle faults and a well-developed crenulation cleavage. He interprets these structures to represent relatively young north-northeast to south-southwest contraction. Garver (1991) also recorded the presence of faults with apparent normal separation and down-dip slickenlines; however, these were scarce. He suggests that the area was subjected primarily to transpressive dextral strike-slip faulting.

3.2.2 Unit II: Blueschist + Greenstone

This unit is similar to Unit I (blueschist unit) but is differentiated by the presence of variable amounts of greenstone. The two rock types are readily distinguished by colour variations. The rocks in this unit are generally massive but locally grade into a phyllite. The tectonic fabric appears to become more intense and penetrative near the thrust fault contact.

In both this unit and the greenstone unit (Unit III) the outcrops locally have bulbous features that are suggestive of pillows and pillow breccias (Figure 3-7), however none can definitely be identified as pillows. Based on Potter's (1983) interpretations of the origin of the greenstones, pillow basalts might be expected.

Veins are prevalent in this unit and appear to be concentrated in the blueschist regions. The veins are composed of quartz and/or carbonate and minor albite and form a web-like array. The relative timing of veining is difficult to interpret but they are inferred to be syn- and post blueschist metamorphism. Some veins are deformed in the local fabric whereas others crosscut this same fabric. Several other studies of subduction-related terranes (e.g. Ernst, 1965; Moore et al. 1981; and Bebout and Barton, 1989) have mentioned the presence of abundant veins and other metasomatic features. Bebout and Barton (1989), in a study of the Catalina Schist Terrane in California, suggest that the veins reflect subduction zone fluid flow and mass transfer of Si and alkali elements that changed the major and trace element bulk chemistry of the protolith. The veins in Unit II therefore

may have acted as conduits for the fluids carrying the components used to produce the blueschist facies assemblages.

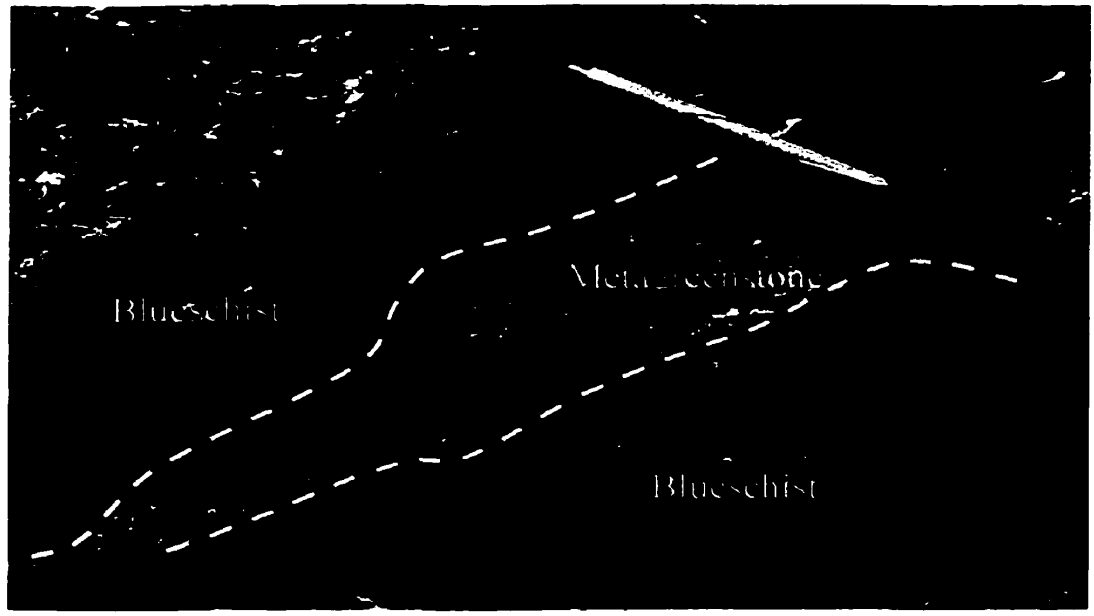

Figure 3-7. Massive, highly veined blueschist unit with greenstone pod.

3.2.3 Unit III: Greenstone

The most prevalent unit in the area is a massive to weakly foliated greenstone. The greenstone is grey-green to dark-brown weathering. Locally the greenstones have strong purple pyrolusite staining. The unit also contains some pillowed and gabbroic varieties. These greenstones locally have relict igneous minerals (e.g. plagioclase and pyroxenes) even at the outcrop scale. Unlike Unit II, obvious veining is not a prevalent feature. Where present however, veins consist of quartz and carbonate but lack albite. The veins tend to be late features that crosscut the local fabric.

The interesting feature of these greenstones is the presence of lenses or foliae of blueschist minerals within the unit. The thickness of the blueschist lenses is typically on

the decimetre to metre scale. The foliae range from approximately 2-10 mm in length and are randomly oriented within the greenstone units (see Figure 3-8). The boundaries between the two rock types range from being relatively diffuse to sharp. As seen in Unit II, these contrasting lithologies may suggest that there may have existed either internal heterogeneities in the original rock or that segregation took place during metamorphism. At one outcrop (station 97-DJH-054), it is possible to see a gradation from a 'pure' greenstone to blueschist composition. Although extremely fine grained, this feature is readily recognized by the increase in blue colour and change to a phyllite.

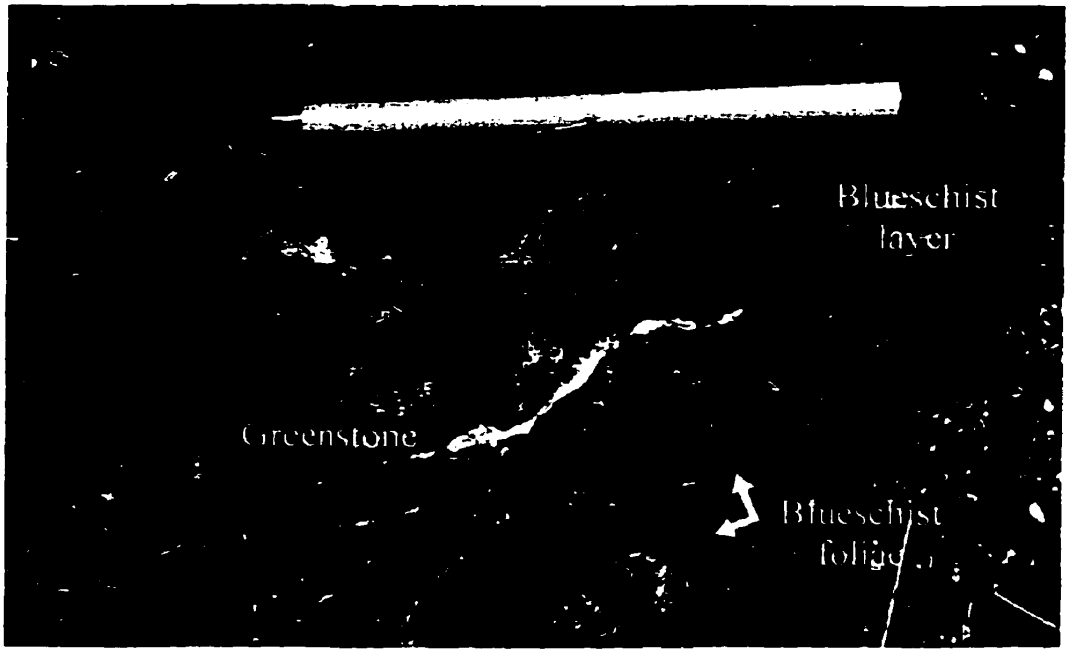

Figure 3-8. Greenstone unit with blueschist lenses and foliae from station 97-DJH-062. Pen magnet for scale.

Several outcrops of this unit display thin slivers of blueschist facies minerals. The Na-amphibole slivers concentrate along former cracks in the greenstone from where they appear to infiltrate further into the rock (see Figure 3-9). Bebout and Barton (1989) regard such features as obvious evidence for at least the local mobility of Na, Al and Si.

The greenstone unit is generally massive to only weakly foliated. Locally, it is highly sheared and fractured with Na-amphibole partings concentrating in these regions. The foliation is defined primarily by anastomosing schistose blueschist regions that wrap around the more resistive greenstone regions (see Figure 3-8). Cowan (1985) describes similar features in mélanges in the western Cordillera of North America and the structure has been described as phacoidal cleavage. The manner in which strain is accommodated in the two regions is emphasized by the juxtaposition of the two lithologies. The blueschist regions are obviously more susceptible to deformation than the greenstone regions.

It may also be possible that the greenstone regions were non-cleaved microlithons that formed during an earlier development of a fracture cleavage. If this is the case and metamorphism followed the formation of the fracture cleavage fluids could have concentrated along these planes and metasomatized these regions. This could then have led to the development of the blueschist facies mineral assemblages (e.g. Wilson, 1982).

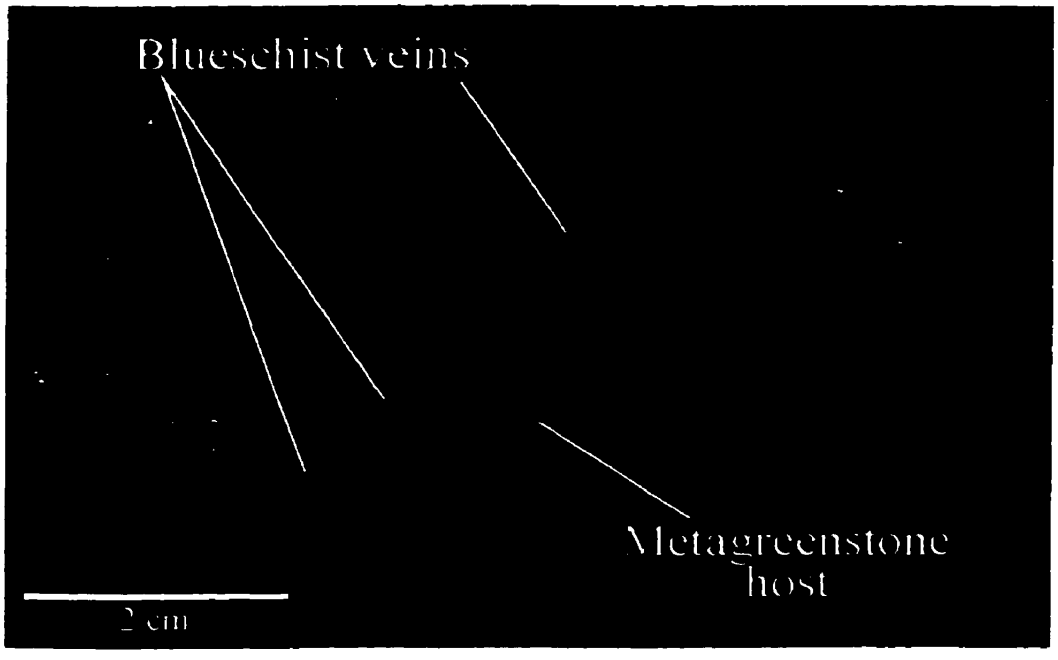

Figure 3-9. Thin blueschist slivers in greenstone. Veins appear to 'infiltrate' into host greenstone.

3.2.4 Unit IV: Metachert

The metachert unit represents a smaller proportion of the rocks found in the study area yet this unit is quite distinctive. The unit consists of blue-grey, green-grey and red-brown coloured beds that range in thickness from a few millimetres to decimetres. Some outcrops commonly appear recrystallized and are veined by quartz and carbonate.

The unit varies structurally from being rhythmically layered to highly disturbed. Locally there is no deformation with primary depositional features (see Figure 3-10) present whereas in other regions, the unit is strongly flattened and locally isoclinally and asymmetrically folded. The asymmetry of some of these folds suggests a vergence to the northeast. Garver (1991) suggests that the variety in colours, lithologic associations and structural disposition indicate that cherts of various affinities and ages are found in the Bridge River Complex. In thin section, the high degree of disruption is obvious. Thin tuffaceous layers now containing sodic amphibole + lawsonite ± stilpnomelane have been complexly folded either syn- or post-blueschist metamorphism (see Figure 3-11). Potter (1986) describes similar wispy, foliated, fragmental tuffaceous layers in other cherts throughout the complex.

Figure 3-10. Well-bedded chert outcrop from the North Cinnabar Creek area (station 97-DJH-104). The unit lies nearly horizontally. Ruler on top of outcrop is 15 cm in length.

Figure 3-11. Photomicrograph of highly disrupted tuffaceous layers in chert unit.

4. WHOLE-ROCK CHEMISTRY

4.1 INTRODUCTION

In an attempt to better understand the tectonic setting of the metavolcanic rocks within the Bridge River area and to determine whether they differ chemically from one another, nine samples were analyzed for their whole-rock chemistry. Five of the samples are metavolcanics, two are blueschists and two are metavolcanics that contain blueschist foliae. These samples are from both the Carpenter Lake area as well as the North Cinnabar Creek area. For sample locations see Figure 1-3.

Major and trace elements were analyzed by wavelength-dispersive X-ray fluorescence (XRF) spectrometry. Measurements were made on fused beads for major elements and pressed pellets for trace elements. The analyses were performed by Mr. Pat Michael using the automated Phillips PW 1440 spectrometer equipped with a Rh X-ray tube housed at The University of Calgary. The operating voltage was 60 kV and 40 μA.

4.2 RESULTS

The results of whole-rock XRF analyses are presented Table 4-1. The variable loss-on-ignition values (LOI) (1.36 – 6.67%) do not appear to reflect variation in hydration (which implies oxidation) between the blueschists and greenstones. Blueschists have LOI values ranging from 1.50 – 6.55% whereas greenstones have LOI values in the range 1.36 – 4.18 %. There also does not appear to be a systematic distribution of alkaline and alkali-earth elements. However, Figure 4-1 suggests that many of these rocks have essentially a basaltic composition.

Normative calculations were performed on the greenstones using the program MELT95 by Nicholls and the classification scheme of Irvine and Baragar (1971). The

results are presented in Table 4-2. The upper limit of Fe_2O_3 was set according to the scheme of Irvine and Baragar (1971) where:

$$\% Fe_2O_3 = \% TiO_2 + 1.5$$

This equation is based on the observation that Fe_2O_3 and TiO_2 generally have similar variation trends (Irvine and Baragar, 1971). Granted, this estimation is somewhat arbitrary particularly for low-grade metamorphic rocks, which are hydrated but some estimation is better than none. The Fe_2O_3/FeO ratio can however appreciably affect the norm and may affect the classification of the rock (e.g. Coombs, 1963). For a further discussion of the recalculation scheme, see Irvine and Baragar (1971).

The normative calculations indicate that the greenstones, including those with minor blueschist foliae, belong to alkaline (hawaiite series), and subalkaline suites (calc-alkaline and tholeiitic series). The subalkaline rocks show highly variable normative hypersthene, orthoclase and olivine contents. The alkaline rocks range in their normative quartz, olivine and nepheline contents. Caution must be exercised when interpreting both the normative calculations and discriminant diagrams. These cannot always be used confidently to determine the characteristics of the primary magma composition since the chemical analyses reflect rock compositions after alteration by seafloor and later metasomatic and metamorphic processes.

4.3 INTERPRETATION

The following section involves the interpretation of these results and comparison to other data presented in the literature for greenstones from the Bridge River area (e.g. Potter, 1983; Church and Pettipas, 1989). Implicit in these comparisons is the assumption that all greenstones within the area were originally from the same basaltic pile.

Table 4-1. Major and Trace element whole-rock geochemistry of selected Bridge River blueschists and related rocks from XRF analysis.

	92-GBR 12†	92-GBR 13A†	92-GBR 13B†	92-GBR 19B[b]	92-GBR 28C†	92-GBR 33*	92-GBR 34[b]	92-GBR 35*	92-GBR 37[b]
SiO_2 %	50.6	49.2	48.9	45.7	48.1	46.0	49.0	42.3	60.1
Al_2O_3	13.4	16.3	15.5	14.7	14.8	10.8	14.87	13.2	9.8
Fe_2O_3	10.5	12.56	10.48	12.12	12.22	13.3	12.6	16.1	16.0
MgO	8.72	5.16	8.92	7.81	5.18	6.52	5.69	7.08	3.68
Na_2O	3.81	0.82	3.90	1.91	3.83	2.80	3.63	2.16	5.10
CaO	7.33	10.75	8.08	8.76	6.38	11.97	8.14	11.34	1.24
K_2O	1.71	0.117	0.174	1.26	1.13	0.136	0.464	0.877	2.258
TiO_2	1.60	1.36	1.16	1.49	3.62	1.28	1.45	1.91	0.614
P_2O_5	0.454	0.137	0.093	0.121	0.666	0.133	0.188	0.199	0.349
MnO	0.153	0.167	0.169	0.195	0.129	0.163	0.185	0.210	0.175
S	<dl	<dl	0.098	<dl	0.13	0.55	<dl	<dl	<dl
LOI	1.364	3.712	3.066	6.553	4.175	6.670	4.607	4.806	1.502
V µg/g	337	418	294	363	317	348	348	480	265
Cr	430	54.8	331	105	85.7	159	236	188	76.8
Ni	86.1	13.6	94.2	58.3	50.3	58.3	113	80.1	76.6
Zn	91.3	96.3	75.7	91.5	126	170	112	132	185
Ga	21.6	21.7	15.1	17.0	22.2	13.2	17.2	17.9	16.6
Rb	39.3	4.8	3.0	32.1	17.0	4.5	11.9	12.6	73.6
Sr	824	527	255	107	295	96	104	65.9	8.1
Y	18.1	27.5	20.8	31.9	31.1	26.8	34.3	50.1	40.4
Zr	98.6	79.0	57.5	89.0	326	73.7	95.7	108	129
Nb	7.1	1.7	1.2	4.0	39.4	3.0	4.6	3.1	12.1
Ba	1295	114	480	54.5	475	58.0	45.5	134	123
La	17.7	<dl	<dl	<dl	27.7	15.4	7.9	16.5	55.6
Pb	<dl	<dl	<dl	<dl	<dl	<dl	<dl	<dl	9.4
Th	<dl	<dl	<dl	<dl	<dl	<dl	<dl	<dl	5.7
Sum %	100.0	100.4	100.7	100.7	100.5	100.5	100.8	100.4	100.9

KEY: † denotes greenstone; [b] denotes blueschist; * denotes greenstone with blueschist foliae; <dl = below detection limit
Analytical Error: < 0.3% for majors elements

Table 4-2. Normative Calculations for the Bridge River Greenstones. Classification scheme of Irvine and Baragar (1971)

	92-GBR 12†	92-GBR 13A†	92-GBR 13B†	92-GBR 19B[b]	92-GBR 28C†	92-GBR 33[a]	92-GBR 34[b]	82-GBR 35[a]	92-GBR 37[b]
SiO_2 %	50.6	49.2	48.9	45.7	48.1	46.0	49.0	42.3	60.1
Al_2O_3	13.4	16.3	15.5	14.7	14.8	10.8	14.87	13.2	9.8
FeO	6.66	8.73	7.04	8.22	6.39	9.47	8.68	11.42	12.49
Fe_2O_3	3.10	2.86	2.66	2.99	5.12	2.78	2.95	3.41	2.11
MgO	8.72	5.16	8.92	7.81	5.18	6.52	5.69	7.08	3.68
Na_2O	3.81	0.82	3.90	1.91	3.83	2.80	3.63	2.16	5.10
CaO	7.33	10.75	8.08	8.76	6.38	11.97	8.14	11.34	1.24
K_2O	1.71	0.117	0.174	1.26	1.13	0.136	0.464	0.877	2.258
TiO_2	1.60	1.36	1.16	1.49	3.62	1.28	1.45	1.91	0.614
P_2O_5	0.454	0.137	0.093	0.121	0.666	0.133	0.188	0.199	0.349
MnO	0.153	0.167	0.169	0.195	0.129	0.163	0.185	0.210	0.175
Normative Calculations									
Q	-	10.43	-	-	2.92	-	-	-	21.61
C	-	-	-	-	-	-	-	-	0.98
Or	10.37	0.72	1.07	8.00	7.00	0.87	2.88	5.51	30.93
pl	47.87	49.61	59.35	47.25	54.81	43.70	56.19	42.88	14.36
(ab)	33.08	7.26	34.20	17.36	33.99	25.76	32.30	17.65	10.77
(an)	14.79	42.35	25.15	29.89	20.82	17.94	23.89	25.23	3.60
ne	-	-	-	-	-	-	-	0.97	-
di	15.72	10.41	12.77	13.02	6.16	37.73	14.27	27.42	-
(wo)	8.15	5.24	6.58	6.67	3.26	19.08	7.22	13.86	-
(en)	5.35	2.50	4.09	3.88	2.55	9.57	3.63	6.96	-
(fs)	2.23	2.67	2.10	2.47	0.35	9.09	3.43	6.60	-
hy	3.51	22.70	3.37	17.01	12.49	0.35	14.65	-	24.18
(en)	2.48	10.96	2.22	10.39	10.98	0.18	7.54	-	0.45
(fs)	1.03	11.74	1.14	6.62	1.51	0.17	7.11	-	23.73
ol	14.78	-	18.34	7.90	-	11.33	5.34	16.91	-
(fo)	10.13	-	11.71	4.64	-	5.54	2.62	8.27	-
(fa)	4.65	-	6.63	3.26	-	5.80	2.72	8.65	-
mt	3.58	3.10	2.61	3.48	7.79	3.03	3.32	4.42	1.37
il	3.12	2.70	2.28	3.04	7.21	2.64	2.90	3.86	1.20
ap	1.09	0.34	0.23	0.31	1.66	0.34	0.47	0.50	5.49

KEY: Q = quartz; C = corundum; or = orthoclase; pl = plagioclase; ab = albite; an = anorthite; ne = nepheline; di = diopside; wo = wollastonite; en = enstatite; fs = ferrosilite; hy = hypersthene; ol = olivine; fo = forsterite; fa = fayalite; mt = magnetite; il = ilmenite; ap = apatite

Figure 4-1 is a total alkalis vs. silica plot after Le Bas et al. (1986) for rocks from the Bridge River area. Despite being subject to varying degrees of metamorphism, these rocks appear to have preserved their original basaltic character. There is significant overlap of this study's data with data from Potter (1983) and Church and Pettipas (1989). This may suggest that the rocks could be related. One data point from this study falls well outside the other data fields. This blueschist sample could indicate relative enrichment in alkalis and silica either prior to metamorphism or during metamorphic segregation.

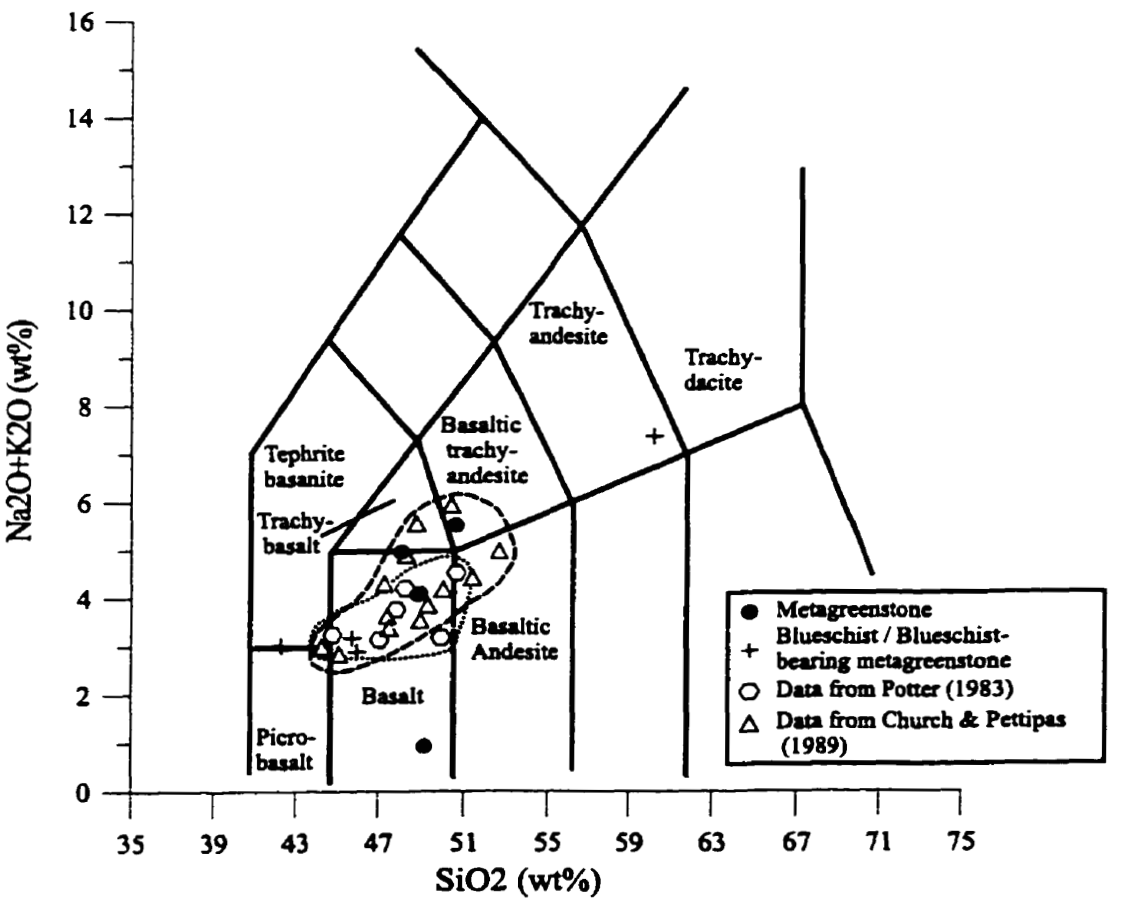

Figure 4-1. Total alkalis vs. silica plot for selected study rocks. The basaltic nature of these rocks is evident.

Pearce and Cann (1973) and Floyd and Winchester (1975) argue that certain trace (e.g. Ti, P, V, Zr Nb, Y) and compatible elements (e.g. Cr and Ni) are useful as discriminants for determination of initial tectonic settings of both fresh and altered basalts. These elements are relatively immobile during metasomatism and low-grade metamorphism. According to the scheme of Pearce and Cann (1973), the Y/Nb ratio is evaluated first to determine the petrologic character of the rocks (i.e. alkalic vs. tholeiitic). In their study, Pearce and Cann (1973) recognized that rocks classified by traditional methods (e.g. where Na_2O+K_2O/SiO_2 is high or where normative olivine is calculated) as alkalic had a greater concentration of Nb with respect to Y. The Y/Nb relationship appears to decrease with increasing alkalic character. Figure 4-2 is a plot of Y/Nb for the rocks in this study. Analyses from the Bridge River blueschist area appear to have less of an alkalic character and more of a tholeiitic character than do the rocks analyzed by Potter (1983).

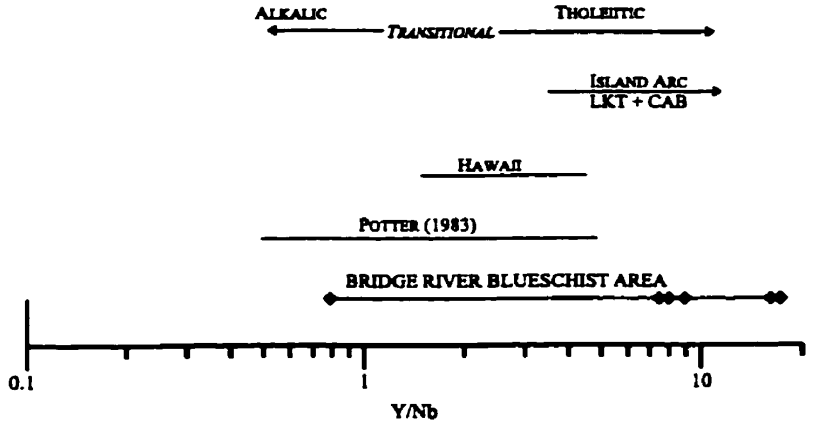

Figure 4-2. Immobile trace element discriminants for basaltic rocks (after Pearce and Cann, 1973). Additional data from Potter (1983).

Plint and Gordon (1997) use a plot of Y vs. Nb, based on the fields of Pearce and Cann (1973), to determine the alkalic nature of greenstones from the Slide Mountain Terrane. Figure 4-3 is a plot of Y vs. Nb for the rocks of this study. All but one of the sampies analyzed falls into the subalkalic field. These results are similar to those of Potter

(1983; 1986). Both Figure 4-2 and Figure 4-3 suggest that the protoliths for the Bridge River greenstones and blueschists were probably transitional between ocean floor tholeiites and alkalic basalts. This data is in agreement with the conclusion reached by Potter (1983; 1986) for the other metavolcanic rocks in the Bridge River area.

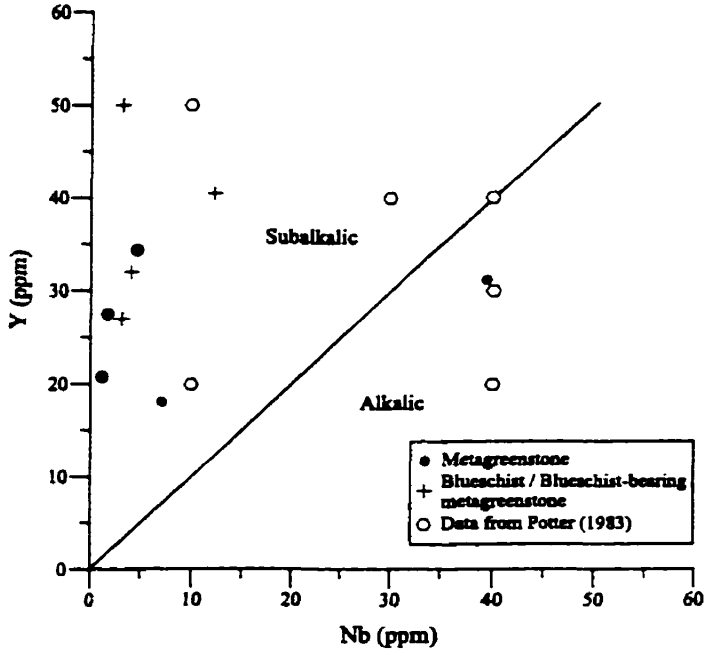

Figure 4-3. Immobile trace element discriminant diagram after Plint and Gordon (1997) Data indicates a mainly subalkalic character to rocks from the Bridge River area.

Pearce and Cann (1973) also suggest a Ti-Zr-Y discriminant plot to determine the original tectonic setting for the rocks. The importance in using these elements lies in their relative insensitivity to secondary processes (Cann, 1970). The analyses from this study fall primarily within 'within-plate basalt' and 'low potassium basalt' fields (Figure 4-4). One sample, a blueschist, plots within the calc-alkaline basalt field. The data would suggest some sort of an island arc to within plate setting for these rocks. Some samples plot outside of the compositional range defined by Pearce and Cann (1973). None, however, plot in the

range of data given by Potter (1983). This lack of correlation may be a function of the limited sample size in both data sets.

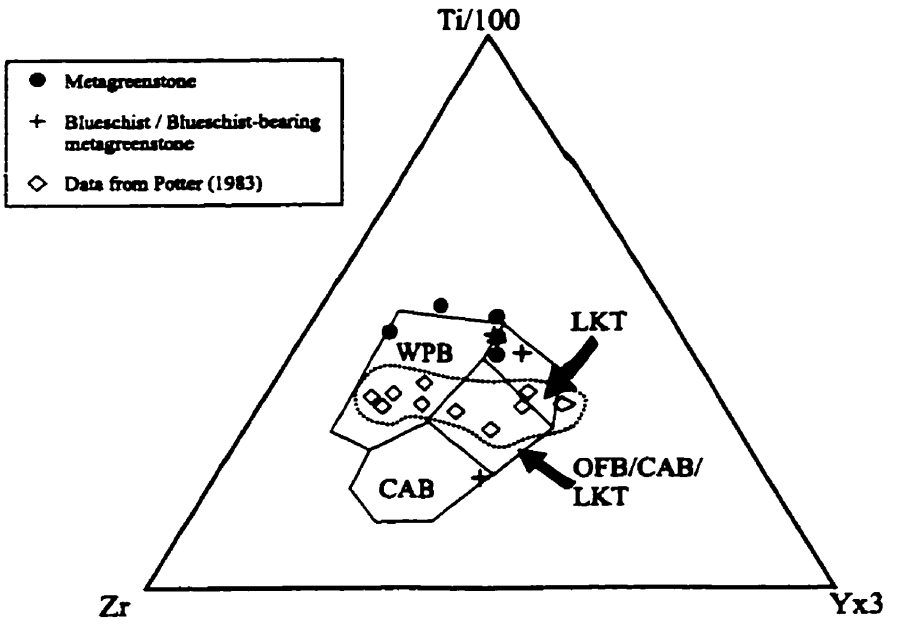

Figure 4-4. Immobile trace element tectonic discriminant diagram for basaltic rocks (after Pearce and Cann, 1973). LKT= low-potassium tholeiite; WPB= within-plate basalt; CAB= calc-alkaline basalt; IAB= island-arc basalt; OFB= ocean-floor basalt; OIB= oceanic island basalt.

Pearce (1975) found that employing a plot of Ti vs. Cr, two elements not greatly affected by alteration, was useful in differentiating between ocean-floor and island-arc basalts. The same plot is used here (Figure 4-5). This plot indicates that the Bridge River rocks have an ocean-floor affinity.

Pearce and Norry (1979) suggest using a Zr/Y vs. Zr plot to distinguish between within-plate, island-arc and ocean-floor basalts. Figure 4-6 shows the Bridge River data plotted on a Zr/Y vs. Zr diagram. Again, a fair degree of variability is observed in the data. Most samples plot within or near the ocean-floor basalt field while some data points plot

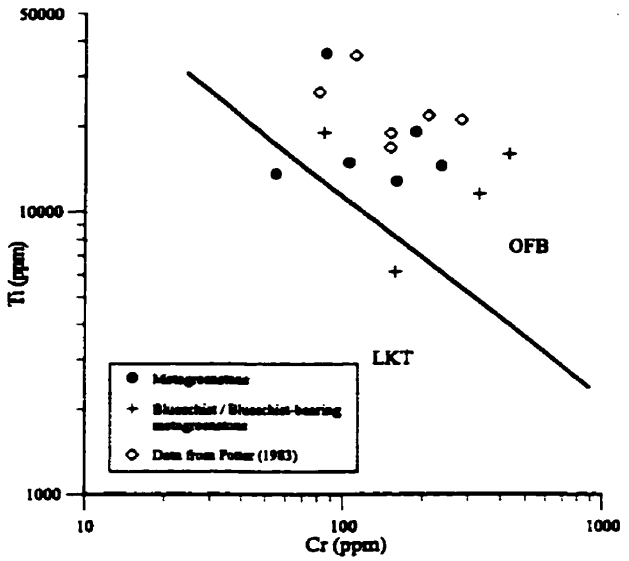

Figure 4-5. Samples from the Bridge River area. The plot suggests an ocean-floor character to the Bridge River rocks.

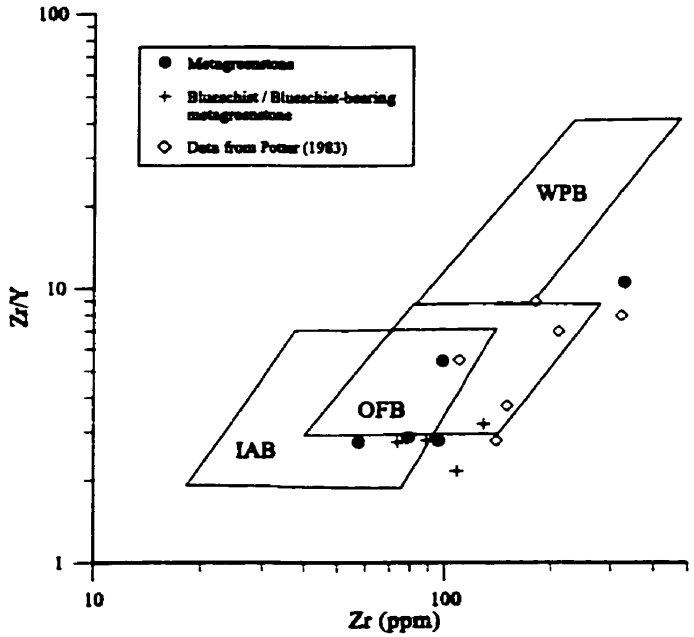

Figure 4-6. Samples from the Bridge River area plotted on a Zr/Y vs. Zr diagram (after Pearce and Norry, 1979). Most samples plot within or near the ocean-floor basalt field.

within the island-arc basalt field while others fall outside the fields defined by Pearce and Norry (1979).

The data presented above for rocks of the Bridge River area suggest that the Bridge River greenstones have a geochemical signature intermediate between that of "typical" spreading ridge generated ocean-floor tholeiites and the more alkalic, ocean–island type basalts. Potter (1983; 1986) indicates that this geochemical signature is consistent with a back-arc basin setting. The data are, however, somewhat ambiguous when one takes into account the limited sample size and the fact that some data points plot outside the compositional fields on the various discriminant diagrams. Field relationships such as the presence of pillowed basalts and the variolitic textures seen in thin section point towards a submarine and therefore possibly oceanic setting for these rocks.

5. MINERALOGY

5.1 INTRODUCTION

5.1.1 Petrography

Petrographic analysis of the Bridge River blueschists and associated rocks was undertaken in order to: 1) define peak metamorphic assemblages; 2) understand textural relationships among the minerals; and 3) choose suitable samples for later electron microprobe analyses. In all, approximately 115 thin sections were examined with the petrographic microscope. Mineral identification was commonly difficult due to the fine-grained nature of these rocks (grain diameters generally less than 20 μm). For this reason, mineral identification was augmented by X-ray diffraction analysis.

X-ray diffraction analyses were performed using the SCINTAG XDS2000 X-Ray Diffractometer housed at the University of Calgary. Radiation was produced using a Cu X-ray tube operating with a filament current of approximately 3.13 amps and a maximum tube power of approximately 1.80 kW. Data were collected in the range from 4.0° to 74.0° 2-theta with a step size of 0.05° and a dwell time of 2.0 seconds. Fifty-five samples were examined by this technique

One sample was also analyzed using a Microbeam X-ray Diffractometer housed at the Department of Mineralogy, Royal Ontario Museum. Analyses were performed by M.E. Back and F.J. Wicks. This technique is extremely useful because it allows for the non-destructive, *in situ* identification of minerals. With this technique a 5 to 100 μm diameter X-ray beam is used in a specially designed camera or diffractometer. Samples can be small and lie entirely within the beam during irradiation or may be much larger so that only a selected part of the sample is irradiated. Microbeam X-ray Diffractometry is ideal for the identification of fine-grained mineral species because the fine-grain size and random to semi-random distribution of orientations produce random to semi-random X-ray diffraction

patterns (Wicks et al., 1995). This technique was used to confirm the identity of fine-grained carbonate minerals.

Petrographic analysis of the Bridge River blueschists and related rocks indicates the existence of three distinctive assemblages. The blueschists in the Tyaughton Creek – Carpenter Lake area typically have an assemblage of Na-amphibole and Lws with various combinations of Stp, Jd, Qtz, carbonate and Ep (all abbreviations after Kretz, 1983). Blueschists from the North Cinnabar Creek area have a peak metamorphic assemblage of Na-amphibole with Ep, Ms with or without Lws or Grt. The third assemblage is found in the greenstones and consists of Chl, Qtz, and Ms with minor Stp. Relict igneous plagioclases and pyroxenes can be found in all areas.. Accessory and vein phases are also present and will be discussed later in this chapter. Representative assemblages for the Bridge River samples are presented in Table 5-1.

5.1.2 Mineral Chemistry

Mineral analyses were obtained using the 9-channel wavelength dispersive ARL-SEMQ electron microprobe at the Department of Geology and Geophysics, University of Calgary. Nine elements were analyzed simultaneously using operating conditions described by Nicholls and Stout (1988). Operating conditions for wavelength dispersive analyses were: accelerating voltage 15kV; beam current 0.15 μA; spot size of 1μm with a counting time of 20 seconds for each analyzed spot. Concentrations were corrected for matrix effects using the methods outlined by Bence and Albee (1968).

Mineral standards were chosen to be as close in composition as possible to the mineral being analyzed or to have a high concentration of the analyzed element (see Appendix 1). The concentration of the element of interest in the chosen standard always exceeded five weight percent and was higher than the unknown.

Table 5-1. Representative mineral summary of the Bridge River samples

	Act	Ab	Arg	Ap	Cpx	Car	Chl	Ep	Grt	Gln	Jd	Lws	Lx	Ms	Opq	Pheno	Pl	Pmp	Qtz	Rt	Stp	Ttn
88-JIG-39-1					x		x	x	x	x				x	x				x			
TL-88-16	x							x		x		x		x							x	x
92-GBR-1							x	x		x				x					x			
92-GBR-2		x						x		x	x	x				x			x		x	
92-GBR-38		x								x		x	x		x					x	x	x
92-GBR-40																			x		x	
92-GBR-43										x		x					x		x		x	
96-DJH-1-2								x		x	x	x	x								x	
96-DJH-3-11		x		x			x			x		x		x		x			x		x	
96-DJH-3-2				x		x				x		x	x		x				x		x	
97-DJH-003-3		x				x	x			x	x	x					x				x	
97-DJH-015-1		x				x	x								x				x	x	x	
97-DJH-018-1						x	x			x		x		x					x			x
97-DJH-018-2						Ank	x			x		x			x				x			
97-DJH-027-3		x					x	x											x			
97-DJH-035-1		x				x	x			x	x							x				x
97-DJH-038-3					x		x			x		x						x				
97-DJH-050-3						x	x			x		x							x			
97-DJH-051-3										x		x		x					x		x	
97-DJH-057-1						x		x		x		x	x	x		x			x		x	
97-DJH-062-4a	x	x				x	x			x		x		x					x			x
97-DJH-110-1	x									x		x										x
97-DJH-125-3		x			x	x	x											x	x			
97-DJH-HC-1	x	x								x		x							x			x
97-DJH-TC-2							x			x	x	x		x			x		x		x	

Note: For sample locations please see Figures 3-1 and 3-2; Abbreviations after Kretz, 1983; Lx = Leuxocene; Pheno = unidentifiable relict igneous phenocrysts; Opq = opaque mineral

5.2 MINERALOGY AND TEXTURES

5.2.1 Amphibole

Sodic amphiboles were the most easily identifiable mineral in the Bridge River rocks because of their distinctive colour. They occur as: 1) vein fillings; 2) overgrowths on relict phenocrysts; 3) distinct, foliation forming, subidioblastic to idioblastic crystals in texturally reconstituted rocks; 4) a 'mesh' of fine-grained crystals in thin (<1 cm thick) deformed argillaceous and/or tuffaceous layers within the chert unit and; 5) discrete foliae within the greenstones. See Figures 5-1 to 5-6.

Sodic amphibole is pleochroic from blue to lavender blue to colourless in thin section. Colour zoning is prevalent in several samples with cores that are commonly lighter coloured than rims. The relation of colour zoning to chemical zoning in the minerals will be discussed later in this chapter. Type 3 sodic amphiboles (see above) commonly have very similar optical orientation. The other sodic amphiboles typically have a more random distribution to their orientations. In the case of Type 2 sodic amphiboles, mineral orientation is related to that of the phenocryst. Many amphiboles display undulatory extinction, a likely result of deformation. Generally, the amphiboles are inclusion-free; however, they locally contain a fine-grained opaque mineral (pyrite).

Generally, sodic amphibole contacts with other mineral grains are sharp and regular. Some contacts, however, can be found in apparent reaction-relationship with stilpnomelane, chlorite, calcite, calcic amphiboles and relict pyroxene phenocrysts. Sodic amphibole can be found interfingered with stilpnomelane; also stilpnomelane occurs along cleavages. Varying degrees of sodic amphibole replacement of calcic amphibole are seen in several samples from both the Carpenter Lake and North Cinnabar Creek areas. This may suggest a blueschist overprint on a greenschist assemblage.

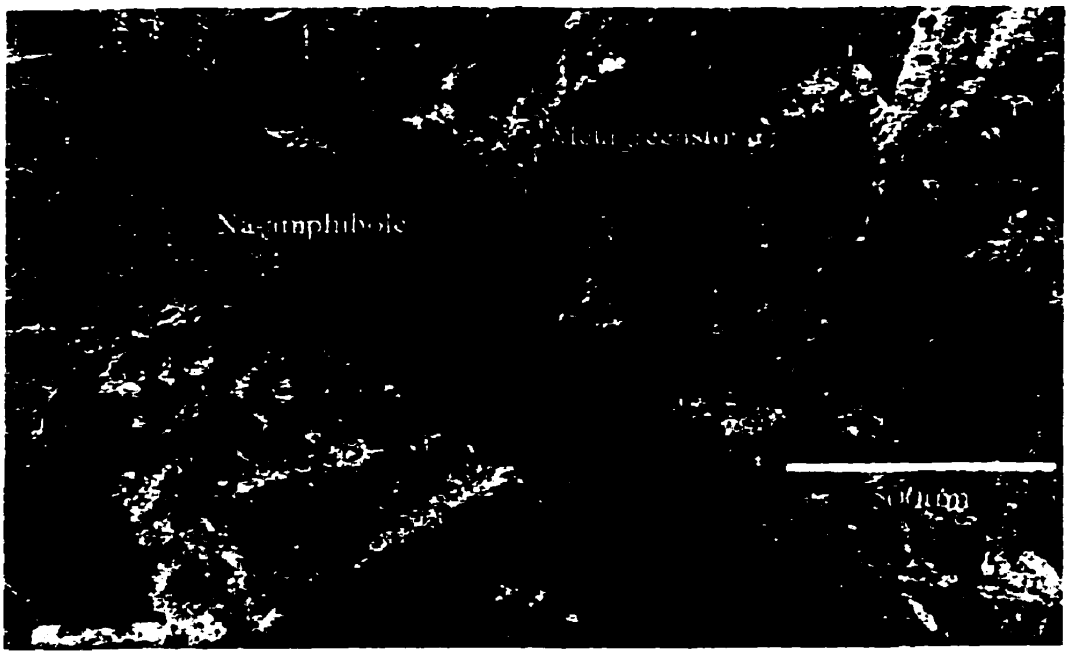

Figure 5-1. Fine-grained vein-filling sodic amphibole cutting metabasalt (Sample 97-DJH-004-6)

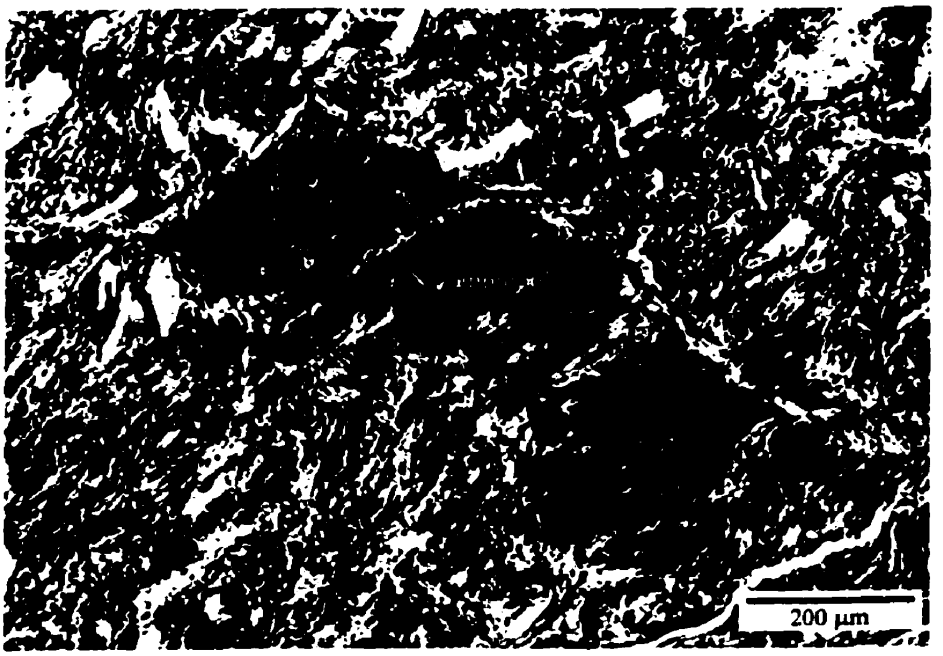

Figure 5-2. Na-amphibole pseudomorphs after relict igneous phenocryst (Sample 92-GBR-22)

Figure 5-3. Sub-idioblastic sodic amphibole with epidote and sphene (Sample 88-JIG-39-1)

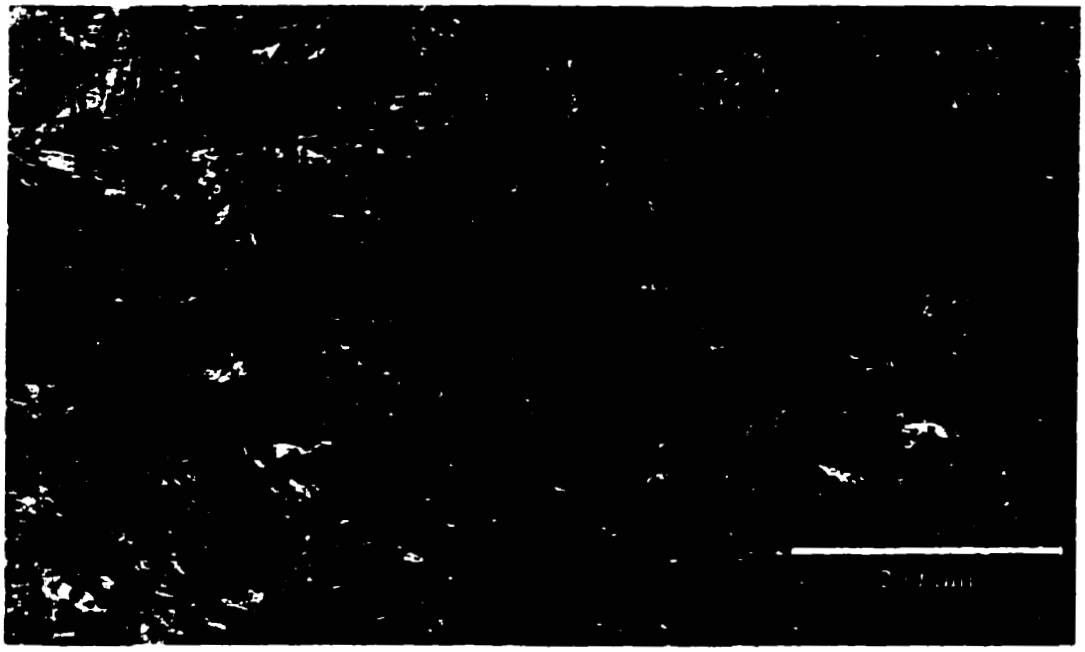

Figure 5-4. Mesh of randomly oriented acicular sodic amphiboles (Sample 97-DJH-062-4)

Figure 5-5. Fine-grained mat of groundmass forming Na-amphibole (Sample 97-DJH-018-3)

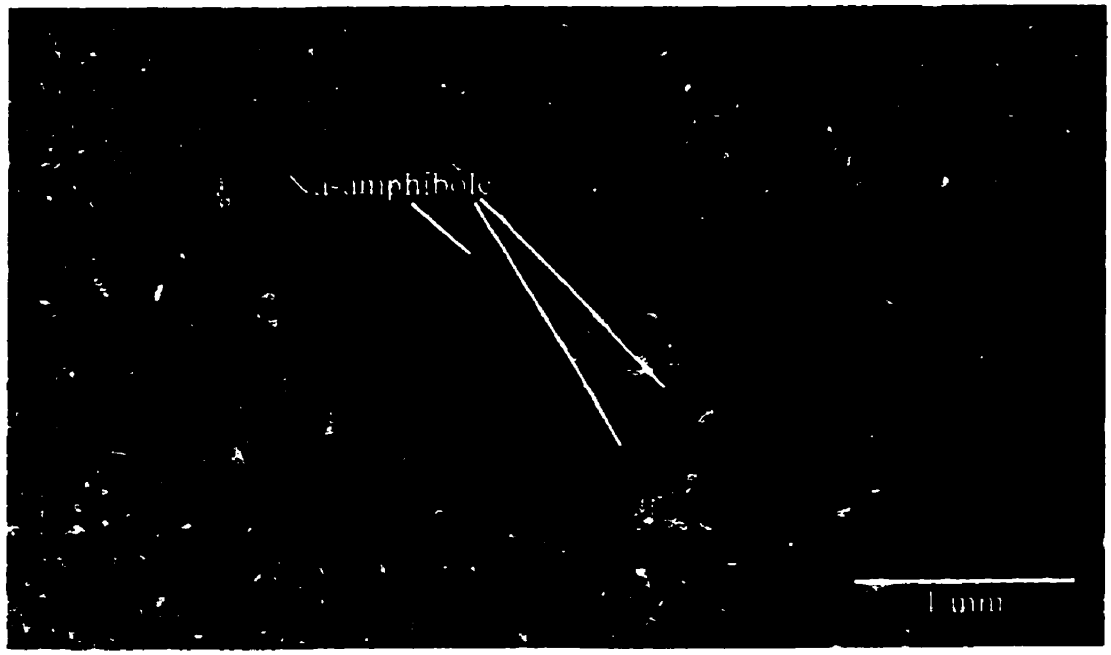

Figure 5-6. Discrete Na-amphiboles in greenstone (Sample 97-DJH-B2)

Representative electron microprobe analyses of amphiboles are presented in Table 5-2 and Table 5-3. Amphibole structural formulae were calculated using the program AMPHIBOL of Richard and Clarke (1990). The program uses the charge balance method described by Robinson et al., (1981) to estimate the ferric iron content. The method used here excludes Na from the A-site and forces it into the B-site with the total number of ions calculated based on 15 cations excluding potassium, and 23 oxygens. Robinson et al. (1981) indicate that this method is most suitable for sodic amphibole analyses since these amphiboles have considerable Na-M(4) site occupancy.

As shown in Table 5-2 and Table 5-3, amphibole compositions range from sodic to sodic-calcic to calcic (see also Figure 5-7) with the majority having sodic compositions. The compositional range does not appear to be related to metamorphic grade since all compositions can be found in both lawsonite- and epidote-bearing assemblages.

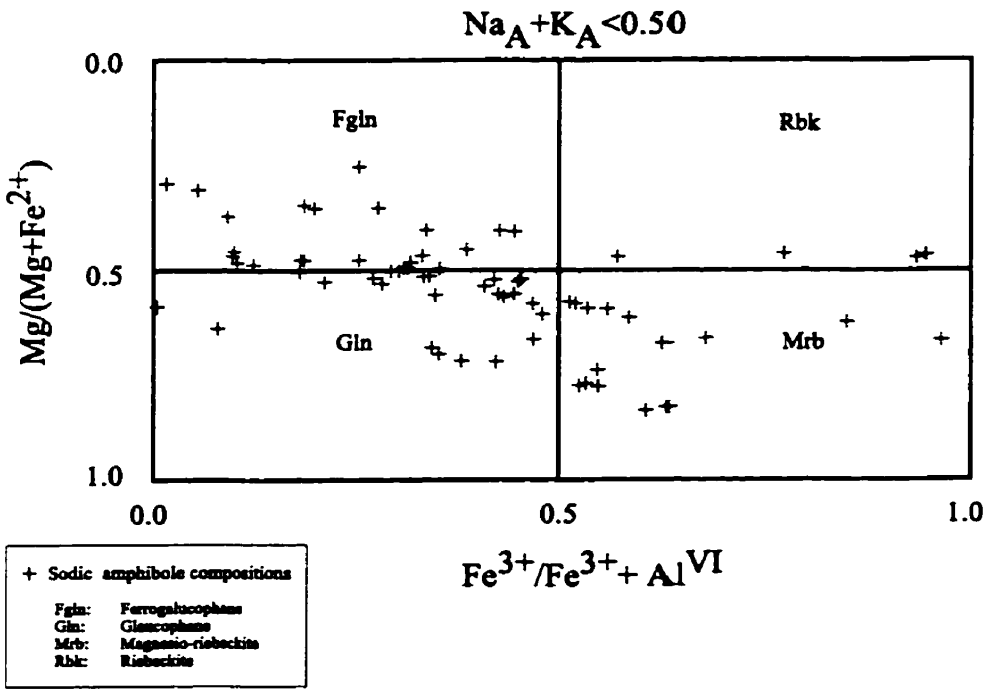

Figure 5-7. Compositional range of sodic amphiboles from the Bridge River blueschists plotted on a modified Miyashiro-type diagram.

Table 5-2. Representative electron microprobe analyses of amphiboles from the Carpenter Lake and North Cinnabar Creek areas.

	97-DJH-018-2	97-DJH-018-2 vein	97-DJH-036-1	97-DJH-036-1	97-DJH-007-1 vein	97-DJH-TC-2	97-DJH-110-1	TL-88-16	92-GBR-43	92-GBR-33	92-GBR-33	97-DJH-031-2	TL-88-16	92-GBR-33	97-DJH-031-2
	Gln	Gln	Fgln	Fgln	Fgln	Gln	Gln	Gln	Fgln	Gln	Mrb	Win	Win	Bar	Act
SiO_2	57.88	57.82	54.28	57.89	57.82	57.50	56.84	55.55	54.15	53.70	47.36	52.49	53.09	50.25	54.01
TiO_2	0.20	0.17	na	0.27	0.09	<dl	na	0.00	0.00	0.00	<dl	0.07	na	<dl	na
Al_2O_3	8.22	8.73	5.78	7.60	5.44	5.98	4.77	7.11	6.80	7.35	2.93	5.86	6.84	0.55	1.11
FeO	12.54	12.44	20.79	18.02	19.84	19.07	19.58	17.98	21.44	16.79	17.73	17.51	17.97	16.28	16.16
MnO	0.12	0.12	0.20	0.11	0.11	0.01	0.25	0.19	0.34	0.13	0.25	0.32	0.12	0.48	0.51
MgO	11.62	10.92	7.47	7.72	8.30	8.60	9.03	8.44	5.92	8.76	6.43	10.29	9.15	8.37	14.27
CaO	2.02	1.59	1.27	1.19	1.39	1.03	2.34	1.33	0.92	2.59	12.70	5.02	4.96	17.20	9.89
Na_2O	5.59	5.98	6.44	6.46	6.15	6.26	5.52	6.04	6.53	5.68	5.98	4.11	4.43	3.62	1.12
K_2O	na	na	0.02	0.00	0.00	0.02	<dl	<dl	0.07	0.04	<dl	<dl	<dl	<dl	<dl
F	0.07	0.09	<dl	<dl	0.14	0.12	0.07	<dl	0.14	<dl	<dl	<dl	0.40	<dl	<dl
Total	98.26	97.86	96.29	99.27	99.28	98.59	98.43	96.67	96.31	95.04	93.40	95.74	96.96	96.75	97.08
Structural formula on the basis of 15 cations, 23 Oxygen															
Si	7.99	8.01	7.86	8.08	8.12	8.09	8.07	7.95	7.90	7.79	7.06	7.64	7.67	7.33	7.84
Al	0.01	0.00	0.14	0.00	0.00	0.00	0.00	0.05	0.10	0.21	0.52	0.36	0.33	0.10	0.16
ΣT	8.00	8.01	8.00	8.08	8.12	8.09	8.07	8.00	8.00	8.00	8.00	8.00	8.00	8.00	8.00
Al	1.33	1.43	0.84	1.25	0.90	0.99	0.80	1.15	1.07	1.05	0.00	0.65	0.84	0.00	0.03
Fe^{3+}	0.13	0.13	1.10	0.29	0.51	0.53	0.59	0.58	0.87	0.75	1.78	0.86	0.74	1.41	0.44
Ti	0.02	0.02	0.00	0.03	0.01	0.00	0.00	0.00	0.00	0.00	0.00	0.01	0.00	0.00	0.00
Mg	2.39	2.25	1.61	1.61	1.74	1.80	1.91	1.80	1.29	1.90	1.43	2.23	1.97	1.82	3.09
Fe^{2+}	1.13	1.17	1.41	1.81	1.82	1.68	1.71	1.47	1.74	1.29	0.00	1.26	1.44	0.00	1.44
Mn	0.00	0.00	0.03	0.01	0.01	0.00	0.00	0.00	0.03	0.02	0.03	0.00	0.02	0.06	0.00
Ca	0.00	0.00	0.00	0.00	0.01	0.00	0.00	0.00	0.00	0.00	1.76	0.00	0.01	1.71	0.00
ΣC	5.00	5.00	5.00	5.00	5.00	5.00	5.00	5.00	5.00	5.00	5.00	5.00	5.00	5.00	5.00
Fe^{2+}	0.19	0.14	0.00	0.00	0.00	0.04	0.03	0.10	0.00	0.00	0.00	0.02	0.00	0.00	0.08
Mn	0.01	0.01	0.00	0.00	0.00	0.00	0.03	0.02	0.01	0.00	0.00	0.04	0.00	0.00	0.06
Ca	0.30	0.24	0.19	0.18	0.20	0.16	0.36	0.20	0.14	0.40	0.27	0.78	0.76	0.98	1.54
Na	1.50	1.61	1.81	1.75	1.68	1.71	1.52	1.68	1.85	1.60	1.73	1.16	1.24	1.02	0.32
ΣB	2.00	1.99	2.00	1.92	1.88	1.91	1.94	2.00	2.00	2.00	2.00	2.00	2.00	2.00	2.00
Na	0.00	0.00	0.00	0.00	0.00	0.00	0.00	0.00	0.00	0.00	0.00	0.00	0.00	0.00	0.00
K	0.00	0.00	0.00	0.00	0.00	0.00	0.01	0.00	0.01	0.01	0.00	0.00	0.00	0.00	0.00
ΣA	0.00	0.00	0.00	0.00	0.00	0.00	0.01	0.00	0.01	0.01	0.00	0.00	0.00	0.00	0.00
Σ cations	15.00	15.00	15.00	15.00	15.00	15.00	15.01	15.00	15.01	15.01	15.00	15.00	15.00	15.00	15.00
Σ oxygens	23.00	23.00	23.00	23.00	23.00	23.00	23.00	23.00	23.00	23.00	22.56	23.00	23.00	22.86	23.00

Note: Abbreviations after Kretz (1983) except for Cro = Crossite; Fgln = Ferroglaucophane; Win = Winchite;
na = not analyzed; <dl = below detection limit

The range in sodic amphibole compositions is presented in Figure 5-7 in a chemical variation diagram for alkali-amphiboles modified after Miyashiro (1957) using the nomenclature of Leake et al., (1997). The majority of sodic amphibole compositions lie within the glaucophane and ferro-glaucophane compositional fields. This range of compositions is similar to those given by Ghent et al (1993) for blueschists at Pinchi Lake, B.C. The Pinchi Lake amphiboles are richer in glaucophane than the Bridge River amphiboles and do not appear to cover the entire spectrum of sodic amphibole compositions, as do the amphiboles from this study.

Table 5-3 and Figures 5-8 and 5-9 show the core-rim compositional variation of selected amphiboles. Core and rim compositions could not be obtained for all amphiboles due to their fine-grained nature. Although some compositions show cores enriched in Ca and depleted in Na and Mg relative to rims the opposite is more commonly the case. This observation may be due to sampling bias since core-rim compositions could only be readily obtained on the larger crystals.

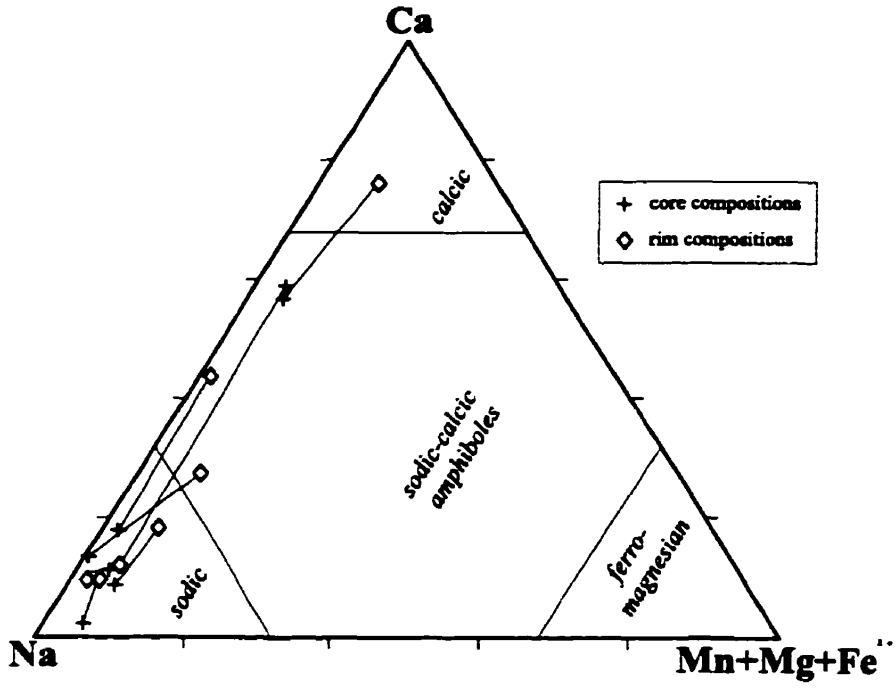

Figure 5-8. Core-rim compositional variation of selected amphiboles from the Bridge River area.

In the sodic amphibole range, colour zoning in the minerals can be correlated with compositional zoning. In Figure 5-8, it is apparent that compositional variation from core to rim is not regular. This compositional heterogeneity is likely not a function of changing physical conditions during mineral growth. It is more likely that the variations are due to complex compositional variation in the reactants of the amphibole-forming reaction. As stated earlier, textural relationships indicate that the sodic amphiboles are commonly found pesudomorphing relict clinopyroxenes. If the clinopyroxenes were complexly zoned to begin with, it could be possible to account for the observed zoning patterns in the amphiboles. Amphibole-forming reactions will be discussed in a later section.

Table 5-3. Representative electron microprobe core and rim compositions of amphiboles from the Carpenter Lake and North Cinnabar Creek areas.

	JIG-88-39-1 core Gln	JIG-88-39-1 rim Gln	92-GBR-1 core Fgln	92-GBR-1 rim Fgln	97-DJH-110-1 core Win	97-DJH-110-1 rim Mrb	97-DJH-110-1 core Mrb	97-DJH-110-1 rim Mrb	TL-88-16 core Mrb	TL-88-16 rim Win	97-DJH-031-2 core Act	97-DJH-031-2 rim Win
SiO_2	56.61	56.05	57.66	57.42	53.62	54.28	54.15	53.66	52.19	53.34	53.11	53.67
TiO_2	<dl	0.04	0.72	0.28	na	na	na	na	na	na	<dl	0.02
Al_2O_3	9.24	8.80	10.32	10.98	2.09	5.00	2.09	4.49	5.49	3.21	1.26	2.88
FeO	14.28	14.81	18.93	19.69	16.24	20.11	19.64	18.80	19.36	18.22	16.12	16.95
MnO	0.05	0.07	0.15	0.19	0.41	0.21	0.24	0.24	0.24	0.37	0.48	0.44
MgO	10.97	11.00	5.84	4.63	14.26	8.82	9.17	10.44	9.30	11.58	14.49	12.14
CaO	1.37	1.80	0.06	0.04	7.70	1.66	2.28	3.61	2.37	5.73	9.91	7.36
Na_2O	6.45	6.21	7.07	7.00	2.64	5.88	5.57	4.57	5.58	3.88	1.10	2.69
K_2O	<dl	0.02	0.06	0.06	0.04	0.00	0.04	0.04	0.03	0.06	<dl	<dl
F	0.13	0.11	<dl	<dl	0.06	0.05	0.06	0.10	<dl	<dl	0.09	<dl
Total	99.10	98.91	100.82	100.30	97.06	96.03	93.24	95.95	94.57	96.44	96.56	96.21
Structural formula on the basis of 15 cations, 23 Oxygen												
Si	7.73	7.69	7.95	8.00	7.69	7.87	8.11	7.80	7.65	7.72	7.75	7.83
Al	0.27	0.31	0.05	0.01	0.31	0.13	0.00	0.20	0.35	0.28	0.22	0.17
ΣT	8.00	8.00	8.00	8.00	8.00	8.00	8.11	8.00	8.00	8.00	8.00	8.00
Al	1.22	1.12	1.63	1.80	0.04	0.72	0.37	0.57	0.60	0.27	0.00	0.33
Fe^{3+}	0.76	0.83	0.15	0.03	1.00	1.06	1.02	0.91	1.32	1.08	0.56	0.60
Ti	-	0.00	0.08	0.03	-	-	-	-	-	-	-	0.00
Mg	2.23	2.25	1.20	0.96	3.05	1.91	2.05	2.26	2.03	2.50	3.15	2.64
Fe^{2+}	0.79	0.80	1.94	2.19	0.91	1.31	1.44	1.26	1.04	1.12	1.29	1.43
Mn	0.00	0.00	0.00	0.00	0.00	0.00	0.03	0.00	0.00	0.02	0.00	0.00
Ca	0.00	0.00	0.00	0.00	0.00	0.00	0.09	0.00	0.00	0.00	0.00	0.00
ΣC	5.00	5.00	5.00	5.00	5.00	5.00	5.00	5.00	5.00	5.00	5.00	5.00
Fe^{2+}	0.09	0.07	0.08	0.08	0.03	0.06	0.00	0.12	0.01	0.00	0.08	0.03
Mn	0.01	0.01	0.02	0.02	0.05	0.03	0.00	0.03	0.03	0.02	0.06	0.05
Ca	0.20	0.27	0.01	0.01	1.18	0.26	0.27	0.56	0.37	0.89	1.55	1.15
Na	1.71	1.65	1.89	1.89	0.73	1.65	1.62	1.29	1.59	1.09	0.31	0.76
ΣB	2.00	2.00	2.00	2.00	2.00	2.00	1.89	2.00	2.00	2.00	2.00	2.00
Ca	0.00	0.00	0.00	0.00	0.00	0.00	0.00	0.00	0.00	0.00	0.00	0.00
Na	0.00	0.00	0.00	0.00	0.00	0.00	0.00	0.00	0.00	0.00	0.00	0.00
K	0.00	0.00	0.01	0.01	0.01	0.00	0.01	0.01	0.01	0.01	0.00	0.00
ΣA	0.00	0.00	0.01	0.01	0.01	0.00	0.01	0.01	0.01	0.01	0.00	0.00
Σ cations	15.00	15.00	15.01	15.01	15.01	15.00	15.01	15.01	15.01	15.01	15.00	15.00
Σ oxygen	23.00	23.00	23.00	23.00	23.00	23.00	23.00	23.00	23.00	23.00	23.00	23.00

Note: Abbreviations after Kretz (1983) except for Cro = Crossite; Fgln = Ferroglaucophane; Win = Winchite; na = not analyzed; <dl = below detection limit

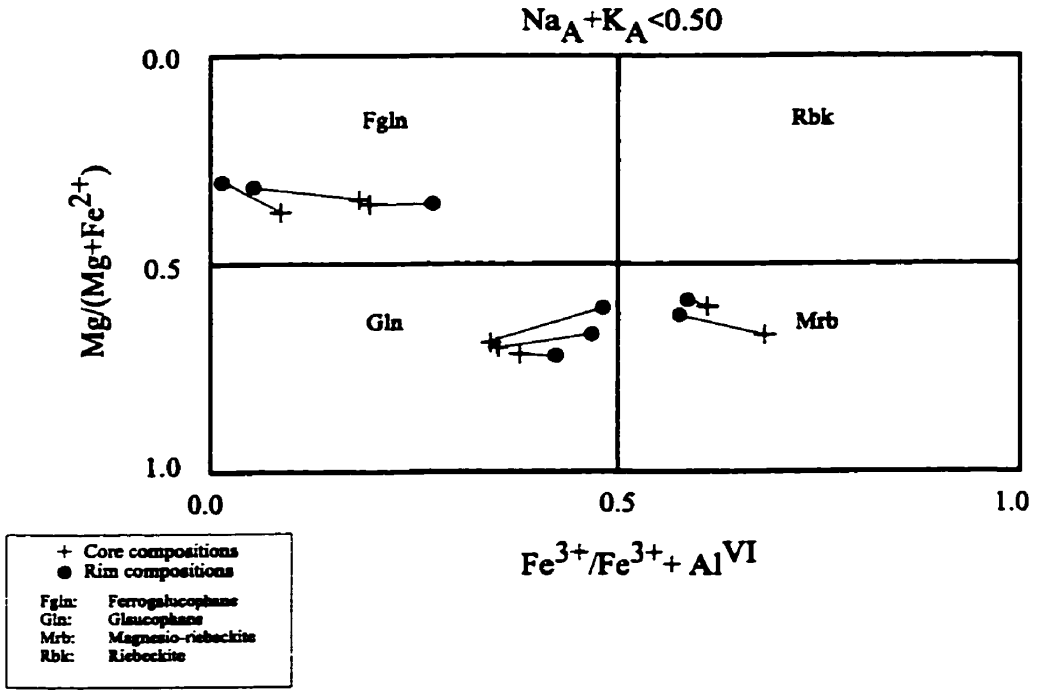

Figure 5-9. Core-rim compositional variation diagram for sodic amphiboles from the Bridge River area plotted on a modified Miyashiro-type diagram

Ca-substitution for Na in amphiboles is presented in Figure 5-10. This plot indicates that since the data plot on or below the 1:1 Ca ↔ Na substitution line there is a range from incomplete to complete filling of the B-site by Ca and Na. Ca ion content in sodic amphiboles range from 0.0 to 0.6 atoms with the majority plotting well above 0.5 Ca atoms. Sodic-calcic and calcic amphiboles range from 0.76 to 1.55 B-site occupancy of Ca. The calcic amphiboles are at the maximum end of this range.

Sodic-amphiboles in assemblages with lawsonite range from 0.13 to 0.6 Ca atoms whereas sodic-amphiboles in epidote assemblages range from 0.00 to 0.39 Ca atoms. For sodic-calcic amphiboles, Ca ion substitution is in the range of 0.76 to 0.98 Ca atoms for lawsonite assemblages and for epidote assemblages, the range is 0.75 to 1.15 atoms. Bradshaw (1978) suggests that large variability in Ca content in amphiboles may be related to local differences in bulk compositions. The Bridge River amphiboles may demonstrate a

relatively significant range in overall bulk chemistry however, there does not appear to be a significant bulk chemical difference between lawsonite-bearing assemblages and the higher-grade epidote-bearing assemblages (see Figure 5-10).

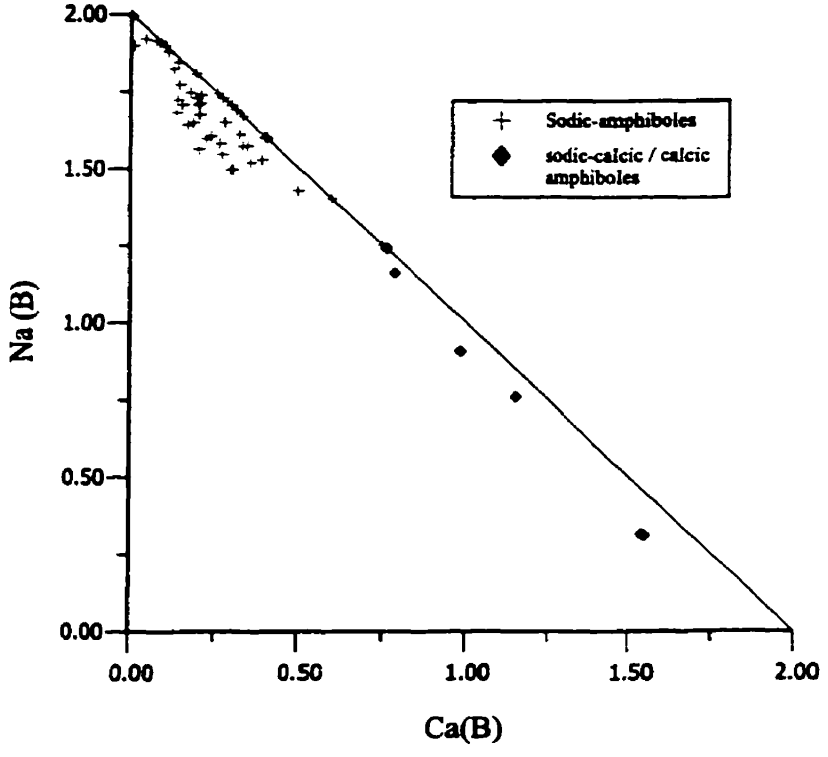

Figure 5-10. Na vs. Ca diagram showing Bridge River amphibole compositions

5.2.2 Lawsonite

Except for some epidote-bearing blueschist assemblages, lawsonite is present in all other samples. Commonly, lawsonite occurs as small (0.025 x 0.01 mm) euhedral, tabular crystals but they can range in size to larger (0.14 x 0.05 mm) subhedral crystals. Larger crystals often show obvious parting (see Figure 5-11). Typically inclusion-free, lawsonite is clear in thin section. Some lawsonite grains found in veins display an acicular habit (see Figure 5-12) with some growing inwards towards the centre of the vein from the margins.

This would suggest that in the veins $P_{fluid} = P_{total}$. Identification of these minerals was confirmed by XRD and electron microprobe analyses (see Table 5-4).

Table 5-4. Comparison of X-ray Diffraction data for acicular lawsonite with calculated pattern. vs = very strong peak intensity (>80); s = strong peak intensity (61-79). Calculated patterns from Borg and Smith (1969).

97-DJH-004-6		**Calculated Pattern**	
d(Å)	Intensity	*d*(Å)	Intensity
2.72	vs	2.721	84
2.63	vs	2.619	100
2.43	s	2.433	80
2.12	s	2.129	76
1.55	s	1.549	76

Lawsonite is commonly found in intimate association with sodic amphiboles and stilpnomelane, suggesting textural equilibrium. It can also be found in apparent equilibrium with white mica and quartz. Less frequently, it is found in textural equilibrium with epidote. Obvious disequilibrium textures are found where lawsonite appears to be replacing relict plagioclase phenocrysts. In these situations there appears to be a preferred alignment to the lawsonite. Ghent (1965) recognized similar features in blueschists from the Black Butte area of California. Lawsonite there shows a strong preferred orientation with the c-axes of lawsonite prisms nearly parallel to the trace of the (010) composition plane of the plagioclase. He suggests that the preferred orientation of the lawsonite indicate epitaxial overgrowth. In addition, Ghent et al. (1996) suggest that these features represent complete replacement of the pre-existing mineral which implies significant mass transfer. The concentration of lawsonite prisms in the core and lack at the margins may reflect original zoning of the feldspar from calcic cores to sodic rims (e.g. Ernst, 1965).

Figure 5-11. Lawsonite in glaucophane matrix. Note variable grain size and partings in lawsonite. (Sample 92-GBR-33)

Figure 5-12. Microphotograph of 'blueschist' vein in a greenstone. Vein consists of sodic amphibole, lawsonite and quartz. Note mat of acicular lawsonite crystals growing inwards from vein walls towards the centre of the vein (Sample 97-DJH-004-6)

Figure 5-13. Lawsonite prisms in relict feldspar phenocryst (Sample 97-DJH-057-1). Note alignment of lawsonite prism in core

Textural occurrence of lawsonite is similar to that of sodic amphiboles. Lawsonite can be found in veins associated with sodic amphiboles. Commonly these occur as small prismatic crystals, however, they may also occur as elongate, acicular crystals growing outwards from the vein margins. As mentioned previously, lawsonite can also be found replacing relict plagioclase feldspars. In well-foliated rocks, lawsonite can be found aligned approximately parallel to the foliation. Also, when found in crenulated rocks, lawsonite crystals are aligned in the crenulation. Commonly, these crystals display minor undulatory extinction that suggests they were deformed. When associated with 'mesh' textured sodic amphiboles, lawsonite occurs as unoriented prisms scattered throughout the sample. In greenstones with variable blueschist components, lawsonite occurs as single crystals within the greenstone host or as distinct lenses associated with sodic amphiboles. Lawsonite is not present in sodic-amphibole bearing cherts.

Representative electron microprobe analyses of lawsonite are presented in Table 5-5. Lawsonite analyses are generally close to end-member compositions. However, some analyses indicate that there are appreciable amounts of Fe_2O_3 present (0.2 – 3.7 wt. per cent). Ghent et al (1993) present data for lawsonites from Pinchi Lake eclogites that contain 0.3 to 0.8 wt. per cent Fe_2O_3. The maximum reported values obtained for Fe in lawsonites (3.2 wt. per cent Fe_2O_3) is presented by Maruyama and Liou (1988), which is closest to the values obtained in this study. The only other measurable impurity in the lawsonite analyses was MgO.

Figure 5-14 shows the range of compositional variability in the lawsonite analyses. Generally, the analyses are consistent from sample to sample and area to area. The only departures from ideal end-member composition occur where there are significant amounts of measured Fe. Multiple analyses of single lawsonite crystals indicate that no obvious chemical zoning was observed.

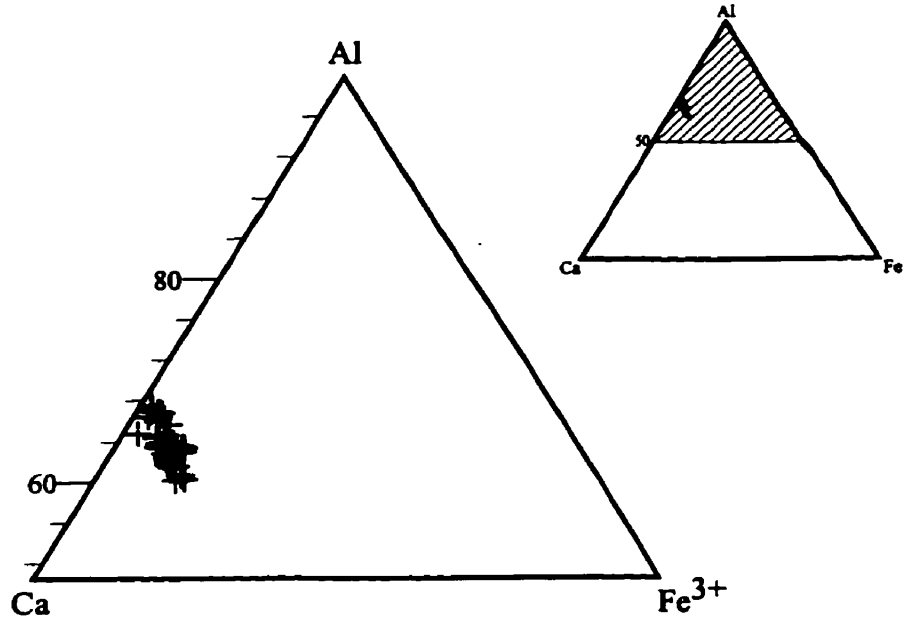

Figure 5-14. Plot of lawsonite analyses

Table 5-5. Representative electron microprobe analyses of lawsonite from the Carpenter Lake and North Cinnabar Creek areas

	97-DJH-004-6 Lws	97-DJH-018-2 Lws	97-DJH-034-6 Lws	97-DJH-TC-2 Lws	97-DJH-TC-2 Lws	97-DJH-034-1 Lws	97-DJH-110-1 Lws	97-DJH-110-1 Lws	92-GBR-1 Lws	92-GBR-43 Lws	TL-88-16 Lws
SiO_2	38.51	38.90	39.07	37.04	35.80	40.70	36.35	36.79	38.36	37.27	36.13
TiO_2	<dl	0.46	<dl	<dl	<dl	0.83	<dl	<dl	<dl	<dl	<dl
Al_2O_3	29.27	30.46	28.03	30.30	30.23	31.72	30.36	29.12	33.79	31.83	33.03
Fe_2O_3	3.02	0.44	3.71	2.29	2.67	3.40	1.81	2.89	0.24	0.40	0.92
MnO	0.06	0.00	0.01	0.01	0.02	0.00	0.00	0.00	0.00	0.02	0.00
MgO	0.25	0.04	0.19	0.09	0.69	0.18	0.01	0.01	0.10	0.02	0.00
CaO	16.95	17.37	16.33	16.68	16.19	16.72	16.98	16.79	17.06	16.65	16.67
Na_2O	0.00	0.00	0.02	0.00	0.00	0.00	0.00	0.00	0.00	0.00	0.00
K_2O	<dl	0.06	<dl	<dl	<dl	<dl	<dl	<dl	0.02	0.01	<dl
H_2O	12.04	12.11	12.79	13.59	14.31	6.54	14.43	14.45	10.32	13.49	13.14
TOTAL	100.10	99.84	100.16	100.01	100.04	100.12	99.94	100.05	99.89	99.82	99.89
Totals Based on 8 Oxygens, 4 OH											
Si	2.04	2.05	2.09	2.00	1.96	2.03	1.98	2.01	1.98	2.00	1.93
Ti	-	0.02	-	-	-	0.03	-	-	-	-	-
Al	1.83	1.89	1.77	1.93	1.95	1.86	1.95	1.88	2.05	2.01	2.08
Fe^{3+}	0.12	0.02	0.15	0.09	0.11	0.13	0.07	0.12	0.01	0.02	0.04
Mg	0.02	0.00	0.02	0.01	0.06	0.01	0.00	0.00	0.01	0.00	0.00
Ca	0.96	0.98	0.94	0.96	0.95	0.89	0.99	0.98	0.94	0.96	0.96
K	-	0.00	-	-	-	-	-	-	0.00	0.00	-
OH	4.00	4.00	4.00	4.00	4.00	4.00	4.00	4.00	4.00	4.00	4.00

Abbreviations: <dl = below detection limit

5.2.3 Epidote

Epidote is a much less abundant phase than lawsonite but its presence is significant. The assemblage glaucophane + epidote suggests higher temperature or lower P_{H_2O} than that of glaucophane + lawsonite (Evans, 1990). This suggests that the Bridge River blueschists consist of rocks of differing metamorphic grade.

Epidote in the area is found primarily in the blueschist facies rocks, however, it also occurs in the greenstones. In the blueschists, epidote occurs as idioblastic to subidioblastic crystals with maximum dimensions of 200 x 40 μm in size (see Figure 5-3). Epidote commonly displays a characteristic pleochroic scheme of α = colourless; β = greenish yellow; γ = yellowish green. No strong colour zoning was observed. In the greenstones, epidote occurs as much finer granular aggregates. Commonly their textural relationships are difficult to interpret. Epidote may appear in textural equilibrium with the other primary phases or as a replacement of relict phases.

Representative epidote analyses are presented in Table 5-6. Structural formulae were calculated on the basis of 12.5 oxygens. H_2O amounts were calculated using the program WATER described by Nicholls et al. (1977) which iteratively adds water to the analysis and corrects all oxides due to the corresponding change in the Bence-Albee factors. Fe was converted to Fe_2O_3 however sufficient Fe^{3+} was converted to Fe^{2+} and allotted to the X-site to allow the sum of cations in X to equal to 2.0. The result of this calculation was a decrease in the sum of Y to slightly below the ideal value of 3.0 cations. The amounts of Fe^{2+} and Mn substitution for Ca may be suspect. Deer et al (1992) indicate that replacement of Ca by Fe^{2+}, Mg and Mn rarely exceed 0.15 atom per formula unit. However, the data do fall within the limits of counting precision.

As mentioned above, no obvious colour zoning was detected during petrographic analyses of the epidotes. Multiple spot analyses of single grains confirm that only minor chemical zoning is present. Representative core-rim presented in Table 5-6 shows that

Table 5-6. Representative electron microprobe analyses of epidote

	97-DJH-031-2	97-DJH-031-2	92-GBR-43-1	92-GBR-43-2	92-GBR-43-2	TL-88-16	TL-88-16	88-JIG-39-1 core	88-JIG-39-1 rim	88-JIG-39-1
	Ep	Ep	Ep	Ep	Ep	Ep	Ep	Ep	Ep	Ep
SiO_2	36.56	37.59	36.75	37.05	37.50	37.05	36.50	37.70	38.13	36.75
TiO_2	<dl	<dl	0.03	<dl	0.04	<dl	0.10	0.05	0.03	0.08
Al_2O_3	25.56	25.77	25.45	25.27	24.63	24.74	24.11	24.41	24.53	25.46
FeO	13.08	12.38	11.54	12.44	14.93	12.44	14.93	14.11	13.87	14.95
MnO	0.42	0.11	0.40	0.41	0.35	0.40	0.35	0.18	0.25	0.40
MgO	<dl	<dl	<dl	<dl	<dl	<dl	<dl	<dl	<dl	<dl
CaO	22.20	22.80	22.48	22.34	22.15	22.34	22.15	22.59	22.54	22.08
Na_2O	<dl	<dl	<dl	<dl	<dl	<dl	<dl	<dl	<dl	<dl
K_2O	<dl	<dl	<dl	<dl	<dl	<dl	<dl	<dl	<dl	<dl
H_2O	1.84	1.17	2.05	2.85	0.33	2.85	1.61	1.00	0.00	0.20
Total	99.70	99.83	98.71	100.39	99.96	99.85	99.78	100.08	99.40	99.93
Structural formula on the basis of 12.5 O										
SiO_2	2.79	2.87	2.94	2.84	2.86	2.83	2.78	2.87	3.00	2.80
TiO_2	-	-	0.00	-	0.00	-	0.01	0.00	0.00	0.00
Al_2O_3	2.30	2.32	2.40	2.28	2.22	2.22	2.17	2.19	2.28	2.29
Fe_2O_3	0.81	0.77	0.75	0.78	0.93	0.77	0.93	0.90	0.89	0.93
MnO	0.03	0.01	0.03	0.03	0.02	0.03	0.02	0.01	0.02	0.03
CaO	1.81	1.86	1.93	1.83	1.81	1.83	1.81	1.84	1.90	1.80
Ca	1.81	1.86	1.93	1.83	1.81	1.83	1.81	1.84	1.90	1.80
Fe^{3+}	0.16	0.13	0.05	0.14	0.17	0.15	0.17	0.14	0.08	0.17
Mn^{3+}	0.03	0.01	0.03	0.03	0.02	0.03	0.02	0.01	0.02	0.03
ΣX	2.00	2.00	2.00	2.00	2.00	2.00	2.00	2.00	2.00	2.00
Al	2.30	2.32	2.40	2.28	2.22	2.22	2.17	2.19	2.28	2.29
Fe^{3+}	0.64	0.62	0.70	0.62	0.74	0.61	0.74	0.74	0.80	0.74
Ti	-	-	0.00	-	0.00	-	0.01	0.00	0.00	0.00
ΣY	2.93	2.94	3.10	2.90	2.96	2.83	2.91	2.93	3.08	3.03
Si	2.79	2.87	2.94	2.84	2.86	2.83	2.78	2.87	3.00	2.80
Al	0.21	0.13	0.06	0.16	0.14	0.17	0.22	0.13	0.00	0.20
ΣZ	3.00	3.00	3.00	3.00	3.00	3.00	3.00	3.00	3.00	3.00

Abbreviations: <dl = below detection limit

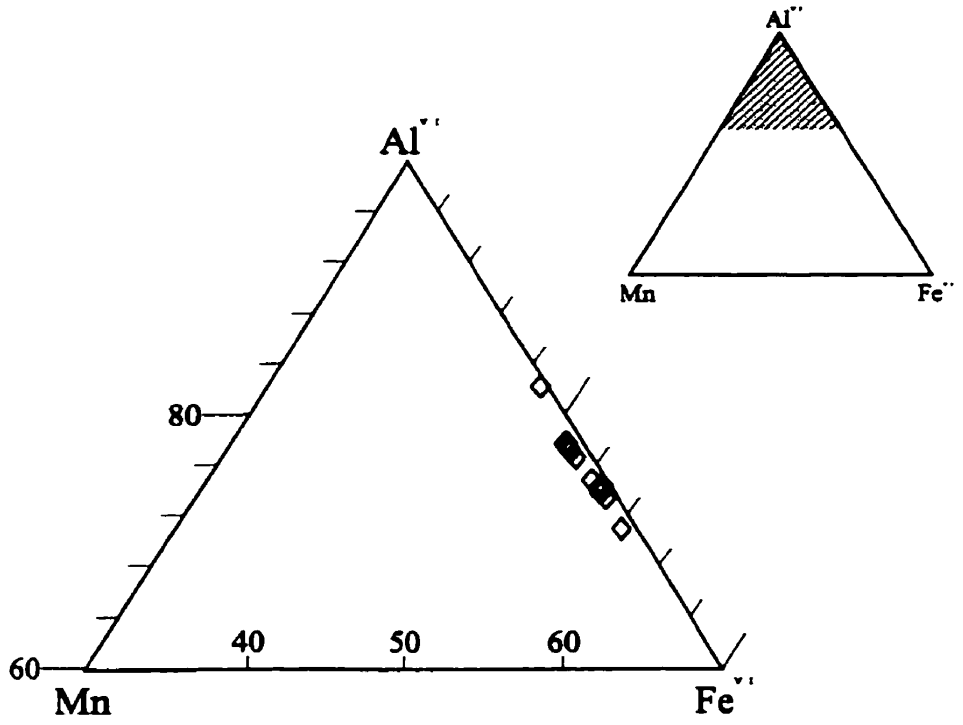

Figure 5-15. Al^{VI} - Fe - Mn diagram showing the compositional variation of epidotes

there is only limited Mn and Fe zoning. The analyzed epidotes are essentially compositionally homogeneous.

Figure 5-15 is a plot of epidote compositions on an Al^{VI}-Mn-Fe diagram. Note that there is very little Mn present in any of the samples. The only compositional variations observed are in the pistacite component. The pistacite range is 17 to 28 mole per cent. There is no obvious difference between blueschist epidotes and those found in the greenstones. Greenstone epidotes have an average pistacite component of approximately 21 mole percent with a very narrow range.

Epidotes from this study are similar in composition to epidotes reported by Maruyama and Liou (1988) for Franciscan blueschists and by Goodge (1995) for

blueschists in the southern Klamath Mountains of northern California. In both cases, analyzed epidotes contain low MnO (0.05 to 0.6 wt. per cent) with rims slightly depleted in Fe^{3+} when compared to cores. Maruyama and Liou (1988) suggest that this depletion in Fe^{3+} indicates progressive growth with increased temperature. Epidote-bearing blueschists have not been previously reported from other localities in the Canadian Cordillera.

5.2.4 Garnet

Sample 88-JIG-39, in the North Cinnabar Creek area is the only known occurrence of garnet-bearing blueschists in the area. In this sample, garnets occur as clear to slightly pinkish grains in distinctive garnet-rich zones approximately 400 μm wide. A bimodal grain size distribution evident among the different layers. Large, idioblastic, inclusion-free garnets (see Figure 5-16) are approximately 300 μm in diameter whereas as the smaller subidioblastic garnets (see Figure 5-17), also inclusion-free, are a maximum of 100 μm in diameter. The smaller garnets are significantly more abundant than the larger ones with an approximate ratio of 3:1. Minor chloritic alteration is apparent along cracks within the garnets.

Garver (1991) describes a synkinematic blueschist-facies metamorphism and deformation in the North Cinnabar Creek area, with the amphibole lying in the schistosity. The garnets lie within this schistosity, however, they appear to overgrow the minerals lying in this schistosity. Few garnets deflect the schistosity, which suggests that they grew late in the deformational history. The lack of inclusions within the garnets makes interpreting the timing of their growth difficult. However, the lack of inclusions does suggest that the garnets grew slowly over a prolonged period enabling the garnet to 'digest' any pre-existing phase.

The garnet-rich layers described above exhibit sharp boundaries with the rest of the rock suggesting an inherent compositional contrast among the layers. The origin of this contrast is difficult to interpret. Garver (1991) indicates that the fabric developed in the blueschists mimics the foliation planes produced in faults during the northeast-vergent

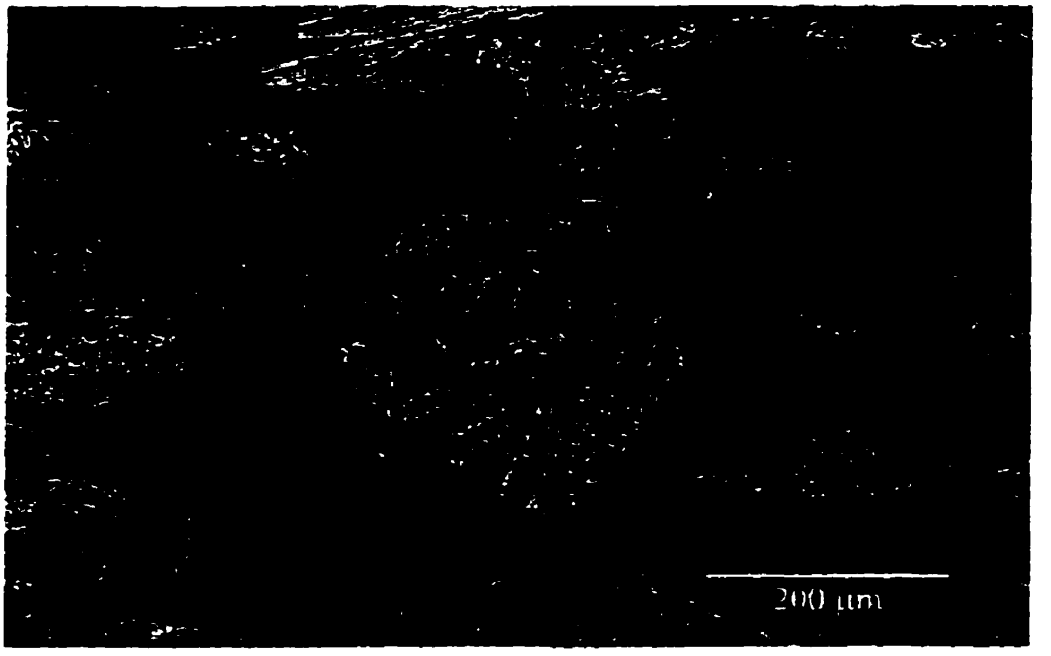

Figure 5-16. Large idioblastic garnet porphyroblast overgrowing blueschist schistosity (Sample 88-JIG-39-1)

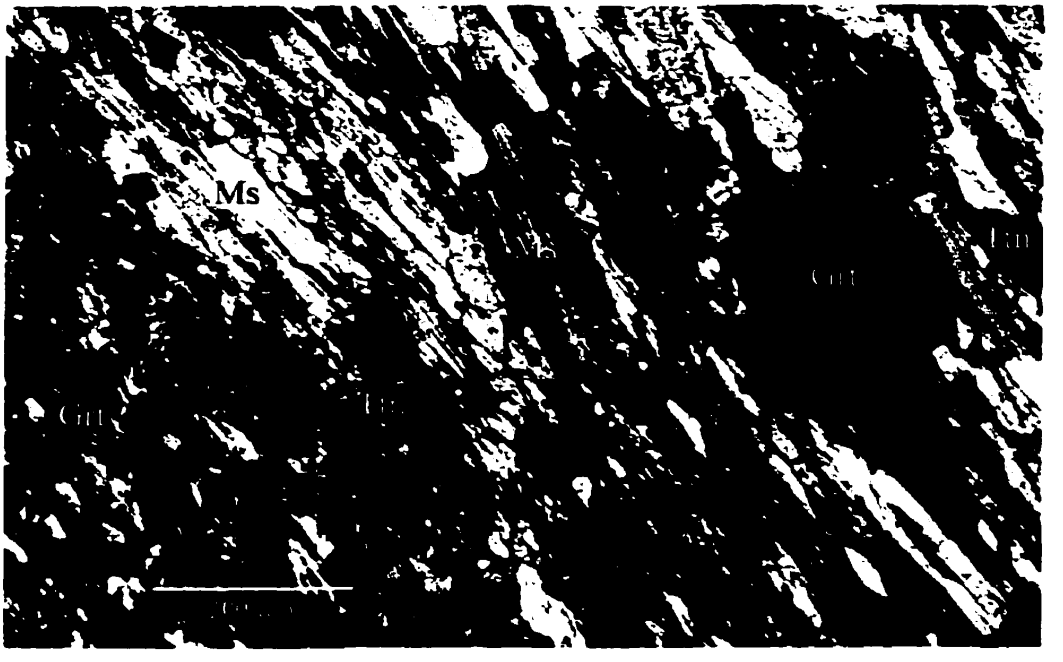

Figure 5-17. Photomicrograph (XPL) showing bimodal size distribution of garnets. Note garnet rich layer in SW corner (Sample 88-JIG-39-1)

Table 5-7. Representative core-rim compositions of Bridge River garnets

	88-JIG-39-1a rim	88-JIG-39-1a core	88-JIG-39-1b rim	88-JIG-39-1b core	88-JIG-39-1e rim	88-JIG-39-1e core	88-JIG-39-1j rim	88-JIG-39-1j core	88-JIG-39-1k rim	88-JIG-39-1k core
SiO_2	37.24	35.72	37.19	36.54	37.40	36.93	36.22	36.29	37.26	37.46
TiO_2	0.04	0.04	0.03	0.05	0.05	0.06	0.09	0.07	0.05	0.03
Al_2O_3	20.79	20.98	21.40	21.34	20.38	20.38	20.78	21.64	21.12	21.01
FeO	29.21	25.15	28.97	24.94	30.11	25.20	28.67	26.21	28.35	25.93
MnO	2.38	9.22	1.91	9.09	2.08	9.12	2.75	7.77	2.53	6.60
MgO	2.43	1.27	2.99	1.31	2.91	1.36	3.19	1.84	2.57	1.92
CaO	7.40	6.74	6.75	6.70	6.41	6.58	6.78	6.10	7.27	6.71
Na_2O	< dl	< dl	< dl	< dl	< dl	< dl	< dl	< dl	< dl	< dl
Total	99.49	99.10	99.33	99.97	100.18	99.63	98.53	99.49	99.53	99.78
Structural formulae on the basis of 12 O										
Si	2.99	2.93	2.98	2.95	2.99	3.00	2.95	2.93	3.00	3.01
Al	0.01	0.07	0.02	0.05	0.01	0.00	0.05	0.07	0.00	0.00
Σ Z	3.00	3.00	3.00	3.00	3.00	3.00	3.00	3.00	3.00	3.01
Al	1.97	1.95	2.00	1.99	1.97	1.95	1.94	1.99	1.99	2.00
Ti	-	-	-	-	-	-	-	-	-	-
Σ Y	2.03	1.95	2.00	1.99	1.97	1.95	1.94	1.99	1.99	2.00
Mg	0.29	0.16	0.36	0.16	0.35	0.16	0.39	0.22	0.31	0.23
Fe^{3+}	1.96	1.72	1.94	1.69	2.02	1.71	1.95	1.77	1.91	1.74
Mn	0.16	0.64	0.13	0.62	0.14	0.63	0.19	0.53	0.17	0.45
Ca	0.64	0.59	0.58	0.58	0.55	0.57	0.59	0.53	0.63	0.58
Σ X	3.06	3.11	3.01	3.05	3.06	3.08	3.12	3.05	3.02	3.00
End member percentages										
% Pyrope	9.54	4.99	11.88	5.18	11.36	5.35	12.41	7.26	10.23	7.67
% Almandine	64.29	55.41	64.54	55.34	65.95	55.64	62.56	58.02	63.27	58.09
% Spessartine	5.31	20.57	4.31	20.43	4.61	20.39	6.08	17.42	5.72	14.98
% Grossular	20.87	19.03	19.27	19.05	18.07	18.61	18.95	17.30	20.79	19.26

Abbreviations: <dl = below detection limit

thrusting event. He states that this observation suggests that the blueschist schistosity has been rotated into parallelism with this younger foliation common throughout the Bridge River Complex. This being the case it would be difficult to ascertain whether this compositional contrast was present prior to blueschist metamorphism or developed as a result of metamorphic segregation during metamorphism.

Table 5-7 presents representative core-rim compositions of the garnets in the North Cinnabar Creek area. All iron in the garnets is assumed to be in the ferrous state. This assumption appears to be correct since no deficiencies in Y-site cations exist. The analyses are presented graphically in Figure 5-18. Although this data only represents a limited sample size, some interesting compositional characteristics are evident.

Compositionally the garnets consist of similar almandine, grossular, pyrope and spessartine components. The garnet cores are typically enriched in spessartine and depleted in almandine and pyrope. The grossular component remains essentially constant. No chemical differences exist between the large and smaller garnets suggesting that: 1) no chemical differences existed among the layers and 2) the bimodal grain size distribution can be attributed variable availability of nucleation sites among the layers.

As described above, variations in core-rim compositions of garnets were detected during electron microprobe analysis and are due to variations in the relative detected amounts of FeO, MgO and MnO. Figure 5-19 is a representative sample of compositional zoning profiles from the Bridge River garnets. These garnets showed the maximum core-rim compositional variation.

Garnets from the Bridge River blueschists show moderate symmetrical 'normal' zoning patterns however the zoning is not very strong. Cores are enriched in spessartine and generally depleted in pyrope and almandine components as compared to rims. The variation from core to rim is essentially smooth and continuous for these components. The variation in the grossular component is less obvious however. Garnet 88-JIG-39-1k shows a relatively constant grossular amount with maximum enrichment between core and rim. This pattern is even more pronounced in garnets 88-JIG-39-1a and 88-JIG-39-1b. Garnet

88-JIG-39-1e also shows this maximum enrichment of grossular between core and rim however the pattern in much more asymmetrical than the other garnets.

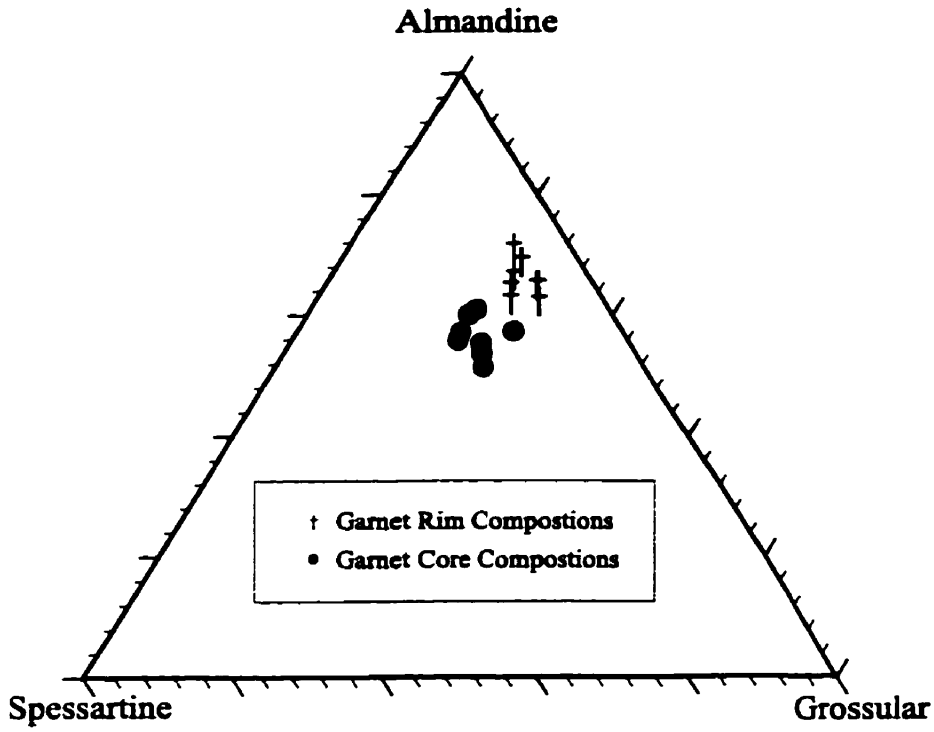

Figure 5-18. Plot of core-rim compositional variation of garnets from the North Cinnabar Creek area.

Similar zoning patterns have been observed in garnets from other blueschist terranes (e.g. Liou et al., 1975; El-Shazly et al., 1990; Faryad 1995). The garnet zoning patterns from these studies were much stronger than those observed in the Bridge River blueschists however. Faryad (1995) also observed maximum grossular contents occurring between core and rim. The minor marginal enrichments observed in these garnets does not provide conclusive evidence for this type of growth zoning.

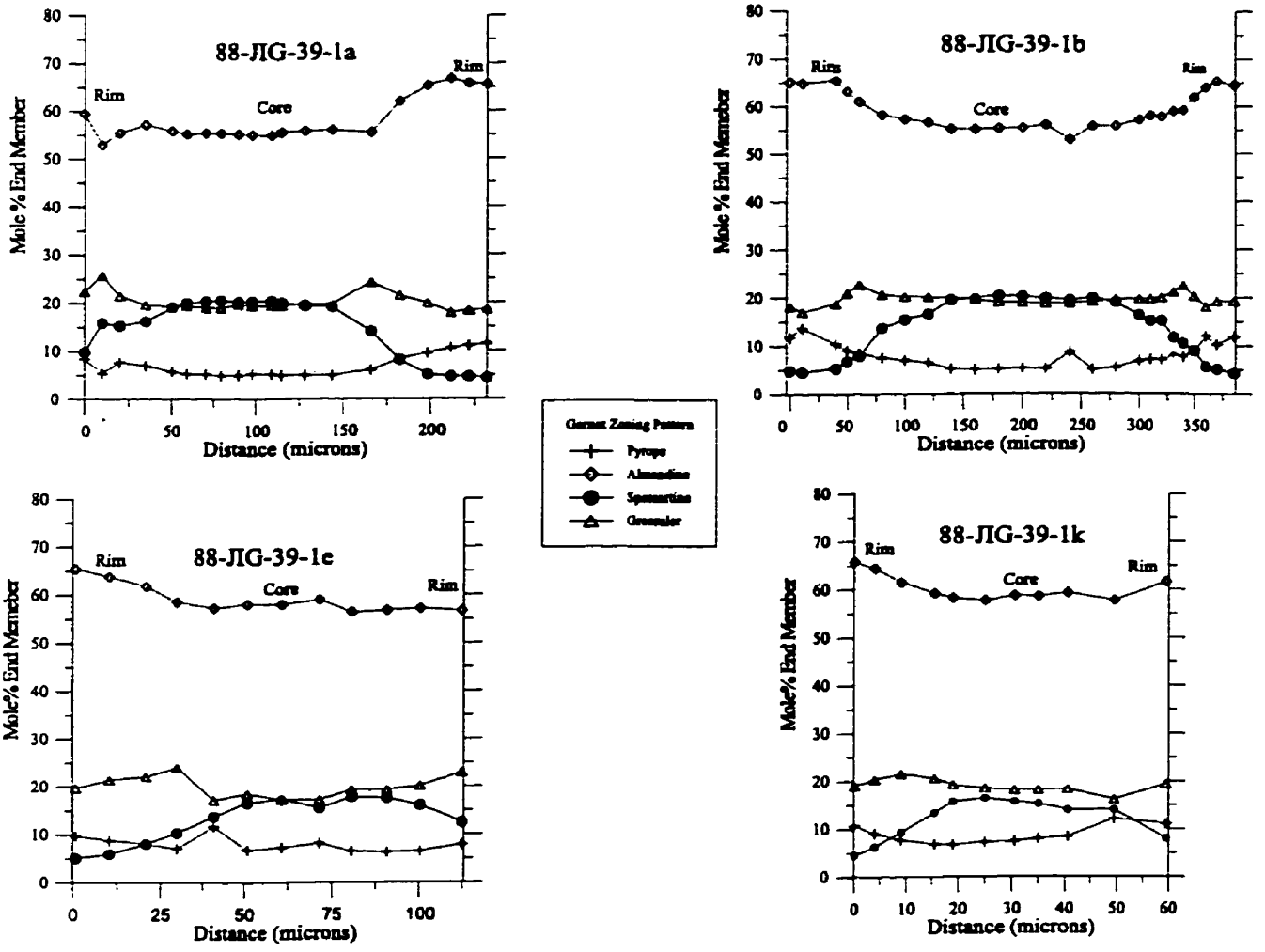

Figure 5-19. Selected garnet-zoning patterns from the Bridge River blueschists

Studies by Hollister (1969) and Räheim (1975) provide explanations for the zoning pattern of MnO, MgO FeO and CaO in these garnets. Variations in MgO, FeO and MnO can be interpreted as resulting from Mn depletion effects (Hollister, 1969). In his study, Hollister (1969) indicates that since Mn, Mg and Fe enter the same site in garnets, as Mn decreases, Mg and Fe must increase to maintain atomic balance in the garnet structure.

Variations in the grossular content of garnets, according to Räheim (1975), are not related to the fractionation model of Hollister (1969). Räheim and Green (1974) determined that grossular component in garnets increases with increasing pressure and a relatively high

grossular content indicates high pressure rather than high temperature. Räheim (1975) suggests that the main reason for CaO zoning is related to physical changes during mineral growth with the concentration of Ca directly reflecting changes in pressure and inversely reflecting changes in temperature. Therefore, the variation of grossular component seen in the garnets from this study may indicate only minor variations in pressure or temperature during garnet growth. However, inferences made about P-T conditions based on changes in composition of only one phase should be regarded as highly suspect

The data presented above suggests that garnet zoning in the Bridge River blueschists is related primarily to depletion of Mn during crystal growth. It is imperative to remember however that these conclusions are based on garnets from the one and only garnet-bearing blueschist outcrop in the area. These conclusions therefore represent only local conditions.

5.2.5 Pyroxene

Pyroxenes in the Bridge River rocks occur as relict igneous pyroxenes and as metamorphic pyroxenes. Relict igneous pyroxenes occur primarily within the greenstones; however, they also occur in the rocks with blueschist facies assemblages. Commonly, the relict igneous pyroxenes occur as euhedral to subhedral phenocrysts (up to 150 x 200 μm in size) (see Figure 5-20) or as smaller groundmass-forming phenocrysts. Generally, they are undeformed to only slightly fractured indicating that they were subject to little or no deformation. The phenocrysts are highly altered and pseudomorphed by a fine-grained irresolvable mesh of minerals with only minor 'fresh' portions remaining. Some relict igneous pyroxenes are rimmed by aegerine and chlorite (Figure 5-20). In the blueschists, relict igneous clinopyroxenes are commonly pseudomorphed by sodic amphibole (see Figure 5-2).

Metamorphic pyroxenes present in the Bridge River blueschists commonly occur as small patches of radiating crystal aggregates (<100 μm across), however, a few samples contain well formed metamorphic pyroxene crystals (Figure 5-20). Metamorphic pyroxenes

range in colour from clear to brownish green to pleochroic pale green to pale emerald green. The fresh, well-formed metamorphic pyroxenes show no obvious colour zoning. Commonly, the most strongly coloured pyroxenes are seen as intimate overgrowths on relict igneous pyroxenes. Other metamorphic pyroxenes are seen replacing relict igneous plagioclase feldspars and are found associated with lawsonite and quartz.

Figure 5-20. Relict clinopyroxene from greenstone (Sample 97-DJH-061-4). Aegerine is the light grey, fine-grained aggregate at the margins of the clinopyroxene.

Although a few metamorphic pyroxenes were identified in thin section, their presence was most commonly detected (and/or confirmed) through X-ray diffraction analysis. Generally, XRD analyses indicated the presence of jadeitic pyroxenes, however some aegerine-augites were also detected. Table 5-8 presents the results of several X-ray diffraction analyses confirming the presence of jadeitic pyroxenes. There is a very close match between the analyses and the calculated pattern of Borg and Smith (1969).

Table 5-8. Comparison of X-ray Diffraction data for jadeitic pyroxenes with calculated pattern. vs = very strong peak intensity (>80); s = strong peak intensity (61-79); m = moderate (21-50); w = weak (<21). Calculated pattern is from Borg and Smith (1969).

Analyses		**Calculated Pattern**	
D(Å)	Intensity	*d*(Å)	Intensity
4.30-4.40	m	4.381	24
2.91-2.94	vs	2.917	100
2.80-2.88	s	2.827	72
2.47-2.50	m	2.488	47
2.39-2.40	m	2.414	30
2.05-2.09	w	2.066	19

Table 5-9 presents electron microprobe analyses of the pyroxenes with end members calculated using the method of Cawthorn and Collerson (1974). Since iron in different oxidation states is not discriminated with the electron microprobe, some assumptions about the distribution of Fe^{2+} and Fe^{3+} were made in calculating mineral formulae and in end member calculations. The amount of ferrous and ferric iron in the pyroxenes was calculated using the method outline by Spear (1995). In this method, the ferric iron content of the pyroxene is calculated by simultaneously normalizing the analysis to 4 cations and 12 positive charges. The total Fe^{3+} amount is determined by calculating the difference between the total number of positive charges based on the normalized 4 cations and the ideal value of 12. This difference is converted to Fe^{3+} atoms in order to achieve charge balance.

Several authors have devised various methods for determining the ferric iron content of pyroxenes (e.g. Spear, 1995; Cawthorn and Collerson, 1974; and Ghent and Coleman, 1973). These estimation schemes have inherent uncertainties attached to the Fe^{3+} value obtained. When one takes into account the analytical errors and propagates them through the Fe^{3+} determinations and subsequent end member calculations, the errors can become extremely large (e.g. Cawthorn and Collerson, 1974). Therefore, any estimation of Fe^{3+} from electron microprobe analyses and subsequent end member calculations must be viewed as only rough approximations.

Table 5-9. Representative electron microprobe analyses of clinopyroxenes.

	97-DJH-035-1 Jd	97-DJH-035-1 Jd	97-DJH-035-1 Jd	97-DJH-034-1 Jd	97-DJH-034-1 Jd	97-DJH-034-1 Jd	97-DJH-034-1 Jd	92-GBR-33 Grn	92-GBR-33 Grn	97-DJH-007-1 Rpx	97-DJH-007-1 Rpx	97-DJH-007-1 Rpx	97-DJH-007-1 Rpx
SiO_2	53.60	56.06	56.78	56.56	58.86	59.31	59.66	51.84	53.43	52.78	52.95	52.77	52.96
TiO_2	<dl	1.18	0.17	0.66	0.39	0.59	0.80	1.36	1.25	0.50	0.52	0.51	0.52
Al_2O_3	11.51	14.85	14.98	15.50	21.55	17.83	22.30	3.57	1.87	1.14	1.03	1.18	1.07
FeO*	15.17	8.45	8.71	8.65	1.45	7.03	1.43	17.59	17.62	16.80	16.81	16.80	16.81
MnO	0.17	0.10	0.08	0.17	0.05	0.07	0.07	0.25	0.35	0.49	0.48	0.49	0.48
MgO	6.58	10.24	10.50	6.12	2.48	1.39	1.42	6.60	6.12	10.80	10.79	11.20	11.19
CaO	6.13	0.95	0.86	3.72	4.05	4.35	4.21	11.99	12.88	12.16	12.21	12.27	12.32
Na_2O	6.67	7.48	7.95	8.27	11.05	10.07	10.52	6.04	6.13	4.67	4.61	4.29	4.24
K_2O	0.11	na.	na	0.14	0.10	<dl	<dl	na	na	na	na	na	na
Total	99.94	99.31	100.03	99.79	99.98	100.64	100.43	99.24	99.65	99.36	99.41	99.53	99.60
Structural formulae on the basis of 4 cations, 12 positive charges													
Si	1.94	1.89	1.89	1.91	1.84	1.97	1.88	1.97	2.03	1.98	1.99	1.98	1.99
Al^{IV}	0.06	0.11	0.11	0.09	0.16	0.03	0.12	0.03	0.00	0.02	0.01	0.02	0.01
Σ	2.00	2.00	2.00	2.00	2.00	2.00	2.00	2.00	2.03	2.00	2.00	2.00	2.00
Al^{VI}	0.44	0.48	0.48	0.53	0.64	0.66	0.70	0.13	0.08	0.03	0.03	0.03	0.03
Ti	-	0.03	0.00	0.02	0.01	0.01	0.02	0.04	0.04	0.01	0.01	0.01	0.01
Fe^{3+} ***	0.40	0.39	0.31	0.38	0.37	0.46	0.40	0.25	0.28	0.20	0.22	0.23	0.25
Fe^{3+} **	0.09	0.07	0.14	0.07	0.06	0.00	0.03	0.27	0.23	0.30	0.29	0.27	0.26
Mn	0.01	0.00	0.00	0.00	0.00	0.00	0.00	0.01	0.01	0.02	0.02	0.02	0.02
Mg	0.36	0.51	0.52	0.31	0.12	0.07	0.07	0.37	0.35	0.60	0.60	0.63	0.63
Na	0.47	0.49	0.51	0.54	0.67	0.65	0.64	0.45	0.45	0.34	0.34	0.31	0.31
Ca	0.24	0.03	0.03	0.13	0.14	0.15	0.14	0.49	0.52	0.49	0.49	0.49	0.50
Σ	1.99	2.00	2.00	1.99	2.00	2.01	2.00	2.00	1.97	2.00	2.00	2.00	2.00
End members													
Aug	0.68	0.66	0.63	0.60	0.43	0.51	0.46	0.71	0.72	0.79	0.80	0.80	0.82
Ac	0.02	0.01	0.03	0.01	0.03	0.00	0.00	0.20	0.23	0.19	0.19	0.18	0.16
Jd	0.30	0.33	0.35	0.39	0.55	0.49	0.54	0.08	0.05	0.02	0.02	0.02	0.02

All Fe as FeO; ** Fe^{3+} is computed by charge balance; *** Fe^{2+} is computed as Fe^{total}-Fe^{3+} (see text for discussion)
Abbreviations: Jd = jadeitic pyroxene; Grn = green pyroxene; Rpx = relict igneous pyroxene;
<dl = below detection limit; na = not analyzed

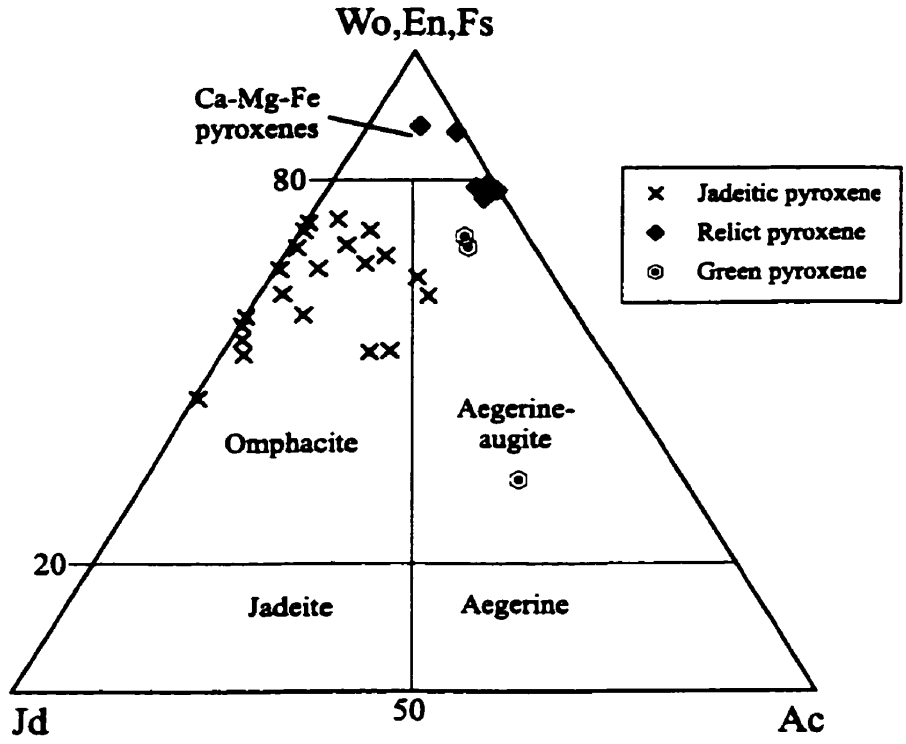

Figure 5-21. Compositions of pyroxenes from the Bridge River rocks. Diagram after Morimoto (1989)

Pyroxene compositions are presented graphically in Figure 5-21, and classified according to the International Mineralogical Association nomenclature given by Morimoto (1989). The fine-grained size of many of the pyroxenes made it impossible to determine core and rim compositions.

Most metamorphic pyroxenes are omphacites with a minimum Jd content of 17 per cent and a maximum Jd content of 55 per cent. Some compositions plot just in the aegerine-augite field. The maximum Jd value obtained from these rocks is significantly lower than the jadeitic pyroxenes reported by Ghent et al. (1996) for the Pinchi Lake blueschists. The Ac content of the omphacites range from 0 to 23 per cent. The green pyroxenes are aegerines to aegerine-augites with a maximum Ac content of 46 per cent and a maximum Jd content of 20 per cent. The relict igneous pyroxenes are essentially Ca-Mg-Fe pyroxenes.

5.2.6 White Mica

White micas are present in all lithologies of the Carpenter Lake – Tyaughton Creek and North Cinnabar Creek areas. They are readily identifiable in thin section and in some hand specimens. In the blueschist and blueschist-bearing rocks, white micas occur as oriented to variably oriented, idioblastic to subidioblastic crystals (see Figure 5-22). Their size range is quite variable with smaller micas having dimensions of 20 x 35 μm and the larger micas with dimensions of 150 x 700 μm. Commonly, these micas occur in contact with sodic amphibole, lawsonite, epidote, garnet, stilpnomelane and quartz. The white micas are inclusion-free in these rocks, indicating, perhaps, a slow rate of growth.

Figure 5-22. Photomicrograph of a sub-idioblastic white mica (Sample 88-JIG-39-1)

Commonly, the white micas are aligned in the schistosity and display uniform extinction. In crenulated samples, the micas are kinked (see Figure 5-23) and display undulatory extinction. White micas found in highly deformed layers within cherts also

display undulatory extinction when warped around fold hinges. Therefore, the micas grew after, or late in the schistosity-forming deformation but prior to the crenulation event.

White micas found within the greenstones are significantly finer grained (< 30 μm x 25 μm) than those found in the blueschists and blueschist-bearing rocks. They typically occur as unoriented, scaly aggregates associated with chlorite and quartz and occur primarily in the groundmass. Many of the relict igneous feldspar phenocrysts have a distinct cloudy appearance suggesting sericitic alteration. Due to the fine-grained nature of these rocks, it is difficult to determine whether the groundmass micas have the same mode of occurrence.

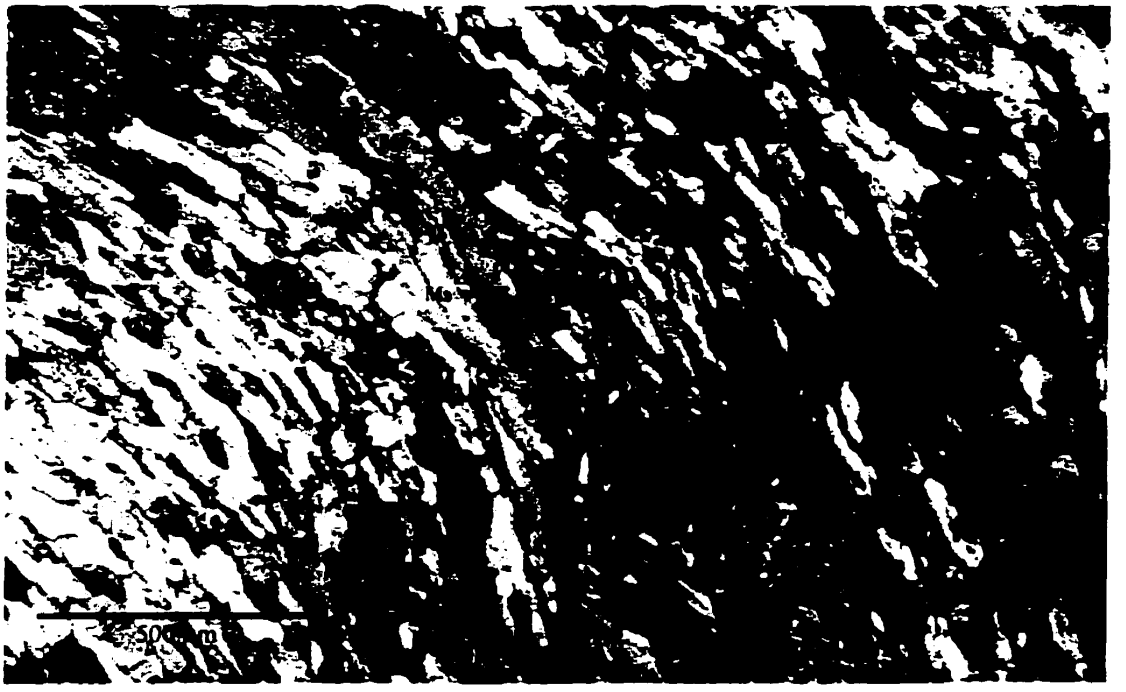

Figure 5-23. Photomicrograph of moderately kinked white micas

Representative electron microprobe analyses and structural formulae from both blueschists and greenstones are presented in Table 5-10. Structural formulae were calculated based on 11 oxygens, with all Fe as Fe^{2+}. Water was assumed to equal four

weight per cent. Estimation of ferric iron content of micas from microprobe analyses is difficult primarily due to the presence of structural vacancies. It was therefore not attempted in this study.

From the analyses, it is evident that the micas are phengites. They all contain significantly more than 3.0 Si atoms per formula unit (3.31-3.61). The formula Mg + Fe^{2+} contents are also greater than the excess of Si atoms above 3.0. This suggests a celadonite substitution (e.g. Ghent and Coleman, 1965). White micas also contain notable amounts of Na_2O (0.25 – 1.0 wt. per cent). The maximum values obtained in this study are lower than those reported by Ghent et al. (1993) for phengites from Pinchi Lake (1.7 wt. per cent) however.

A comparison of blueschist and greenstone mica compositions is presented in Figure 5-24. Both data sets have a relatively wide compositional range; however, greenstone micas contain greater amounts of Fe_{total} and Mg and are more celadonitic than the blueschist micas.

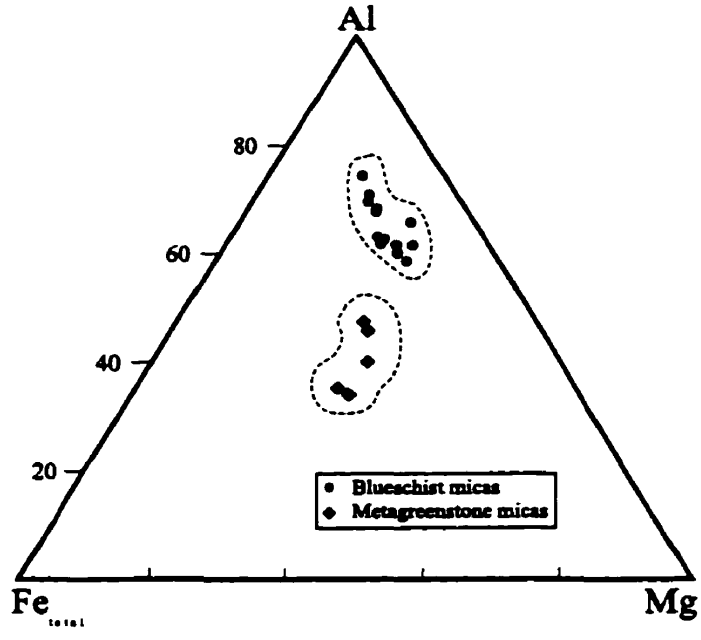

Figure 5-24. Al-Fe-Mg plot comparing compositions of blueschist and greenstone micas.

Table 5-10. Representative electron microprobe analyses of white micas

	97-DJH-110-1	97-DJH-110-1	88-JIG-39-1 core	88-JIG-39-1 rim	92-GBR-35	97-DJH-062-4	97-DJH-062-4	97-DJH-062-4	92-GBR-43	92-GBR-43
SiO_2	49.26	48.80	49.56	49.00	51.64	51.11	51.63	53.31	53.15	53.44
Al_2O_3	26.31	27.90	26.57	26.41	22.57	22.28	21.58	21.67	20.34	21.77
FeO*	4.52	4.20	4.46	4.57	5.49	5.29	5.47	3.99	4.96	3.30
MnO	<dl	<dl	<dl	<dl	<dl	0.10	0.09	0.09	0.10	0.06
MgO	3.40	2.80	3.44	3.38	4.49	4.56	4.65	5.72	5.22	5.02
CaO	<dl	<dl	<dl	<dl	<dl	0.14	0.13	0.12	<dl	<dl
Na_2O	0.78	1.00	0.55	0.56	0.67	0.60	0.58	0.41	0.59	0.58
K_2O	10.43	10.30	10.47	10.40	11.01	11.09	11.09	10.25	11.21	10.99
F	<dl	<dl	0.09	0.20	<dl	<dl	0.12	<dl	<dl	0.09
H_2O	4.00	4.00	4.00	4.00	4.00	4.00	4.00	4.00	4.00	4.00
Total	98.78	99.40	99.14	98.52	99.97	99.17	99.34	99.63	99.62	99.28
Structural formulae on the basis of 11 oxygens										
Si	3.36	3.31	3.36	3.35	3.50	3.50	3.53	3.58	3.61	3.60
Al^{IV}	0.64	0.69	0.64	0.65	0.50	0.50	0.47	0.42	0.39	0.40
Σ	4.00	4.00	4.00	4.00	4.00	4.00	4.00	4.00	4.00	4.00
Al^{VI}	1.47	1.54	1.49	1.48	1.31	1.30	1.27	1.29	1.24	1.33
Fe	0.26	0.24	0.25	0.26	0.31	0.30	0.31	0.22	0.28	0.19
Mg	0.35	0.28	0.35	0.34	0.45	0.47	0.47	0.57	0.53	0.50
Σ	2.08	2.06	2.09	2.09	2.07	2.06	2.06	2.09	2.05	2.02
Na	0.10	0.13	0.07	0.07	0.09	0.08	0.08	0.05	0.08	0.08
K	0.91	0.89	0.91	0.91	0.95	0.97	0.97	0.88	0.97	0.94
Σ	1.01	1.02	0.98	0.98	1.04	1.05	1.04	0.93	1.05	1.02

*All Fe as FeO; <dl = below detection limit; na = not analyzed

5.2.7 Chlorite

The presence of chlorite in blueschist facies rocks is well documented in the literature (e.g. Ernst, 1965; Ghent and Coleman, 1973; and Ghent et al., 1996) and is also found in most rocks of the Bridge River study area. In the blueschist and blueschist-bearing rocks, chlorite is present but not common. It is typically found as a secondary phase associated with stilpnomelane replacing sodic amphiboles and is present in small veinlets crosscutting the local fabric and metamorphic minerals. The chlorites found in these units range in size from submicroscopic to maximum dimensions of approximately 200 x 80 μm. The larger crystals display anomalous blue-brown interference colours and are optically negative (see Figure 5-25).

Greenstone chlorites are typically present as the main groundmass-forming mineral. Chlorites commonly occur as a fine-grained mesh of intergrown muscovite, quartz in these metavolcanics. Chlorite also replaces relict igneous phenocrysts. It is most commonly found rimming relict pyroxenes and associated with white mica replacing relict feldspars. Unlike the blueschist-related chlorites, these chlorites tend not to show the anomalous blue-brown interference colours.

Most commonly, the greenstones contain a very fine-grained brownish coloured mineral. This mineral could be similar to the 'chlorite-vermiculite' of Brown (1967). He indicates that the rocks from Otago, New Zealand, much like the greenstones from this study, show evidence of alteration and concludes that the 'chlorite-vermiculite' is actually altered chlorite. X-ray diffraction patterns of many greenstones show weak 7 Å peaks in the absence of obvious chlorite in thin section. This is likely due to small amounts of chlorite in the sample.

Table 5-11 is a representative summary of chlorite compositions from the Bridge River study area. The structural formulae were calculated on the basis of 28 oxygens per formula unit; all iron was assumed to be in the ferrous state. H_2O was calculated using the program WATER (Nicholls et al., 1977) which iteratively adds water to the analysis and

corrects all oxides due to changes in the Bence-Albee factors. The best chlorite results were obtained from the larger crystals. The small grain size of most unaltered flakes and the presence of interleaved chlorite and white mica produced spurious results. Chlorites present in the study area have a wide compositional range when grouped as a whole: SiO_2 ranges from 24.4 – 29.5% (by weight), Al_2O_3 from 11.8 – 23.3%, FeO from 18.0 – 32.7%, MnO from 0.1 – 0.7% and MgO from 9.3 to 22.6%. The Fe/Mg ratio ranges from 0.5 – 1.9, with Al^{VI} between 1.8 – 3.6. However, when grouped by occurrence the compositions cover a much narrower range. Typically, greenstone chlorites have lower Al_2O_3 and FeO values and higher MgO values than the replacement chlorites. No systematic variation in SiO_2 or MnO was observed. Detectable amounts of Ca were also present. Chlorites show a range in weight per cent H_2O of 9 to 16. Published data indicate that these values should be 12 weight per cent H_2O.

Figure 5-25. Photomicrograph of late chlorite vein in greenstone (XPL) (Sample 97-DJH-035-1). Greenstone comprised of a mesh of chlorite, white mica, quartz and relict igneous feldspars

Table 5-11. Representative electron microprobe analyses of chlorite

	88-JIG-39-1 s	88-JIG-39-1 s	97-DJH-TC-2 s	97-DJH-TC-2 s	97-DJH-031-2 s	97-DJH-034-6	97-DJH-034-6	97-DJH-035-1	97-DJH-031-2	97-DJH-TC-2
SiO_2	24.38	24.85	28.73	28.74	27.45	28.65	27.37	29.16	28.11	29.15
Al_2O_3	18.52	19.35	23.07	23.30	16.57	15.76	16.17	17.02	14.57	16.8
FeO*	32.66	31.07	24.71	26.02	32.41	25.86	26.50	18.69	27.91	22.67
MnO	0.65	0.46	0.16	0.12	0.20	0.42	0.41	0.19	0.25	0.56
MgO	9.56	10.45	10.00	10.90	10.52	16.87	17.29	22.42	12.28	18.22
CaO	<dl	<dl	0.85	0.70	1.17	0.24	0.32	0.13	0.75	1.34
F	0.16	<dl	0.77	0.30	0.07	0.14	0.09	<dl	0.13	0.18
H_2O	13.76	13.48	10.74	9.12	11.37	11.52	11.61	12.13	15.84	10.86
Total	99.73	99.74	99.81	99.84	99.78	99.77	99.78	99.84	99.85	99.81
Structural formulae on the basis of 28 oxygens										
Si	5.52	5.53	5.94	5.83	5.99	6.04	5.81	5.93	6.31	6.00
Al^{IV}	2.48	2.47	2.06	2.17	2.01	1.96	2.19	2.07	1.69	2.00
Σ	8.00	8.00	8.00	8.00	8.00	8.00	8.00	8.00	8.00	8.00
Al^{VI}	2.46	2.60	3.57	3.41	2.24	1.96	1.85	2.00	2.17	2.07
Fe	6.18	5.78	4.27	4.42	5.91	4.56	4.70	3.18	5.24	3.90
Mn	0.12	0.09	0.03	0.02	0.04	0.08	0.07	0.03	0.05	0.10
Mg	3.23	3.46	3.08	3.30	3.42	5.30	5.47	6.79	4.11	5.59
Ca	-	-	0.19	0.15	0.27	0.05	0.07	0.03	0.18	0.30
Σ	12.01	11.94	11.34	11.46	11.88	11.96	12.17	12.03	11.76	11.96

*All Fe as FeO; <dl = below detection limit; na = not analyzed; s = secondary/replacement chlorite

Chlorite compositions are plotted on an Al-Fe_{total}-Mg diagram in Figure 5-26. The difference between the two occurrences is obvious from this plot. Greenstone chlorites plot on a trend that is approximately related to the Mg-Fe solid solution. Chlorites present as replacement minerals appear to fall on a trend related to variations in Al-Fe amounts. The presence of chlorites in the greenstones and the absence in the blueschist assemblages may reflect slight compositional differences between the lithologies.

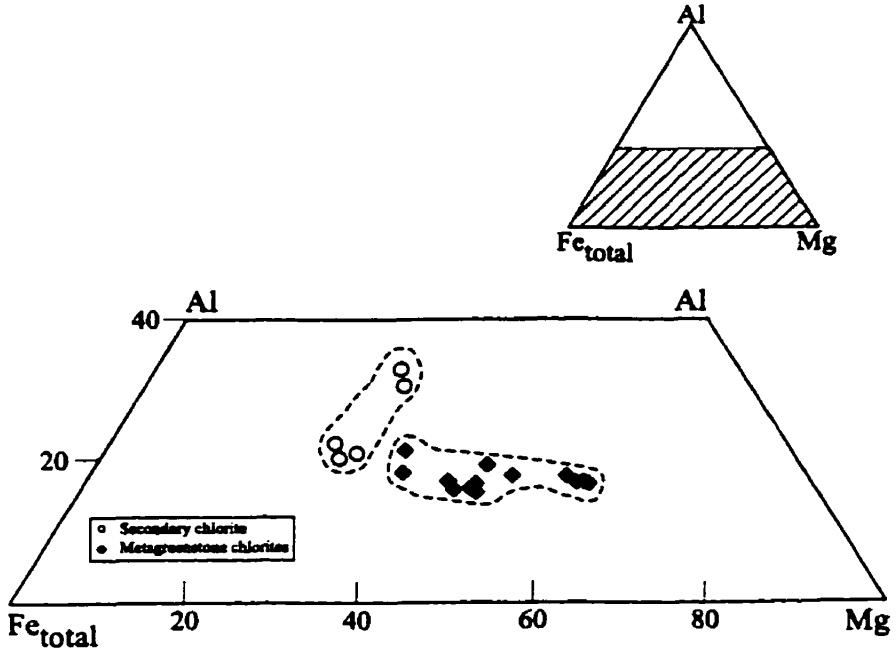

Figure 5-26. Al-Fe_{total}-Mg plot illustrating chlorite compositions. Dashed lines enclose composition of replacement chlorites and 'primary' greenstone chlorites

5.2.8 Stilpnomelane

Stilpnomelane is a common constituent of the blueschist and blueschist-bearing rocks within the Bridge River Complex. Commonly, stilpnomelane occurs as reddish-brown aggregate crystal masses with no apparent orientation (see Figure 5-27). According to Brown (1971), this distinctive colour indicates the stilpnomelane is rich in ferric iron. Stilpnomelane also occurs in segregations, as small (typically < 80 x 15 μm), subidioblastic crystals aligned with the local foliation. It is also found in both blueschists and greenstones as thin veinlets that crosscut other minerals or the local fabric. In one sample, 97-DHTC-2, stilpnomelane is found in the intermediate region between a blueschist assemblage and the greenstone.

Stilpnomelane commonly occurs with quartz and carbonate in the veins. It can also be found in apparent textural equilibrium with blue amphibole and lawsonite in the blueschist assemblages. Several blueschist samples display apparent intergrowths of blue amphibole and stilpnomelane. In some greenstones samples, stilpnomelane is found rimming what appear to have been relict igneous phenocrysts that have been subsequently replaced by carbonate.

Electron microprobe analyses are presented in Table 5-12. Structural formulae are calculated on the basis of 8 Si with H_2O calculated using the program WATER (Nicholls et al., 1977). Stilpnomelanes from this study have wide compositional ranges. Of particular note is the range in Mn content. Mn varies from 0.01 to 1.7 atoms. The higher Mn values were obtained from metacherts from the North Cinnabar Creek area with the lower values coming from samples in the Carpenter Lake – Tyaughton Creek area. The distinction between the two occurrences is not necessarily this straightforward. Some analyses from the North Cinnabar Creek area have values considerably lower than the maximum (e.g. 97-DJH-110-1). Stilpnomelane from the Bridge River Complex also has notable variations in K (0.08-0.3), Na (0.07-2.0) and Ca (0-0.5) atoms per formula unit. Comparable data has not been found elsewhere in the literature.

Figure 5-27. Mesh of late stilpnomelane cross-cutting greenstone. Note relict igneous feldspars in greenstone

Figure 5-28 is an Al-Fe+Mn-Mg plot of stilpnomelane compositions from the study area. Typically stilpnomelane from the North Cinnabar Creek area is richer in Fe + Mn and generally poorer in Al than Carpenter Lake stilpnomelane. When compared to stilpnomelane analyses from Pinchi Lake, the minimum and maximum values obtained from this study are significantly different from those reported by Ghent et al. (1990; 1996)

Table 5-12. Representative electron microprobe analyses of stilpnomelane

	97-DJH-110-1	97-DJH-110-1	97-DJH-34-6	92-GBR-43	92-GBR-43	92-GBR-40	92-GBR-40	92-GBR-40
SiO_2	43.91	45.66	48.42	45.48	45.66	47.01	48.47	48.98
Al_2O_3	5.58	5.52	9.09	5.37	5.52	6.11	6.01	5.79
FeO*	19.78	20.29	20.04	20.35	20.29	20.73	20.32	20.20
MnO	13.28	10.30	0.20	10.23	10.30	11.69	9.80	11.45
MgO	4.76	4.49	8.16	4.48	4.49	4.31	4.13	4.38
CaO	0.00	0.00	2.99	0.00	0.00	0.00	0.00	0.00
Na_2O	0.20	1.54	6.31	1.97	1.54	1.11	2.74	1.70
K_2O	1.38	1.17	1.01	1.41	1.17	0.39	0.72	0.60
F	0.10	0.05	0.10	<dl	<dl	<dl	<dl	<dl
H_2O	10.82	10.78	3.42	10.45	10.78	8.48	7.42	6.64
Total	99.81	99.80	99.74	99.80	99.80	99.83	99.70	99.74
Structural formulae on the basis of 8 Si								
Si	8.00	8.00	8.00	8.00	8.00	8.00	8.00	8.00
Al	1.20	1.14	1.77	1.11	1.14	1.23	1.17	1.11
Fe	3.01	2.97	2.77	2.99	2.97	2.95	2.80	2.76
Mn	2.05	1.53	0.03	1.52	1.53	1.68	1.37	1.58
Mg	1.29	1.17	2.01	1.17	1.17	1.09	1.02	1.07
Ca	-	-	0.53	-	-	-	-	-
Na	0.07	0.52	2.02	0.67	0.52	0.37	0.88	0.54
K	0.32	0.26	0.21	0.32	0.26	0.08	0.15	0.13

*All Fe as FeO; <dl = below detection limit; na = not analyzed

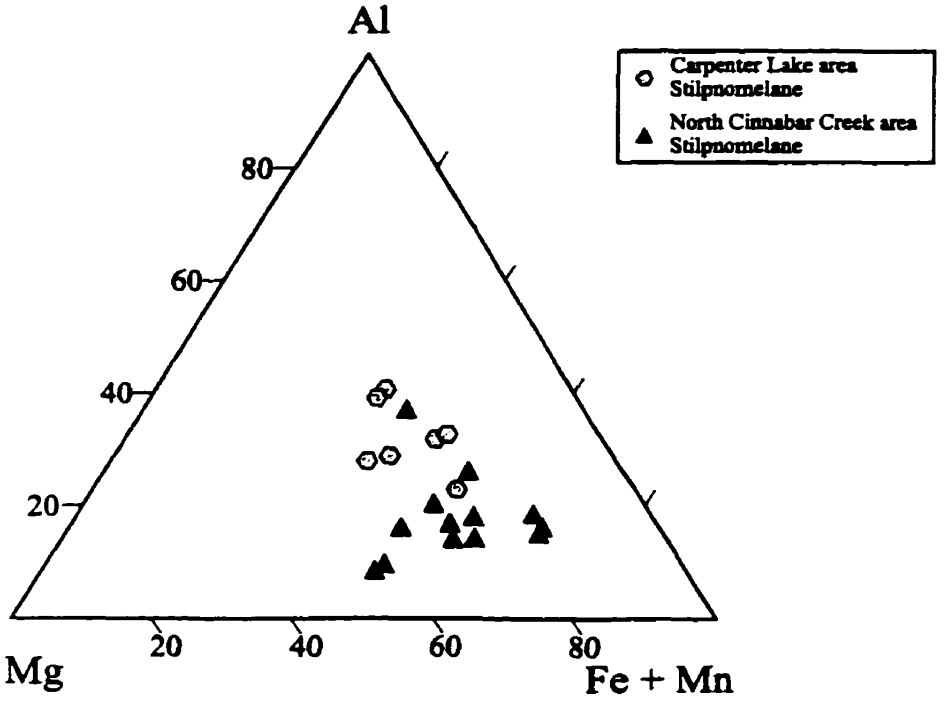

Figure 5-28. Al-Fe+Mn-Mg plot of stilpnomelane compositions

5.2.9 Feldspars

Feldspars are present as intergranular crystals in some blueschists and metacherts; as a vein phase in crosscutting most lithologies, and as a relict igneous phase of the greenstones. In the blueschists and metacherts, feldspars occur as small (<40 x 20 μm), blocky crystals aligned with the local fabric. In the metacherts, the feldspars occur in the deformed mafic/argillaceous layers. Vein feldspars occur as larger (40 x 20 μm to 1.2 x 0.6 mm) simply twinned crystals associated with quartz and carbonate (Figure 5-29). Relict igneous feldspars are heavily altered to white mica, chlorite and quartz in most samples yet retain a variolitic texture (Figure 5-30). Several relict igneous feldspars are also replaced by jadeitic pyroxene, however, no assemblage of jadeite + lawsonite + quartz was found.

Table 5-13 presents representative electron microprobe analyses of the various feldspars. All feldspars are albite (see Figure 5-31) and occur in the compositional range

Figure 5-29. Late albite + quartz vein. Note simply twinned albite (Sample 97-DJH-003-1)

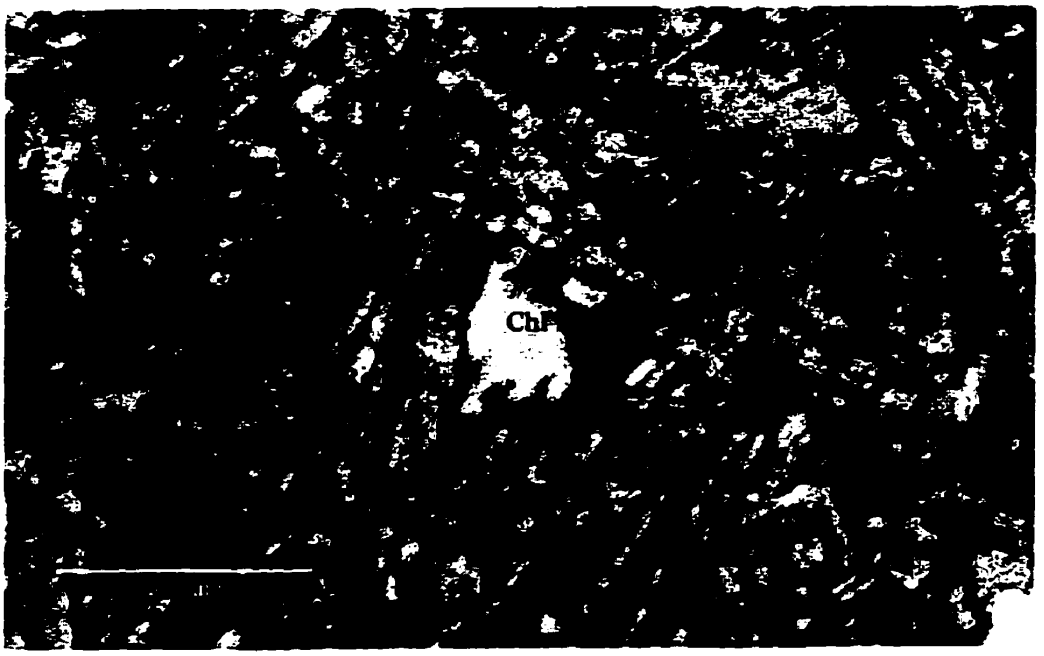

Figure 5-30. Altered relict igneous feldspars from a greenstone. Note variolitic texture (Sample 97-DJH-061-4)

Table 5-13. Representative electron microprobe analyses of feldspars

	97-DJH-031-2 vein	97-DJH-031-2 vein	97-DJH-003-11 vein	97-DJH-003-11 vein	97-DJH-035-1 r. ig	97-DJH-035-1 r. ig	97-DJH-125-3 igx	97-DJH-125-3 igx	92-GBR-38 igx	97-DJH-HC-1 igx
SiO_2	68.01	68.15	67.88	68.45	68.72	68.18	68.34	68.54	68.49	68.34
Al_2O_3	19.12	19.94	19.97	19.19	20.16	19.05	20.11	19.07	19.40	19.60
MgO	0.02	<dl	<dl	<dl	0.03	0.02	<dl	<dl	<dl	<dl
CaO	0.27	0.26	0.15	0.17	0.40	0.40	0.25	0.31	0.15	0.14
Na_2O	11.70	11.30	11.73	11.55	10.75	11.85	11.69	11.94	11.64	11.51
K_2O	0.06	0.04	0.05	0.08	0.10	0.10	0.04	0.10	0.04	0.03
F	<dl	<dl	0.07	<dl	<dl	<dl	<dl	<dl	<dl	<dl
Total	99.18	98.70	99.86	99.44	100.16	99.60	100.46	99.96	99.72	99.66
Structural formulae on the basis of 32 O										
Si	11.99	11.93	11.89	12.02	11.94	11.98	11.89	12.00	11.99	11.97
Al	3.98	4.11	4.12	3.97	4.13	3.94	4.12	3.93	4.00	4.05
Σ	15.97	16.04	16.01	15.98	16.07	15.93	16.02	15.93	15.99	16.02
Mg	0.01	-	-	-	0.01	0.01	-	-	-	-
Na	4.00	3.97	3.98	3.93	3.62	4.04	3.94	4.05	3.95	3.91
Ca	0.05	0.05	0.03	0.03	0.07	0.08	0.05	0.06	0.03	0.03
K	-	-	0.01	-	-	-	-	-	-	-
Σ	4.07	4.03	4.03	3.98	3.73	4.14	4.00	4.13	3.99	3.94
Mole per cent end member										
Ab	98.4	98.5	99.0	98.8	97.4	97.6	98.6	98.1	99.1	99.2
An	1.3	1.3	0.7	0.8	2.0	1.8	1.2	1.4	0.7	0.7
Or	0.3	0.2	0.3	0.4	0.6	0.5	0.2	0.5	0.2	0.1

Abbreviations: <dl = below detection limit; r.ig = relict igneous; igx = intergranular crystal

$An_{0.7}$ to $An_{2.0}$ with only a negligible Or component. Analyses of relict igneous feldspars produce a compositional range of $An_{1.3}$ to $An_{2.0}$ indicating that they have undergone albitization during alteration. This process would have involved significant mass redistribution.

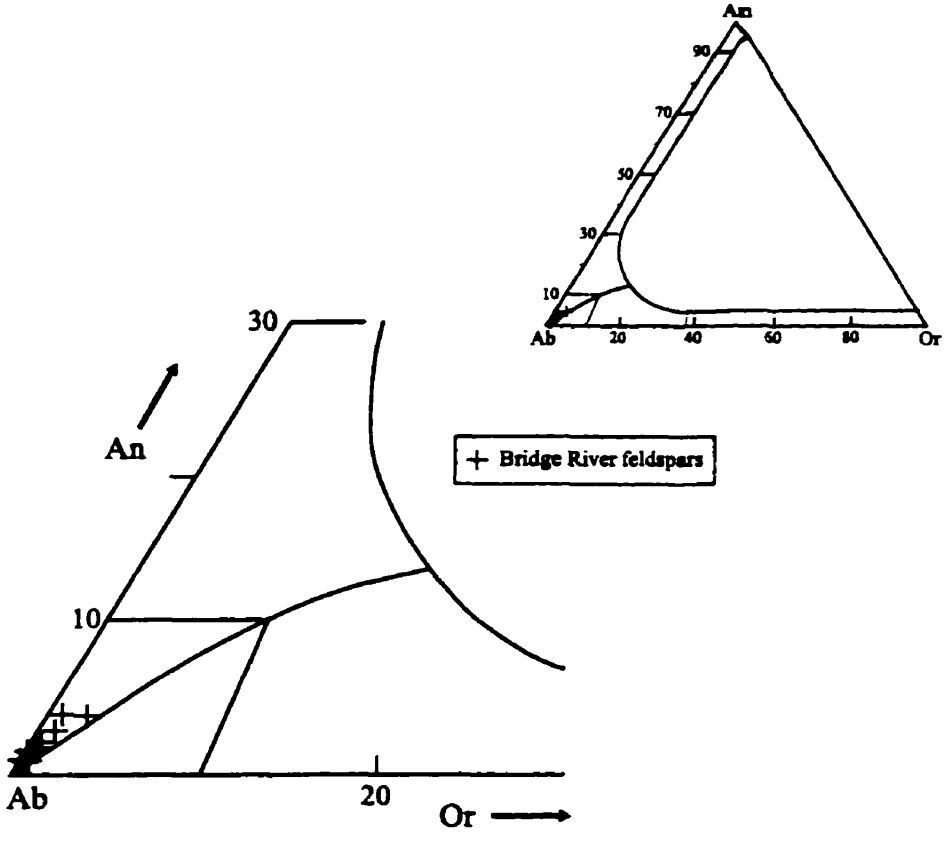

Figure 5-31. Compositional variation diagram of feldspar from the Bridge River Complex study area.

5.2.10 Other Phases

Several other, less abundant, phases are present in the study area. These include: titanite, rutile, leuxocene, quartz, carbonate, datolite and pyrite. The characteristics of each of these phases are presented below.

Titanite is the dominant Ti-phase in blueschists and blueschist-bearing rocks but is rarer in greenstones and absent from metacherts. It forms as either small granules (< 10 μm) or as coarse, idioblastic to sub-idioblastic crystals (approximately 50 x 20 μm) in epidote-blueschist assemblages (see Figure 5-32).

Figure 5-32. Coarse-grained, idioblastic and subidioblastic titanites (Sample TL-88-16)

Representative electron microprobe analyses of titanites are presented in and are shown on a Ti-Al-Fe_{total} plot (Figure 5-33). Analyses indicate that the Carpenter Lake-Tyaughton Creek area titanites show the greatest compositional variability. Titanite from the North Cinnabar Creek area is close to end member composition whereas titanite from the Carpenter Lake-Tyaughton Creek area contains significant Al_2O_3 (maximum value 7.3 weight per cent). Besides variations in Al_2O_3 content, significant variability in MgO content exist between the two occurrences. Titanite from the North Cinnabar Creek area typically has insignificant amounts of MgO whereas those occurring in the Carpenter Lake-

Table 5-14. Representative electron microprobe analyses of titanite

	97-DJH-034-1 core	97-DJH-034-1 rim	TL-88-16 core	TL-88-16 rim	97-DJH-018-1	TL-88-16	97-DJH-HC-1	97-DJH-110-1	97-DJH-110-1	92-GBR-38
SiO_2	32.99	31.92	33.31	32.14	32.47	30.69	31.33	32.01	31.82	31.43
TiO_2	34.08	39.22	36.17	39.00	26.72	38.77	38.74	34.21	39.18	33.76
Al_2O_3	4.18	1.03	2.45	1.03	7.32	1.99	1.30	4.01	1.05	5.06
FeO*	1.49	0.65	1.02	0.59	4.65	0.60	0.66	1.36	0.65	1.05
MnO	<dl	<dl	<dl	<dl	0.1	0.07	0.07	<dl	0.06	0.10
MgO	0.37	<dl	0.45	<dl	3.93	0.08	<dl	0.27	0.07	3.76
CaO	27.41	27.35	25.70	27.27	23.09	27.00	27.23	27.43	27.35	23.26
Na_2O	<dl	<dl	<dl	<dl	<dl	<dl	<dl	<dl	<dl	<dl
F	<dl	<dl	0.16	0.09	1.45	0.32	0.13	1.25	0.22	0.78
Total	100.59	100.23	99.26	100.12	99.73	99.77	99.46	100.54	100.40	99.2
Structural formulae on the basis of 4 Si										
Si	4.00	4.00	4.00	4.00	4.00	4.00	4.00	4.00	4.00	4.00
Ti	3.11	3.70	3.27	3.65	2.48	3.8	3.72	3.22	3.70	3.23
Al	0.60	0.15	0.35	0.15	1.06	0.31	0.20	0.59	0.16	0.76
Fe	0.15	0.07	0.10	0.06	0.48	0.07	0.07	0.14	0.07	0.11
Mn	-	-	-	-	0.01	0.01	-	-	-	-
Mg	0.07	-	0.08	-	0.72	0.02	-	0.05	0.01	0.71
Ca	3.56	3.67	3.31	3.64	3.05	3.77	3.72	3.67	3.68	3.17

*All Fe as FeO; <dl = below detection limit; na = not analyzed

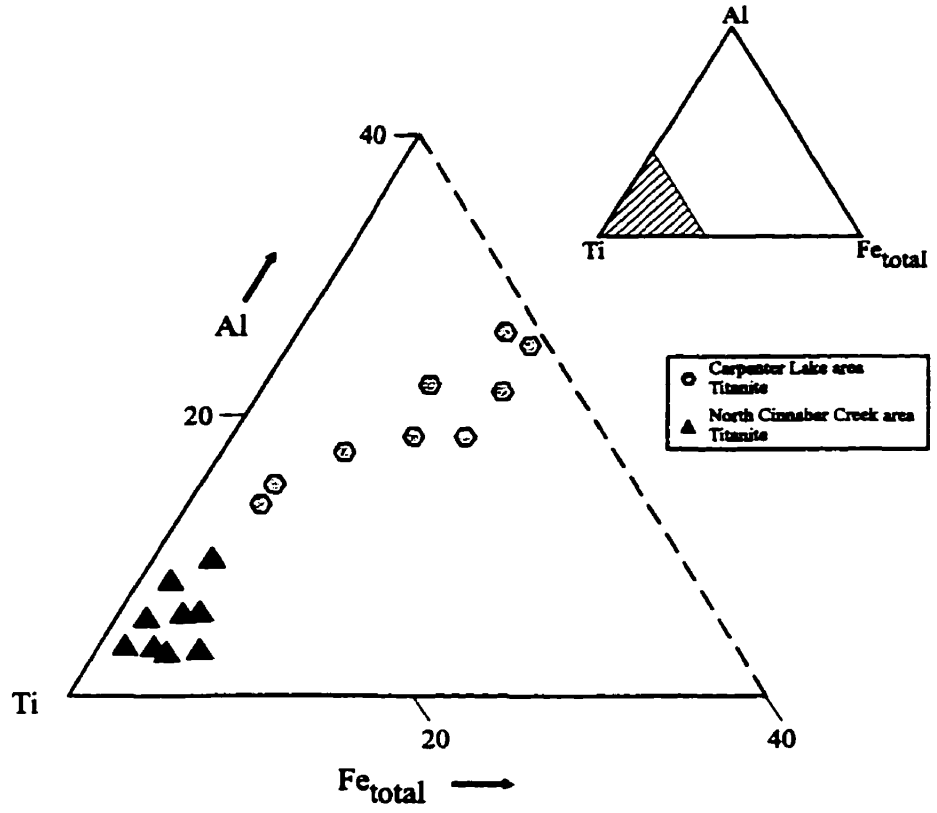

Figure 5-33. Ti-Al-Fe$_{total}$ plot depicting the compositional variation of titanite

Tyaughton Creek areas have a very wide range in MgO content (0.37 – 3.93 weight per cent).

Rutile and leuxocene are the other major Ti-phases present in these rocks. Rutile was found in only two samples, both from the North Cinnabar Creek area. It occurs as small, reddish brown oval shaped crystals with approximate dimensions of 15 x 20 μm. Generally, the long dimensions of these crystals are aligned in the foliation. Leuxocene is most common in the greenstones of the Carpenter Lake-Tyaughton Creek area; it is, however, also present in the North Cinnabar Creek area, within greenstones and some blueschists. It occurs as a fine-grained, grey-brown alteration product of Ti-rich minerals (e.g. Deer et al., 1992) in large patchy regions in greenstones and in 'mafic' metachert layers. Commonly, these patchy regions are greater than 0.5 mm in diameter. The presence

of leuxocene was first reported in these rocks by Schiarizza et al. (1995) as an alteration product, presumably of relict igneous phenocrysts, within many greenstones.

Quartz occurs as a fine to coarse grained, inclusion free phase in many rocks of the Bridge River study area. In some quartz-rich rocks, it appears clastic. It is most common in metacherts and rarer in blueschists and greenstones. Quartz is the major component of veins that crosscut both greenstones and blueschists. It commonly occurs in contact with sodic amphibole, lawsonite, white mica, stilpnomelane, chlorite, carbonate, albite and less commonly, jadeitic pyroxene. Quartz is variably deformed and/or recrystallized in these rocks. Vein quartz is of variable grain size and is primarily undeformed with only a few crystals displaying moderate strain shadows. Typically, these crystals show sutured grain boundaries. Quartz found in the interstices of some blueschist shows evidence of recrystallization (e.g. uniform grain size, triple junctions) and appears relatively unstrained. Metachert quartz is commonly recrystallized with well-developed triple-junction grain boundaries and generally little evidence of strain. Some regions remain cryptocrystalline.

Carbonate is present in the study area as calcite and the dolomite-group member ankerite. These minerals were identified petrographically and through X-ray diffraction analysis. M.E. Back and F.J Wicks confirmed the presence of ankerite in these samples using microbeam X-ray diffraction (see Wicks et al., 1995 for a further description of the technique). In greenstones and blueschists, carbonate occurs in veins along with quartz and carbonate as relatively coarse crystals that range in size up to 1.0 x 1.0 mm; in the blueschists as small crystal aggregates typically less than 40 x 40 μm in size; and replacing relict phenocrysts or filling void spaces in greenstones.

Aragonite was not detected either petrographically nor through X-ray diffraction analysis. Several crystals did display an apparent small 2V of approximately 18-20°, which suggests aragonite. However, these sections did not display the characteristic {110} lamellar twinning cut normal to the acute bisectrix ($2V_{\alpha} \approx 20°$). Therefore, it was determined that these grains were deformed calcite sections cut normal to the c-crystallographic axis.

Datolite is found in two greenstones from the Carpenter Lake area. It occurs in cavities and veins as coarse (up to 500 x 300 μm) radiating crystal bundles (see Figure 5-34). Datolite was originally misidentified petrographically as prehnite. However, when electron microprobe analysis at the University of Calgary was attempted, the results were consistently well below acceptable values for prehnite (e.g. Deer et al., 1992) with the results yielding a Ca/Si ratio of close to 1.0. X-ray diffraction patterns (Table 5-15) confirmed the presence of datolite. Qualitative analysis of the mineral by M. Raudsepp at the University of British Columbia using a Cameca SX-50 electron microprobe with synthetic multi-layer diffracting crystals for detecting light elements confirmed the presence of significant amounts of boron. This further confirmed the mineral's identity.

Table 5-15. Comparison of X-ray Diffraction data for datolite with calculated pattern. vs = very strong peak intensity (>80); s = strong peak intensity (61-79); m = moderate (21-50). Calculated patterns are from Borg and Smith (1969).

97-DJH-031-2		**Calculated Pattern**	
d(Å)	Intensity	*d*(Å)	Intensity
3.77	s	3.761	61
3.12	vs	3.116	100
2.86	s	2.856	79
3.0	m	2.989	44
2.24	m	2.244	49

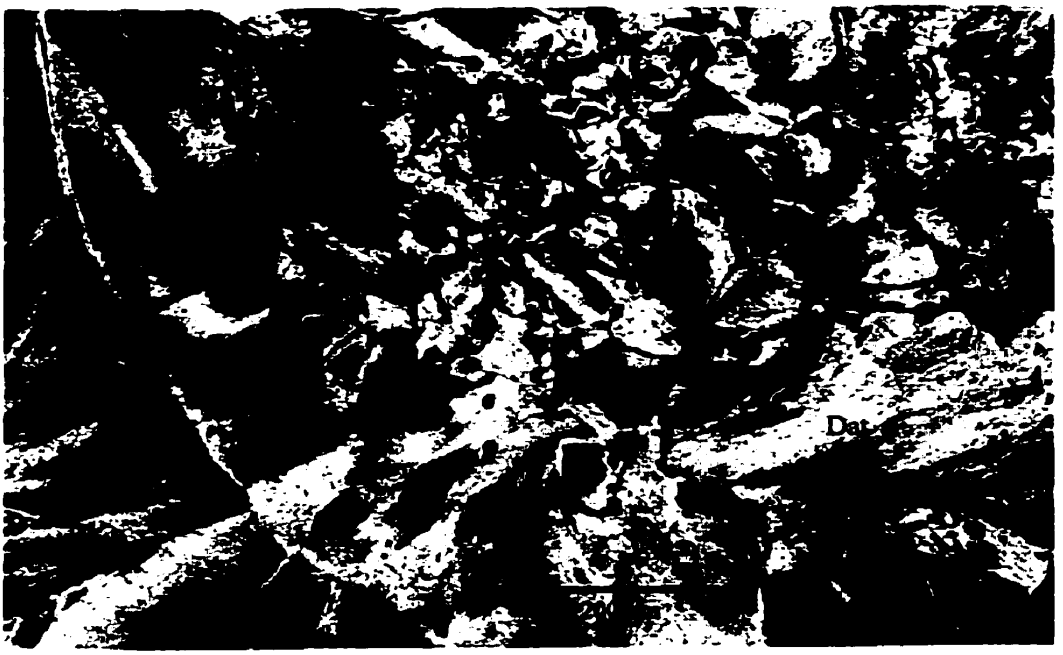

Figure 5-34. Coarse-grained radiating bundles of datolite with minor albite (Sample 97-DJH-031-2)

6. METAMORPHISM

6.1 PROTOLITHS

Protoliths from the Bridge River complex are inferred from relict mineralogy, textural relationships, metamorphic mineral assemblages, bulk rock chemistry and field relationships. As discussed in previous chapters, the fine-grained nature of these rocks and the local, limited, outcrop exposure made it difficult to establish a meaningful stratigraphic succession (e.g. Potter, 1983; 1986; Schiarizza et al., 1989).

Based upon the above criteria, the dominant lithology in this portion of the Bridge River Complex consists of metavolcanic rocks: basaltic flows and mafic tuffs. From rock chemistry, discussed in Chapter 4, I infer that the greenstones and some blueschists are chemically intermediate between spreading ridge generated ocean-floor tholeiites and more alkalic, ocean-island type basalts. Apparent pillows as well as well-developed variolitic texture suggest that some of the Bridge River rocks represent the extrusion of a basic magma into a submarine setting.

Many greenstones are metamorphosed tuffs that consist of altered glass shards with no obvious crystals or crystal fragments. Variable alteration (spilitization) and metamorphic segregation (to be discussed in the following section) of these rocks produced the most abundant lithologies seen in the study area. Other greenstones may be of sedimentary origin. These sedimentary greenstones are massive and may be argillites with a significant tuffaceous component. They commonly contain relict igneous pyroxene crystals. These greenstones may be similar to the argillaceous crystal tuffs described by Ghent et al (1996).

Metamorphosed cherts comprise the remaining protolith in the study area. They are characterized by highly contorted, thin laminae (less than 400 μm wide) of blue amphibole, white mica and locally stilpnomelane. These blueschist laminae occur as distinctive layers separated from each other by millimeter to centimeter-scale quartz-rich layers. The laminae

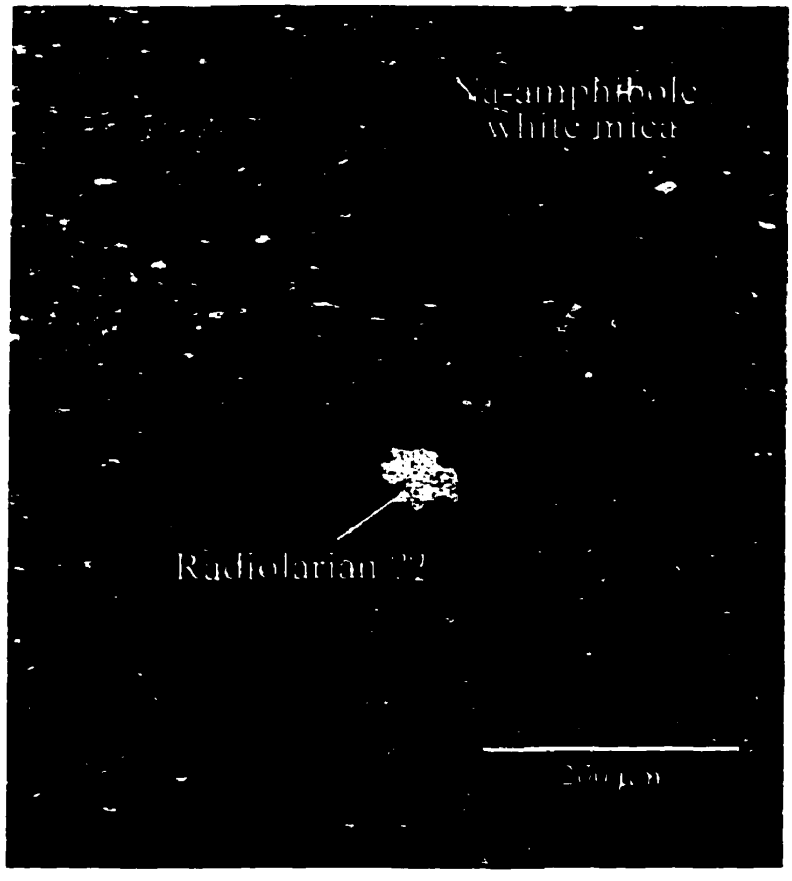

Figure 6-1. Microphotograph of a well layered tuffaceous/argillaceous unit. Note possible radioarian suggesting a marine depositional environment. (Sample 97-DJH-110-1).

also occur interlayered with quartz at the scale of 50 to 100 μm. These layers probably reflect thin laminae of either argillaceous sediment or possibly volcanic tuff deposited during chert deposition. These may be similar to the more massive argillaceous tuffs described above. The widespread chaotic folding seen in these rocks is probably due to the accretion-subduction process and may include soft sediment deformation since textural evidence suggests that the folding occurred prior to blueschist metamorphism.

One locality (97-DJH-110; see Figure 3-2) yielded a very well layered blueschist sample. Sodic amphibole and white mica-rich layers occur along with lawsonite-rich layers. The presence of a possible radiolarian fossil (see Figure 6-1) suggests that the

parent material for this rock was deposited in a deep ocean setting, spatially associated with cherts and possibly tectonically associated with a convergent plate margin.

6.2 BLUESCHIST –GREENSTONE RELATIONSHIP

As described in previous chapters, the Bridge River blueschists consist of the critical assemblage of glaucophane, lawsonite or epidote ± jadeite whereas the greenstones consist primarily of chlorite, white mica and quartz ± epidote. Attempts were made using the program REACTION (Ball and Robin, 1990), with reference to reactions found in Chatterjee (1971), to chemically balance the assemblages found in the greenstones to those found in the blueschists. It quickly became obvious that the greenstones lack the necessary sodic phase (e.g. Ab) to balance the chemistry. It is therefore possible that the mineral assemblage found in the greenstones is isofacial with the blueschist mineral assemblage. This is not to say that the greenstone assemblage is indicative of the blueschist facies but that this assemblage has an extremely large pressure-temperature stability field (e.g. Yardley, 1989) which overlaps with the blueschist facies (e.g. Evans, 1990).

The coexistence of diverse assemblages in the same rock unit, similar to that seen in the Bridge River Complex, have been well documented in the literature (e.g. Dungan et al., 1983; Moore, 1984; Barrientos and Selverstone, 1993; Baltatzis, 1996). The interlayering of these assemblages could be attributed to: (1) differences in the pressure–temperature conditions of equilibrium in the different layers (e.g. Reinsch, 1979); (2) Tectonic interleaving of rocks of the different metamorphic facies; (3) fluid interaction with the protolith prior to and perhaps during metamorphism (e.g. Moore, 1966; Bebout and Barton, 1989; 1993); (4) bulk chemical differences among the layers (e.g. Dungan, et al., 1983; Evans, 1990); and (5) metamorphic segregation. This section will discuss whether any of the above hypotheses can explain the juxtaposition of the Bridge River blueschist and greenstone assemblages.

As I have demonstrated throughout this study the mineralogical differences between the blueschists and greenstones indicate that the units are not chemically equivalent. Therefore, these bulk compositional differences indicate that variable pressure, temperature and a_{H_2O} cannot account for the difference in the mineralogy observed. Consequently, the rocks could have been metamorphosed under identical pressure, temperature and a_{H_2O} conditions.

Of the five hypotheses, number (1) is the most difficult to envision for the rocks of the study area. The close proximity of these rocks and reported thin layers make it difficult to imagine large variations in pressure (perhaps several kilobars), temperature (perhaps tens of degrees).

Tectonic interleaving (2) is one process that could be used to account for the apparent coexistence of greenstone and blueschist assemblages. In this scenario, the two units would have been metamorphosed under different metamorphic conditions and then juxtaposed against one another. Despite the tectonic disruptions so evident on the maps, little field evidence exists for this hypothesis in the Bridge River rocks. Contacts between the greenstones and blueschists are rarely sharp but more commonly are gradational. There is no evidence for fault contacts between adjacent blueschists and greenstones. It is also difficult to imagine how the small lenses and thin foliae of blueschists could be produced by a tectonic process. Therefore, it is unlikely that the assemblages were tectonically juxtaposed.

As mentioned in an earlier chapter, there may be evidence for a mechanism by which infiltrating fluid aided in the production of blueschist facies minerals (hypothesis 3). Several studies (e.g. Badger, 1993; Bebout and Barton, 1993; 1989) have looked at the effect of fluid-rock interaction, prior to metamorphism, on the development of metamorphic mineral assemblages and textures. Badger (1993), in a study of central Appalachian metabasalts determined that schistose zones of metabasalts reflect metamorphic textures and mineralogies whereas massive regions retain igneous textures and minerals. Very similar features have been reported in the rocks of the study area (e.g. Schiarizza et al.,

1995). Therefore, portions of the rock mass that were hydrated could have been more easily strained and thus became schistose.

Moore (1966) studied the palagonitization of Hawaiian basalts. He determined that during submarine weathering of pillowed basalts Na, Ca and Mn were removed and K, Ti and Fe were gained due to the interaction with seawater. A similar interaction between a basaltic protolith and seawater may have contributed to the overall lithologic variations seen in the Bridge River rocks. The metamorphic mineral assemblage of muscovite-quartz –chlorite in a metabasalt implies significant metasomatism and hydration whereby there was a depletion of Na and Ca and relative enrichment in K and Fe.

Nelson (1991) states that the occurrence of mineral-filled veins and vugs within the Franciscan metamorphic rocks is evidence for widespread fluid infiltration and metasomatism. Bebout and Barton (1993; 1989) suggest that these features reflect the presence of an aqueous fluid phase capable of controlling metamorphic reactions and which modified trace and major element compositions of rocks within the subduction complex. Earlier in this study I described the presence of multiple episodes of veining (pre- to post-metamorphic) within the Bridge River rocks. Commonly, greenstones in the study area are free from veins; however, when present, the veins (or segregations) consist of sodic amphibole with or without lawsonite, quartz or albite. Other veins in the greenstones contain variable amounts of quartz, albite and carbonate. Several blueschist outcrops are heavily veined by quartz, albite and carbonate.

Bebout and Barton (1989; 1993) indicate that vein compositions and alteration of host rocks record the relative mobilities of elements in the fluids during subduction. Therefore, sodic amphibole, albite, lawsonite and quartz indicate the local mobility of Na, Al, Ca and Si. When applied to the Bridge River rocks, this hypothesis suggests that the veins of blueschist facies minerals could result from the metasomatic alteration of host rocks by these fluids. The source of these fluids is inferred to be from deeper regions within the subducting slab.

Further evidence for the alteration of the Bridge River rocks is presented in Figure 6-2, modified from Bebout and Barton (1993). Utilizing a different set of elements than those used in Chapter 4, the compositions of rocks presented here are different from likely protolith compositions. Greenstones and blueschists show the greatest departures from inferred original compositions. It is interesting to note that greenstones with blueschist foliae have compositions nearest those presumed for the protolith. This feature may reflect internal heterogeneities, either original or due to metamorphic segregation, rather than being related to circulating fluids.

Metasomatism of the protolith, prior to blueschist metamorphism, may provide a mechanism by which rock chemistry could be altered sufficiently to produce the assemblages found within the Bridge River rocks. However, no direct petrologic evidence can be used to prove fluid interaction with the protolith occurred. Therefore, for this study, metasomatic alteration of the protolith is not considered a likely mechanism to explain the coexistence of the blueschists and greenstones in the Bridge River Complex.

The only plausible explanation for the differences in mineralogy is a variation in bulk chemistry between the greenstones and blueschists (e.g. Dungan et al., 1983; Evans, 1990). The question that stems from this explanation is how did this difference in bulk chemistry arise?

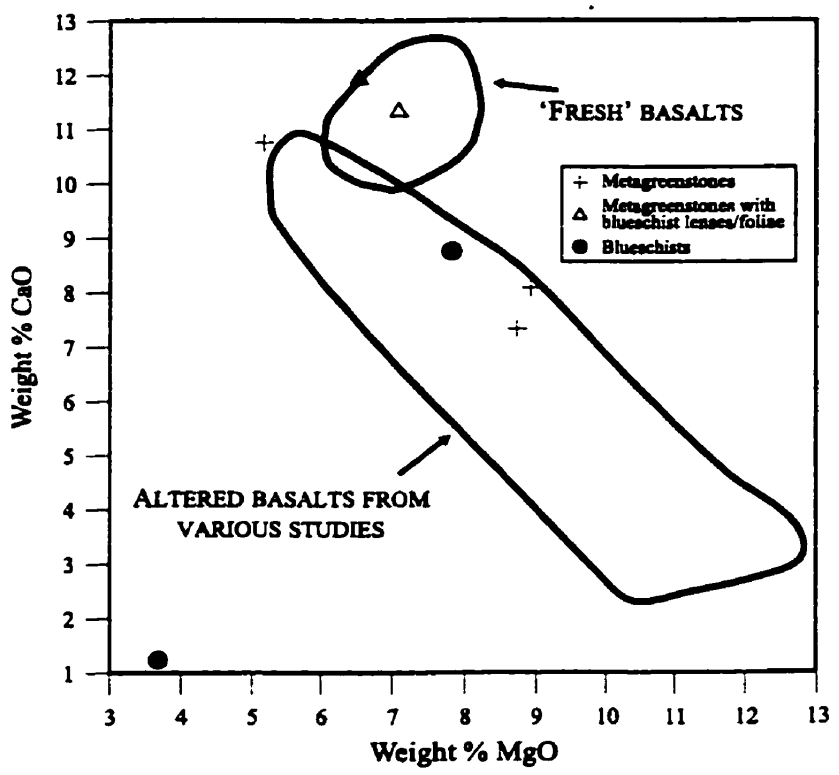

Figure 6-2. Plot of CaO versus MgO, demonstrating variability in the compositions of metabasaltic rocks from the study area (modified from data presented in Bebout and Barton, 1993).

The simplest origin for bulk chemical differences between adjacent regions within the same rock body is heterogeneities within the protolith. In the case of the Bridge River rocks, these differences would reflect local concentrations of elements that were sufficient to allow the crystallization of sodic amphibole and a Ca-Al phase at blueschist conditions. The replacement of igneous phenocrysts by sodic amphibole (see Figures 5-2 and 5-6) is also evidence for this concentration of components. Dobretsov et al (1967) describe spotted glaucophane-bearing greenschists, from the Penzhinsk Range of Northwestern Kamchatka, characterized by concentrations of Ca-Al minerals set in a groundmass of glaucophane. These features are conspicuously similar to the lenses and foliae found within greenstones from this study. Dobretsov et al (1967) ascribe these spots to primary heterogeneities within the basaltic protolith.

From the limited whole rock chemical analyses available (Table 4-1) there is evidence for chemical variations between the greenstones and blueschists, similar to those described by Dungan et al (1983) for the Shuksan greenschists. Generally, the greenstones have low values of Na_2O/CaO (0.07-0.6) whereas blueschists have the highest values (4.1). Furthermore, values for CaO/Fe_2O_3 are highest in the greenstones (0.5 –0.9) and low in the blueschists (0.08). No systematic variation in Na_2O/ Fe_2O_3 values is seen in the Bridge River blueschists and greenstones; values obtained for blueschists are similar to those in the greenstones. Analyses of greenstones with blueschist foliae are not necessarily intermediate between the blueschists and greenstones and cover a range of values for Na_2O/CaO, CaO/Fe_2O_3 and Na_2O/ Fe_2O_3. This variability is likely due to the actual amounts of blueschist lenses or foliae in the rocks.

Sample 92-GBR-19B, described as a blueschist (E.D. Ghent, pers. comm.), presents anomalous data, often contrary to that presented by the other blueschist (92-GBR-37). I am unable to comment on the homogeneity or degree of alteration of this sample, which would significantly affect the rock's chemistry. Although the analysis of sample 92-GBR-37 conforms to the variations discussed by Dungan et al (1983), additional blueschists analyses would be useful. These analyses would serve to determine whether sample 92-GBR-19B is simply the result of analytical error or is in fact representative of the variability in the composition of the blueschists.

Dungan et al (1983) indicate that the variations observed in the Shuksan rocks may roughly define compositional fields for greenschists and blueschists. They also indicate that the multi-element compositional controls that determined the mineralogy reflect the primary differentiation that produced moderately to highly evolved basalt bulk compositions.

Metamorphic segregation, as defined by Robin (1979), is the formation and growth of regions of different bulk compositions within an originally homogenous rock. This differentiation of a metamorphic rock in to mineralogically and chemically different portions appears contrary to the law of increasing entropy (e.g. Robin, 1979; Ehlers and

Blatt, 1982). Harker (1950) describes metamorphic segregation as "...a selective effect in which like is drawn to like, and to that extent separated from unlike by a process which is described rather than explained...". To the knowledge of the author, the same holds today in that few studies have adequately described the processes and mechanisms involved in metamorphic segregation.

According to Robin (1979), it is commonly accepted that metamorphic segregation requires some form of diffusion. The various explanations that have been proposed to drive the diffusion are based either on mineral compatibilities or on gradients in composition, temperature or pressure in the rock system. The thermodynamic reasoning behind metamorphic segregation is probably that grain boundaries between crystals of the same or structurally similar phase are likely to have a lower surface energy than those between unlike phases (e.g. Yardley, 1989). Thus, metamorphic segregation would act to reduce the surface free energy of the system (e.g. Robin, 1979; Yardley, 1989). Again, though, the exact mechanisms of material transfer through the rock system are not fully understood (e.g. Robin, 1979).

Rocks from the Bridge River area display several textural features which suggests that the mineralogical differences between the greenstones and blueschists result from metamorphic segregation. As described earlier, numerous segregations and lenses of blueschist assemblages occur within the various greenstones. Some of these patches are discontinuous and range in length from a few millimetres to less than ten centimetres. These regions may reflect, according to Bowes and Park (1966), the locations of earlier cracks or fissures in the protolith. Bowes and Park (1966) indicate that such features are essential for differentiation due to heterogeneous pressure. Also, the complete replacement of relict plagioclase by lawsonite and of relict phenocrysts by sodic amphibole documented in the Bridge River rocks is evidence for significant mass transfer (e.g. Ghent, 1965)

Differentiation through deformation results from the unequal application of stress. Segregations may be parallel to a metamorphically derived cleavage or may develop in rocks with no evidence of heterogeneous strain (e.g. Robin, 1979; Ehlers and Blatt, 1982).

Bowes and Park (1966) indicate that the cracks and fissures within the Loch Kerry basites are analogous to foliation planes. Differentiation occurs because the constituents with higher molar volumes (and consequently higher free energy) will be unstable in high-pressure areas and will migrate to the low-pressure areas. Ramberg (1952) states that the minerals that will concentrate in the cracks consist of the most mobile elements: Si, Na, K and Al. The elements are essential to forming the minerals found in the segregations within the Bridge River rocks.

Ramberg (1952) also provides a possible explanation for the segregations that are found in the undeformed greenstones. He states that if pressure and temperature conditions are constant throughout a rock body, then the likelihood of new nuclei forming depends on the concentration of the necessary constituents, the mobility of the constituents and free energy relationships. Therefore, if chemical heterogeneities exist in the protolith, it is conceivable that elements of the same type will diffuse from other regions within the protolith into those areas where there is a higher concentration of the element. The pre-existing phase in these highly concentrated areas will then act as nucleation sites. In the Bridge River rocks, original heterogeneities within the protolith are enhanced through metamorphic segregation.

The petrographic and field observations discussed above indicate that metamorphic segregation enhanced by heterogeneities within the protolith, contributed to the formation of the diverse lithologies found within the Bridge River rocks. The effect that fluids had on changing the composition of the rock mass prior to or during metamorphism cannot easily be determined, yet their possible role cannot be discounted. Subduction zones are complex geologic environments where the effects of abundant volatiles (e.g. Bebout and Barton, 1989; 1993; Barrientos and Selverstone, 1993) could readily develop the features documented in the Bridge River blueschists and greenstones.

6.3 METAMORPHIC CONDITIONS

6.3.1 Calculation of Pressure-Temperature Conditions

As discussed earlier, the Bridge River rocks do not contain reaction assemblages. Commonly, blueschists contain high variance assemblages, thus, constraining the pressure, temperature and fluid composition conditions associated with metamorphism requires the study of calculated phase equilibria rather than simple petrogenetic grids (e.g. Ghent et al., 1996). In metabasaltic rocks, this can be done by describing the mineralogy within the system Na_2O-CaO-MgO-FeO-Fe_2O_3-Al_2O_3-SiO_2-H_2O. According to Liou et al (1985), this system accounts for more than 95% by weight of most basaltic rocks. Other components such as K_2O, P_2O_5, CO_2 and TiO_2 can be neglected because each additional component introduced into the system will add only one new mineral. For example, K_2O will add phengite, P_2O_5: apatite, CO_2: calcite and TiO_2: rutile and/or titanite (e.g. Schliestedt, 1986).

The phase equilibria discussed below were calculated using the program PTAX of Brown et al (1989) and databases from Berman (1988) and from Holland (1988) compiled by E.D Ghent (1996, pers. comm.) was used.

Various activity models for solid solution minerals were used in P-T-X calculations that act to displace the equilibria of the solution from its pure end-member. Table 6-1 is a listing of maximum and minimum values for activities used in calculating the phase diagrams.

For glaucophane, the activity model of Evans (1990) was used. The activity of the glaucophane phase component is given by $a_{Na_2Mg_3Al_2Si_8O_{22}(OH)_2} = [Na]^2\,[Mg]^3\,[Al]^2$, where [Na], [Mg] and [Al] refer to the mole fractions of the elements in the specific sites. Models for glaucophane in tremolite was assumed to be charge balanced in terms of activities (Evans, 1990). The activity of tremolite was estimated by $([Na][Ca])^2$ (see Spear, 1993). [Na] and [Ca] refer to the mole fractions of Na and Ca in the M4 site.

The activity model of Bird and Helgeson (1980) was adopted for clinozoisite. The activity of the clinozoisite phase component of epidote was taken to be equivalent to the

mole fraction of Al on the M3 site. Evans (1990) indicates that this is a satisfactory approximation at low temperatures despite the lack of information on which epidote compositions coexist in FeAl exchange equilibirum with sodic amphibole. Lawsonite is near end-member composition, therefore, the activity of the lawsonite phase component is assumed to be 1.0 (e.g. Ghent et al., 1993).

The activity of the clinochlore component of chlorite was modeled after Chernosky et al (1988) and Gordon et al (1991). The activity was estimated by:

$$\left[\left(X^{VI}Mg\right)/\frac{5}{6}\right]^5 \times \left[\left(X^{VI}Al\right)/\frac{1}{6}\right]^1$$

where $X^{VI}Mg$ and $X^{VI}Al$ are the mole fractions of Mg and Al in the octahedral site respectively. The activities used in calculating phase diagrams were from 'fresh' chlorites in the greenstones.

According to Ghent et al. (1996), the activity of the jadeite component of clinopyroxene in low temperature blueschists is approximately equal to X_{jd}^{cpx}, i.e. the mole fraction of jadeite. In cases where diopside was required to set limits on phase equilibria, a_{di} was estimated as 1-a_{jd} for simplicity.

Where grossular and pyrope activities were required for setting limits on phase equilibria, ideal activity models modified from Evans (1990) were used. Pyrope activity was modeled as $(X_{Mg})^3$, grossular as $(X_{Ca})^3$, i.e. the mole fractions of Mg and Ca in the analyzed garnets respectively.

Other phases such as quartz, titanite, rutile, albite and laumontite were modeled as pure phases and thus the activities of their phase components were taken to equal 1.0. The activity of H_2O was assumed to equal 1.0. Evans (1990) adopted an activity of 0.9 for H_2O to allow for other fluid species. In this study, constraints on fluid compositions were not determined and thus any contribution other species may have had to changing the activity of H_2O were assumed to be negligible. Evans (1990) suggests using an activity of 0.95 for paragonite to allow for small amounts of other components, most notably muscovite.

Table 6-1. Component activities used in phase diagram calculations

	Na-amphibole	*Ca-amphibole*	*Jadeite*	*Epidote*	*Pyrope*	*Grossular*	*Chlorite*
Maximum activity	0.18	0.59	0.55	0.36	0.002	0.03	0.14
Minimum activity	0.02	0.14	0.30	0.22	0.002	0.03	0.04

Phase diagrams calculated for the Carpenter Lake -Tyaughton Creek and the North Cinnabar Creek areas are presented in Figure 6-3 and Figure 6-4 respectively. The choice of equilibria used to calculate the diagrams was based on the previously described petrographic analyses. Minerals considered to be in equilibrium were either in contact or were within 0.05mm with one another and showed no obvious signs of reaction. Calcite and/or aragonite do not appear to be a stable phase with either Na-amphibole or lawsonite. Therefore, the following equilibria, calculated in PTAX, were discounted as being distinctive:

$$3\ cal + 3\ chl + 10\ ab + 7\ qtz \Leftrightarrow 5\ gln + 3\ lws + 3\ CO_2 + H_2O$$

$$3\ cal + 3\ chl + 10\ ab + 7\ qtz \Leftrightarrow 2\ czo + 5\ gln + 6\ H_2O + 3\ CO_2$$

The presence of several Ca-amphibole cores rimmed by Na-amphibole suggest that the Bridge River rocks underwent the classic greenschist to epidote-blueschist transition (Evans, 1990) given by:

$$50\ ab + 9\ chl + 6\ tr \Leftrightarrow 25\ gln + 6\ czo + 7\ qtz + 14\ H_2O$$

or alternatively for the transition to lawsonite-blueschist by the reaction:

$$10\ ab + 2\ chl + tr \Leftrightarrow 2\ lws + 5\ gln$$

Minimum pressures for the Bridge River rocks are given by the presence of lawsonite and quartz instead of laumontite. From Figure 6-3 the minimum pressures (for $P_S = P_{H_2O}$; where P_s is lithostatic pressure) are $P > 3$ kbar at 200°C. The lawsonite blueschist assemblage yields minimum pressures of greater than 4.9 kbar at 200°C and greater than 10

kbar at 475°C. For the epidote blueschist assemblage, minimum pressures are greater than 5.5 kbar at 200°C and 8.9 kbar at 500°C (see Figure 6-4). Evans (1990) calculated a significant temperature overlap for lawsonite- and epidote-blueschist parageneses that is dependent on the Fe/Al ratio of epidote and Na-amphibole. The epidote + Na-amphibole field calculated by Evans (1990) is smallest for Al-rich and Fe-poor mineral compositions and largest for Al-poor and Fe-rich compositions. This is related to the preferential incorporation of Fe^{3+} by epidote and Na-amphibole relative to lawsonite, actinolite and chlorite. The apparent coexistence of lawsonite- and epidote blueschists seen in the Bridge River rocks is best explained by local compositional variations (e.g. Evans, 1990).

The presence of jadeitic pyroxene and quartz in the Bridge River rocks instead of albite indicates that the pressures were greater than 7.1 kbar at 200°C and 10.6 kbar at 400°C for $X_{jd}^{cpx} = 0.55$. For $X_{jd}^{cpx} = 0.30$ the conditions change to greater than 5.6 kbar at 200°C and 8.5 kbar at 400°C (see Figure 6-3).

The presence of lawsonite and glaucophane instead of epidote, quartz, pyrope and pyroxene ($X_{jd}^{cpx} = 0.55$) suggest that temperatures did not exceed 480°C at 12 kbar and 498°C at 14 kbar. The presence of epidote and glaucophane instead of pyroxene ($X_{jd}^{cpx} = 0.55$; $X_{di}^{cpx} = 0.45$), lawsonite and pyrope suggest that temperatures were in excess of 305°C at 10 kbar and 400°C at 14 kbar (see Figures 6-3 and 6-4). The equilibrium:

$$lws + gln \Leftrightarrow czo + qtz + prp + jd + H_2O$$

is only moderately affected by using the lower activities (see Figure 1-5). However, the combined effects of decreasing all other activities and increasing the activity of diopside drastically alters the position of the equilibrium:

$$di + jd + lws + prp \Leftrightarrow gln + czo + H_2O$$

This change moves the equilibirum to 248°C at 10 kbar and 336°C at 14 kbar.

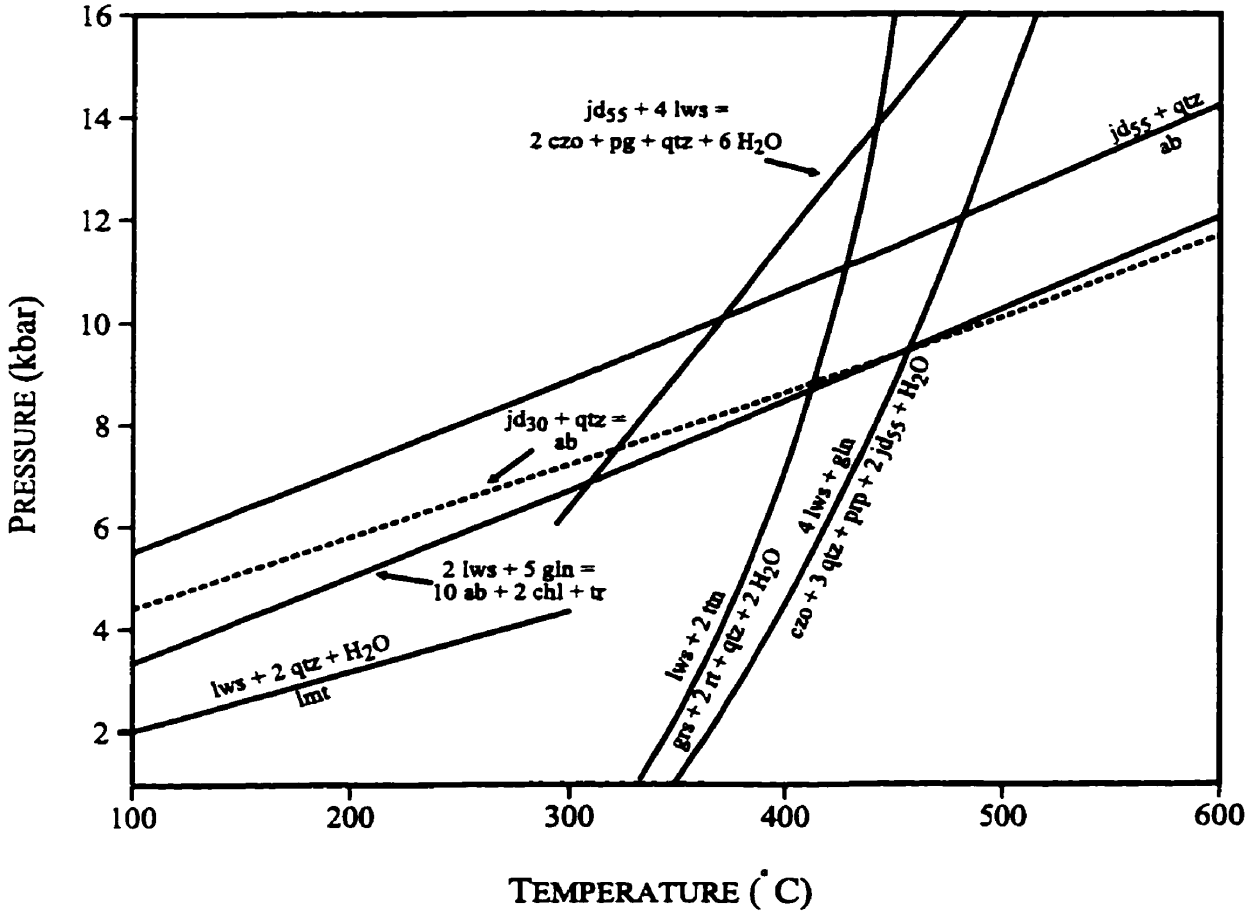

Figure 6-3. Pressure-temperature diagram for phases related to the Carpenter Lake - Tyaughton Creek areas. Phase diagram calculated using the program PTAX (Brown et al., 1989) and the databases of Berman (1988) and from Holland (1988), compiled by Ghent (1996, pers. comm.)

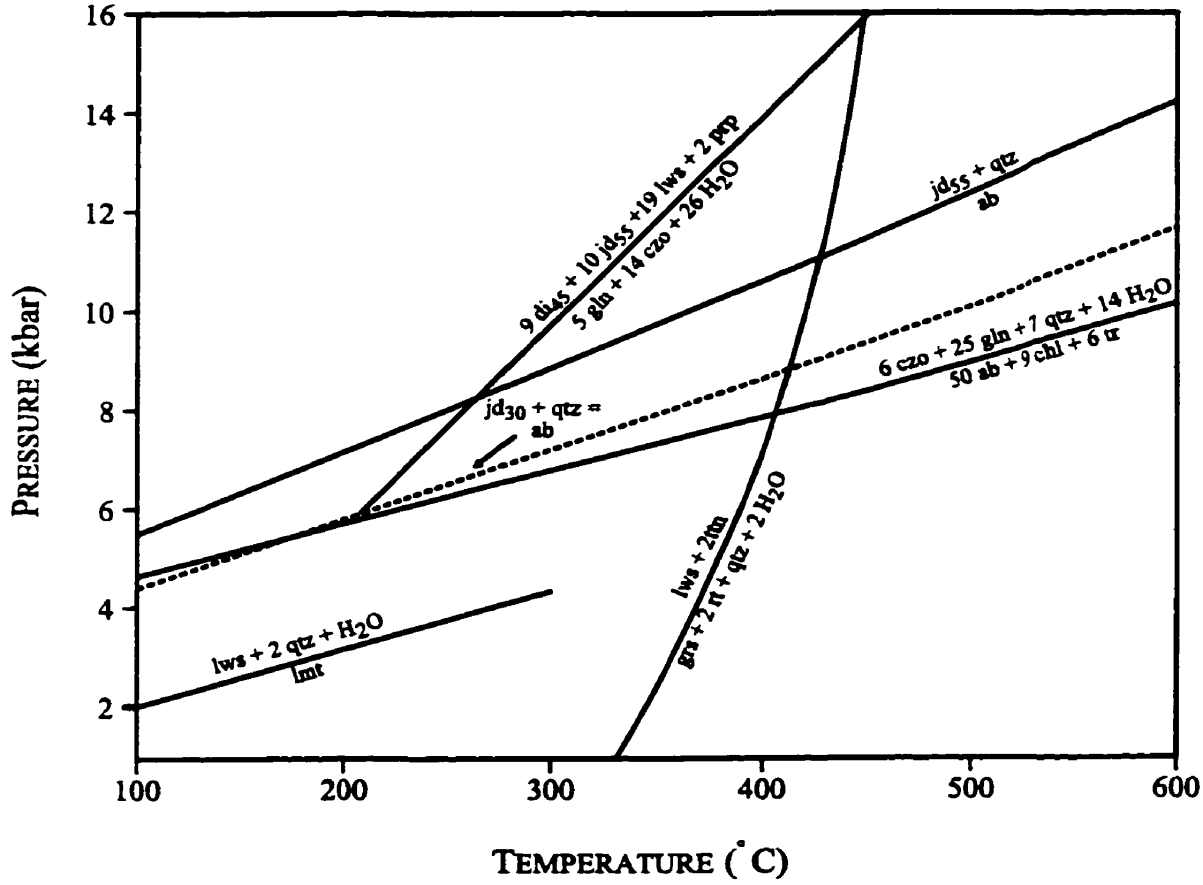

Figure 6-4. Pressure-temperature diagram for phases related to the North Cinnabar Creek area. Phase diagram calculated using the program PTAX (Brown et al., 1989) and the databases of Berman (1988) and from Holland (1988), compiled by Ghent (1996, pers. comm.)

The presence of jadeitic pyroxene ($X_{jd}^{cpx} = 0.55$) and lawsonite instead of epidote, paragonite and quartz within the Tyaughton Creek blueschists suggests that temperature did not exceed 404°C at 12 kbar. The presence of lawsonite and titanite instead of grossular, rutile and quartz (for $a_{H_2O} = 1.0$) suggests that temperatures were less than 430°C at 11 kbar and 440°C at 14 kbar.

Based upon the equilibria described above, brackets can be placed on the pressure and temperature conditions of blueschist metamorphism within the Bridge River complex. Within the Carpenter Lake-Tyaughton Creek areas metamorphic conditions did not exceed the stability limits of lawsonite + glaucophane (Figure 6-3). However, the local presence of jadeitic pyroxene + quartz, jadeitic pyroxene + lawsonite and lawsonite + titanite set minimum pressures at maximum temperatures for the area (Figure 6-3). Minimum temperature limits cannot be determined for the area. In the North Cinnabar Creek area, metamorphic pressure-temperature conditions are better constrained. Minimum temperatures are defined by the equilibirum Na-amphibole + epidote, whereas maximum temperatures are controlled by the local presence of lawsonite + titanite in the rocks (Figure 6-4). Minimum pressures are a constrained by the occurrence of epidote + glaucophane + quartz. However, the presence of jadeitic pyroxene elsewhere in the complex would indicate that minimum pressures are constrained by the pyroxene + quartz equilibrium (Figure 6-4).

Figure 6-5 is a comparison of phase equilibria using the calculated maximum and minimum mineral activities. The effect of varying phase component activities ($a_{H_2O} = 1.0$) is least for equilibria with steep reaction curves (e.g. lws + 2 ttn ⇔ grs + 2 rt + qtz + 2 H_2O). The greatest variability is observed for equilibria with shallow reaction curves (e.g. jd + qtz ⇔ ab). For the equilibrium:

$$6\ czo + 25\ gln + 7\ qtz + 14\ H_2O \Leftrightarrow 50\ ab + 9\ chl + 6\ tr$$

the effect of decreasing the activities is that the classic transition from greenschist to blueschist assemblages is brought to significantly lower pressures.

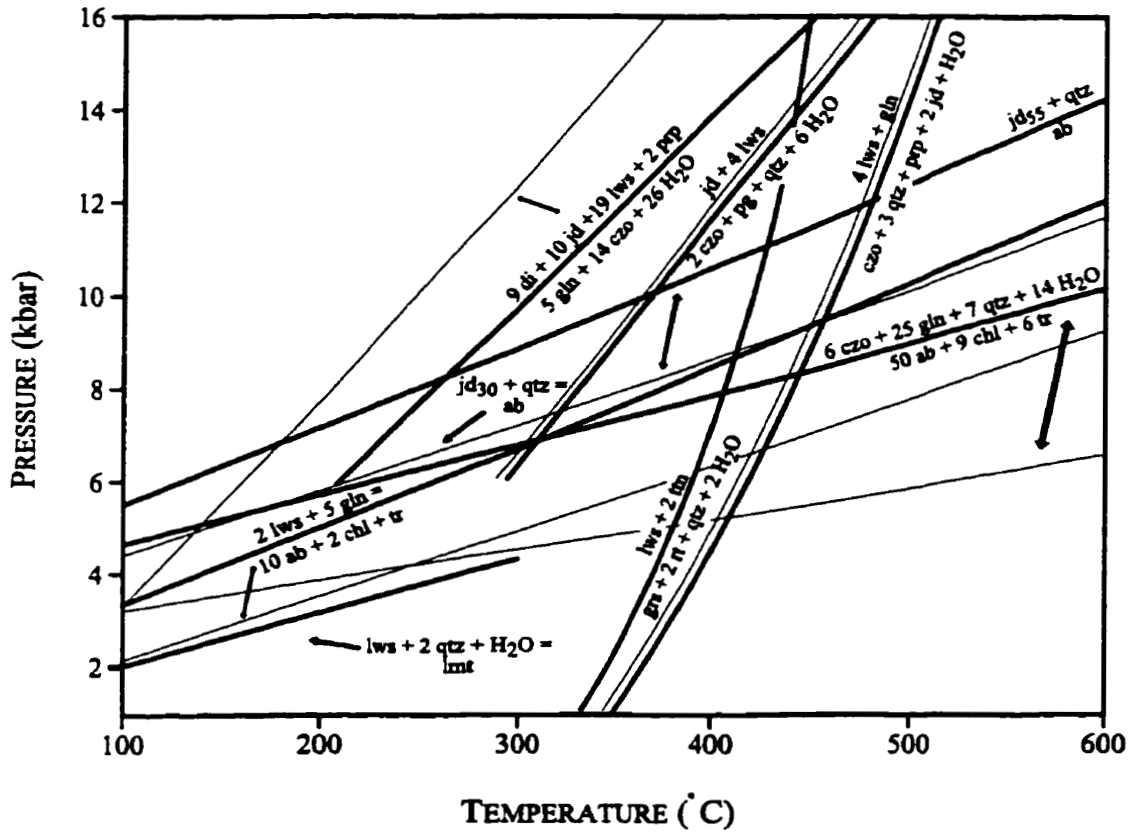

Figure 6-5. Pressure-temperature diagram for phases particular to the Bridge River blueschists. Thick lines are for equilibria calculated with maximum phase activities; thin lines are for equilibria calculated with minimum phase activities. Arrows connect equilibria of maximum and minimum activities. Phase diagram calculated using the program PTAX (Brown et al., 1989) and the databases of Berman (1988) and from Holland (1988), compiled by Ghent (1996, pers. comm.)

6.3.2 Fluids Accompanying Metamorphism

The presence of a fluid phase prior to and perhaps during metamorphism, and its possible role in developing the lithologic variations, was discussed earlier. Two distinctive features that resulted from the fluid phase are 1) veins and segregations of blueschist facies minerals; and 2) the complete replacement of igneous phenocrysts by lawsonite and sodic amphibole. These features suggest that at least some components were mobile during metamorphism (e.g. Ghent, 1965; Bebout and Barton, 1989; 1993).

To better constrain the fluid composition associated with blueschist metamorphism in the Bridge River complex the following T-X_{CO_2} diagram (Figure 1-6) was computed, using PTAX (Brown et al., 1988), for equilibria pertinent to these rocks. Based on the presence of lawsonite and titanite in the Bridge River rocks, the metamorphic fluids were low in CO_2. This is consistent with the presence of titanite instead of calcite (or aragonite), rutile and quartz (e.g. Ghent et al., 1996). According to the PTAX calculation, X_{CO_2} was less than approximately 0.02 at 8 kbar and 350°C. From Figure 6-6, it is also evident that the stability field for lawsonite + Na-amphibole is confined to lower X_{CO_2}. Given the temperatures bracketed for blueschist metamorphism in the Bridge River complex, low values of X_{CO_2} are also indicated.

According to the T- X_{CO_2} diagram (Figure 1-6) it appears that the earlier assumption of a_{H_2O}=1.0 should be satisfactory since the reactions indicate low values of X_{CO_2}. However, several authors (e.g. Barrientos and Selverstone, 1989; Bebout and Barton, 1989; 1993; El-Shazly et al., 1997) mention the presence of a number of volatile species in fluids associated with blueschist metamorphism. Therefore, it is unlikely that a_{H_2O} = 1.0 and the approximation of Evans (1990), where a_{H_2O} = 0.9, may be more appropriate. Figure 6-7 is a comparison of different a_{H_2O} values for the reactions examined earlier. It is apparent that as a_{H_2O} decreases the equilibrium curves shift to lower temperatures, thus expanding the stability field of the H_2O-side of the reaction. This has the effect of slightly increasing the

stability field of the North Cinnabar Creek area rocks (i.e. epidote blueschists) and slightly decreasing the maximum temperature stability of the Carpenter Lake – Tyaughton Creek rocks (i.e. lawsonite blueschists). According to the diagram, there is very little effect on the classic greenschist to blueschist transition reaction.

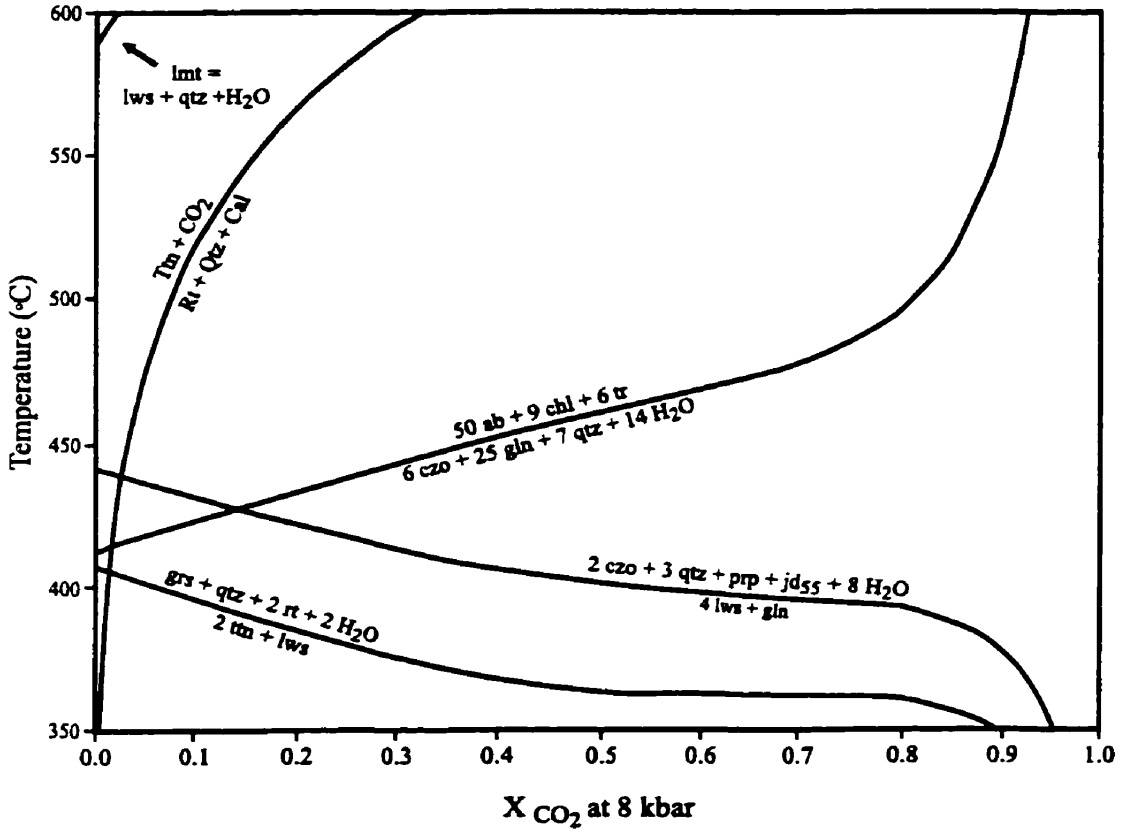

Figure 6-6. T-X_{CO_2} diagram calculated using PTAX for reactions pertinent to the Bridge River rocks.

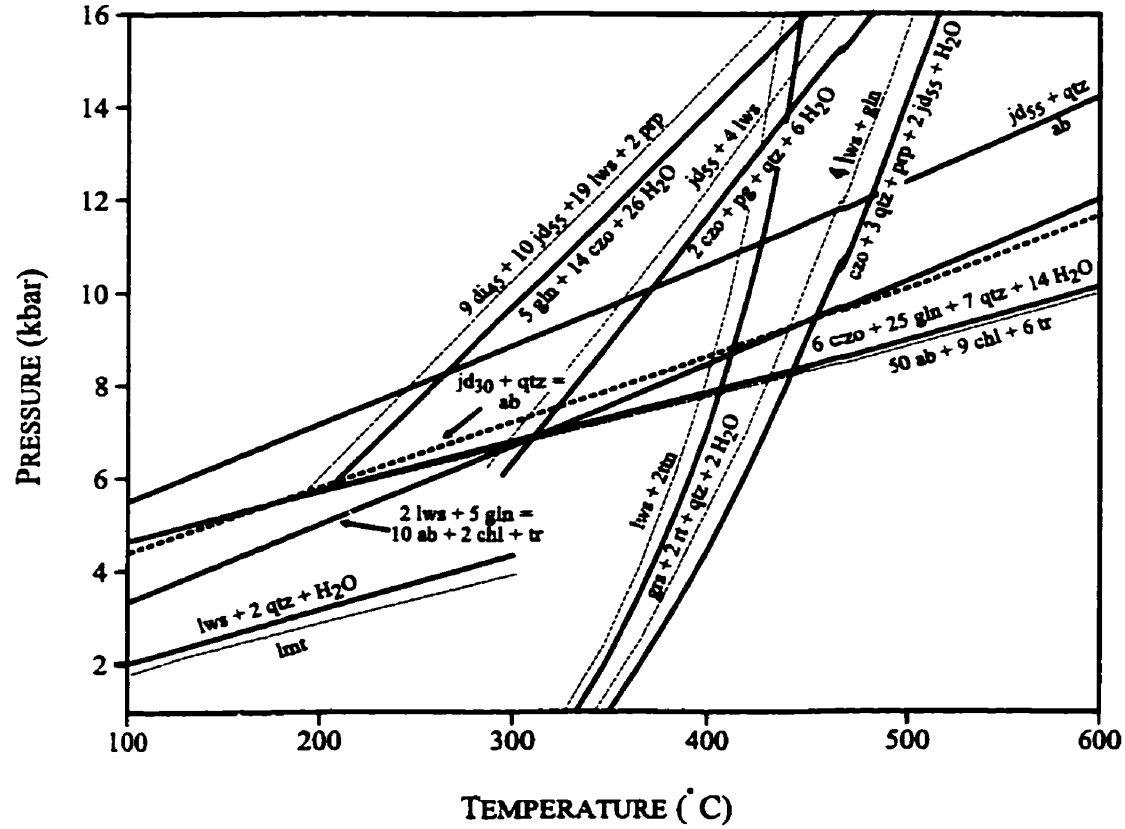

Figure 6-7. Pressure-temperature diagram calculated using PTAX. Solid lines refer to reactions with a_{H_2O}=1.0; dashed lines refer to reactions where a_{H_2O}=0.9.

6.3.3 Constraints on the *P-T* path of the Bridge River Blueschists

The inferred P-T paths experienced by blueschists are summarized by Ernst (1988). Prograde P-T trajectories typically involve the protolith passing through zeolite to prehnite-pumpellyite and sometimes into greenschist grades before reaching blueschist conditions (e.g. Ernst, 1988). According to Spear (1993) most prograde P-T paths have slopes on the order of 35 to 40°C/kbar (approximately 10°C/km). For the preservation of blueschists assemblages without any overprinting, retrograde paths must be nearly coincident with the prograde paths.

For the Bridge River blueschists, few constraints can be put on the P-T path other than those related to peak metamorphic conditions. The lack of stable aragonite (or calcite) makes it difficult to comment on the geothermal gradients at the time of uplift. According to Brown et al (1962), if aragonite were present the geothermal gradient at the time of metamorphism could not have been much greater than 10°C/km and the aragonite must have been 'dry' during unroofing. If either of these conditions were not met, aragonite would not have been preserved. Furthermore, Liu and Yund (1993) suggest that preservation of aragonite in dry rocks can only occur if the calcite stability field is entered at approximately 235°C or less.

Figure 6-8 is the inferred P-T path (dashed line) followed by the Bridge River blueschists. Assuming the maximum pressure and temperatures attained by these rocks was 10 kbar and 300°C, the slope of the prograde P-T path would be approximately 9°C/km. The retrograde path would have been nearly coincident with the prograde since overprinting by higher temperature assemblages did not occur. From Figure 6-8 it is apparent that the maximum P-T conditions reached fall within the stability field for the lawsonite blueschists (given a_{H_2O} = 1.0) since no low temperature limit for the assemblage can be defined. However, given the same conditions it appears that the *P-T* path falls outside the stability field for the epidote blueschists. Therefore, it is likely that each block followed its own, separate *P-T* path with the North Cinnabar Creek blueschists entering the stability field for epidote blueschists and the Carpenter Lake – Tyaughton Creek blueschists being confined to the lawsonite blueschist stability field.

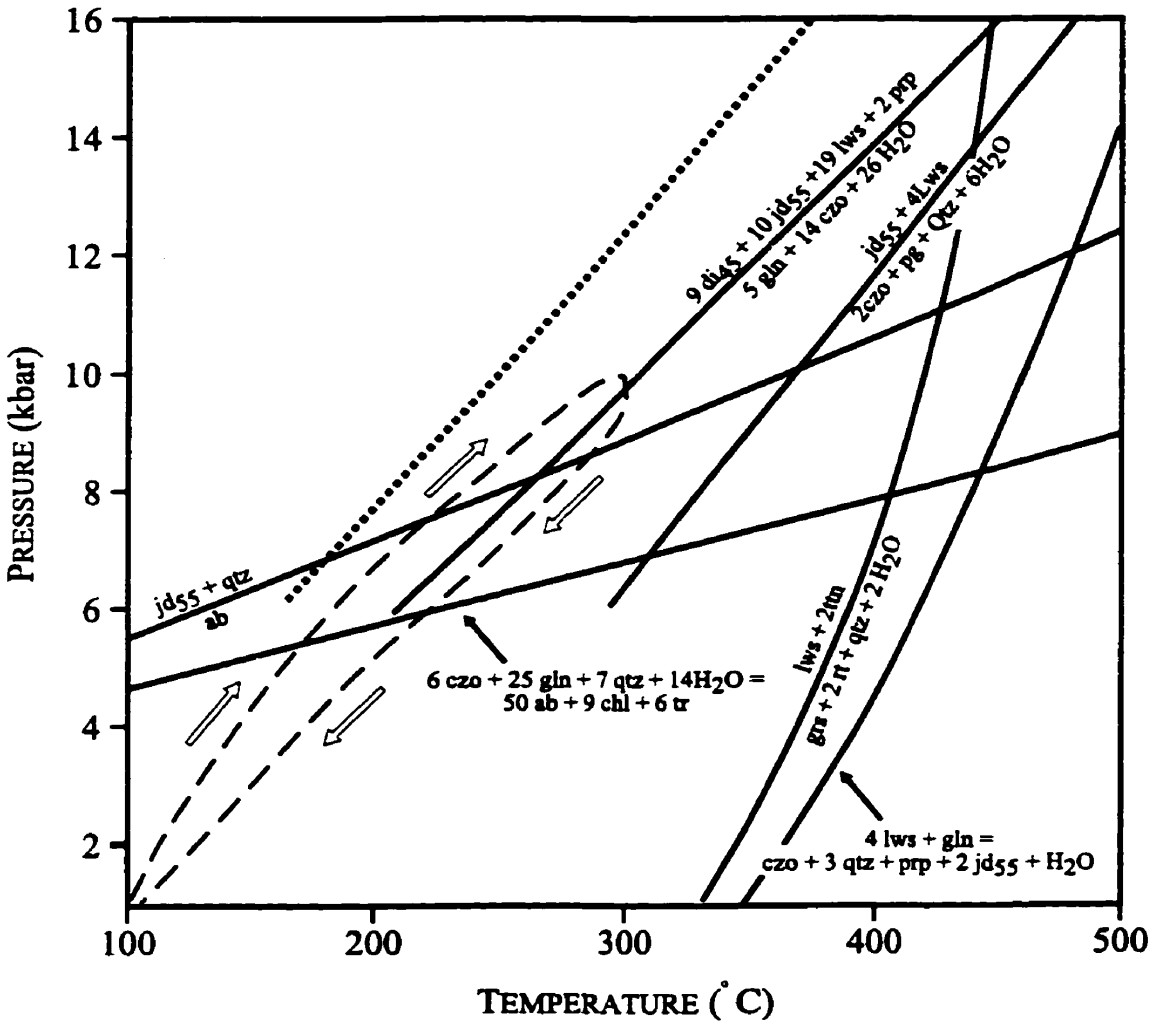

Figure 6-8. Inferred P-T path (dashed line) for burial and exhumation of the Bridge River blueschists. Maximum P-T conditions reached are assumed to be 10 kbar at 300°C with $P_{H_2O} = P_s$. Given local decrease in a_{H_2O} the epidote blueschist assemblage is encountered along this path. The dotted line corresponds to the stability limits for epidote blueschist paragenesis given $a_{H_2O} = 0.9$ rather than $a_{H_2O} = 1$ (solid line)

6.4 TECTONIC EVOLUTION

Detailed studies (e.g. Potter, 1983; 1986; Garver et al., 1989; Schiarizza et al., 1989) have concluded that the Bridge River complex accumulated as an accretion-subduction complex. This conclusion is based primarily upon the wide age range, lack of an internal stratigraphy, and the presence of blueschists.

As discussed in Chapter 2, Potter (1983; 1986) proposed three models that describe the paleotectonic setting of the Bridge River complex. These are: (A) telescoping of a back arc basin after a colliding fragment has stalled forearc subduction; (B) underplating of undeformed slabs of oceanic rocks in a subduction complex; (C) transpressional collapse of a small sea of unspecified origin (see Figure 2-3). Given additional data provided by Garver et al., (1989), Schiarizza et al., (1989), Archibald et al, (1991) and Garver (1991), and models presented by several workers (e.g. Draper and Bone, 1981; Cloos, 1986; Platt, 1986; 1987; Ernst, 1988; and Peacock, 1993) regarding blueschist generation, preservation and exhumation, I propose that a setting similar to Potter's model (B) is most consistent with the observations.

It has been well established that pressure-temperature conditions for blueschist generation exist at subduction zones (e.g. Ernst, 1988, Peacock, 1993). At these plate margins, relatively rapid lithospheric destruction is taking place and oceanic sediment piles up within an accretionary prism, against the landward side of the subduction complex. Furthermore, Ernst (1977) indicates that a major feature of subduction zones is a pronounced downwarp of the isotherms in the upper portions of the descending slab and in the complex itself. According to Oxburgh and Turcotte (1971), the rate at which accretion is taking place is too great for sediments to reach thermal equilibrium as they accumulate. Therefore, thermal gradients within the prism tend to be extremely low. If the accretionary prism is sufficiently thick, blueschist metamorphic conditions would be attained in its lower parts. An essential component of this model is that subduction of the oceanic crust must

continue to prevent the thermal conditions within the accretionary prism from equilibrating with its surroundings.

Peacock (1993) indicates that subducting oceanic crust, on its own, will encounter different metamorphic facies as the subduction zone evolves. This results from the progressive cooling of the thermal structure of the subducting zone, with time, until a steady-state regime is achieved. According to Peacock (1993), once a subduction zone has reached a steady-state thermal structure, the subducting slab can undergo blueschist to eclogite facies metamorphism. The variation in metamorphism with time depends primarily on the rate of shear heating. Different metamorphic regimes are encountered at different levels within the oceanic crust because the rocks within the crust are located at various distances away from the subduction shear zone. Although the Peacock (1993) model allows for the development of blueschist metamorphic conditions, I believe that the geologic evidence described earlier (i.e. variable assemblage of lithologies, chaotic structural style and large age range) indicates that Bridge River rocks in the study area were derived from the subduction of oceanic crust and the associated accretionary prism.

Once blueschist metamorphic conditions have been achieved, it is necessary for exhumation to occur quickly so that temperature conditions within the accretionary prism do not equilibrate with the surroundings and overprint the blueschist assemblage (e.g. Ernst, 1988). Several studies have attempted to provide mechanisms for the uplift of blueschists from depth. In their scaled model of an accretionary prism, Cowan and Silling (1978) observed upward flow of material within the prism during continued subduction. This upward flow of material could provide a mechanism of moving blueschist up from depth. However, as material is added to the base of the prism, the entire prism grows and the blueschists never get any closer to the surface (Platt, 1986; 1987). Cloos (1986) proposes that syn-subduction uplift is required for blueschist preservation. Therefore, to preserve and then expose blueschists at the Earth's surface, it is necessary to remove material stratigraphically above the blueschists.

Platt (1986; 1987) indicates that continued underplating makes the accretionary prism become gravitationally unstable which results in the formation of listric normal faults. These faults allow for significant extension, which can aid in exposing the blueschists. Thrust faults described by Garver (1991) could have provided some of the transport mechanism that brought the Bridge River blueschists to the surface.

The rates of unroofing necessary for the preservation of blueschists during exhumation have been modeled by Draper and Bone (1980). They indicate that exhumation is the result of both fluvio-glacial erosion and large-scale mass movement either by tectonic mechanisms or through large scale mass wasting. Draper and Bone (1980) stated that denudation rates slower than 0.14 cm per year would result in the prograde metamorphism of the blueschists to higher temperature assemblages. For the Bridge River rocks, assuming a pressure of 8 kbar and a density of 2.85 g cm^{-3}, metamorphism would have taken place at a depth of approximately 29 km. Assuming a denudation rate of 0.14 cm per year, the Bridge River blueschists would have a maximum time of approximately 21 Ma to reach the surface.

The requirement of continued subduction for the preservation and exhumation of blueschists discussed by Ernst (1988) is consistent with observations made during several studies of the Bridge River complex. $^{40}Ar/^{39}Ar$ dating by Archibald et al., (1991) indicate that the blueschist metamorphic event in the area ended at approximately 230 Ma. However, Cordey and Schiarizza (1993) provide a radiolarian age range for the complex from Mississippian to late Middle Jurassic. Cordey and Schiarizza (1993) conclude that this information indicates that the ocean basin behind the subduction zone must have been large because of this large age range (approximately 180 Ma). These studies indicate that the blueschist metamorphic event is older than some parts of the complex.

One possible explanation is that the Bridge River complex is not one coherent unit but is actually several units whose structural relationships are obscure and hide the true nature of the complex. Alternatively, the Bridge River complex is in fact one unit that has developed over an extremely long period. This alternative model is consistent with Ernst

(1988). The long time span recorded in the Bridge River complex reflects the long, continuous subduction required for blueschist preservation and exhumation. This process allowed for depression of the isotherms at depth allowing high pressure, low temperature metamorphism to take place (e.g. Ernst, 1988). Furthermore, continued subduction aids in bringing blueschists at depth, closer to the surface (e.g. Cloos, 1986; Platt, 1986; 1987). As blueschist metamorphism was occurring at depth, the other assemblages were being formed within the accretionary prism and outboard of the subduction zone, in the ocean basin. These younger rocks were accreted within the subduction complex and eventually exposed at the surface. Blueschist metamorphism, therefore, was able to occur prior to the formation of other rocks within the complex.

7. CONCLUSIONS AND SUGGESTIONS FOR FURTHER WORK

7.1 CONCLUSIONS

Five distinctive, fault-bounded blocks of blueschist facies rocks occur within the Bridge River Terrane in southwestern British Columbia. The Bridge River Terrane in the area is represented by the Bridge River complex, a highly disrupted Mississippian to late Middle Jurassic unit consisting primarily of chert, argillite and minor greenstone that likely formed in an accretion-subduction complex (e.g. Garver, 1989; Schiarizza et al., 1989; 1993; Cordey and Schiarizza, 1993).

Archibald et al (1991) reported that the blueschist metamorphic event in the Bridge River complex ended at approximately 230 Ma that suggests that the age of metamorphism is older than other rocks in the complex. This apparent contradiction is rectified through realization that for blueschists to be preserved and exhumed, long, continued subduction is required (e.g. Ernst, 1988). Therefore, as blueschist metamorphism occurred at depth, the other lithologies were still actively forming, within and outboard of the subduction-accretion complex.

Field studies delineated four units within the study area. These include blueschists, blueschists with minor greenstone components, greenstones with blueschist lenses or foliae and metamorphosed cherts. The lack of internal stratigraphy reported by Potter (1986) is very evident within the study area; it is extremely chaotic and disrupted. Many of the structures are discontinuous and cannot be traced beyond any one outcrop.

Petrographic analyses, aided by X-ray Diffraction analyses (required due to the fine-grained nature of the rocks), defined two distinctive blueschist mineral assemblages. The Carpenter Lake-Tyaughton Creek assemblage, in the eastern portion of the study area, consists of sodic amphibole + lawsonite ± jadeitic pyroxene ± stilpnomelane. In the North Cinnabar Creek area, blueschists commonly contain the assemblage sodic amphibole +

epidote ± garnet ± white mica. According to Evans (1990) the epidote blueschists reflect higher temperatures or lower P_{H_2O} than the lawsonite blueschists.

Whole-rock chemical analyses of a limited number of greenstones and blueschists suggest that the rocks have geochemical signatures intermediate between spreading-ridge, ocean floor tholeiites and more alkalic, ocean-island type basalts. These results are consistent with analyses of other greenstones within the Bridge River complex (e.g. Potter, 1983; Church and Pettipas, 1989).

Electron microprobe analyses indicate that sodic to sodic-calcic amphiboles are present in the rocks. Calcic amphiboles are only found in some greenstones as crystal cores rimmed by blue, sodic amphibole. Sodic amphiboles range from glaucophane and ferro-glaucophane to riebeckite and magnesio-riebeckite. Lawsonite and titanite are near end-member composition. Epidote compositions from both blueschists and greenstones range from Ps_{17} to Ps_{28}. Garnets from one locality in the North Cinnabar Creek area show moderate symmetrical 'normal' zoning patterns with cores enriched in spessartine and depleted in pyrope and almandine. Sodic pyroxenes have compositions ranging from Jd_{30} to Jd_{54}. Green, metamorphic pyroxenes are aegerine-augites. White micas are phengitic and are present, locally, in all lithologies. Chlorite is present both as a replacement phase in some blueschists and a primary component in greenstones. Greenstone chlorites show a range in Mg-Fe_{Total} compositions whereas replacement chlorites appear to range in Al-Fe_{Total} composition. Feldspars, regardless of their occurrence, are albite-rich.

The juxtaposition of blueschists and greenstones in the Bridge River complex is likely the result of original heterogeneities within the protoliths, metasomatic alteration, localized fluid flow and metamorphic segregation.

Metamorphic P-T conditions, calculated using the program PTAX, are inferred to be in the range of 8 to 10 kbar at 250-300°C, assuming $P_s = P_{H_2O}$. The inferred metamorphic P-T path with a slope of 9°C/km, indicates that all rocks within the study area followed the same path. The variation in blueschist assemblages present is due to lower, local, P_{H_2O} conditions in the North Cinnabar Creek area. Fluids accompanying metamorphism were

likely low in CO_2 due to the presence of lawsonite and titanite. The stability fields for both of these phases are confined to low values of X_{CO_2}.

Blueschist metamorphism within the Bridge River complex likely took place at approximately 29 to 36 km depth with exhumation taking approximately 21 to 26 Ma. These rates are consistent with those derived for other blueschist terranes (e.g. Ghent et al., 1996) and necessary to prevent overprinting of the blueschist assemblage by lower pressure, higher temperature assemblages (e.g. Draper and Bone, 1980).

7.2 FURTHER WORK

During the course of this study several questions and obscurities arose, the answers to which remain unresolved. The following suggested work would provide further insights into the nature of the Bridge River blueschists and related rocks specifically and to the Bridge River complex as a whole. This work should include:

I. Development of a meaningful stratigraphic column for the Bridge River Complex. This would involve a significant amount of detailed structural and petrological work, on a large scale, to decipher the geological relationships

II. Additional bulk rock analyses of the blueschists and the various greenstones in order to do a more thorough comparison of the lithologies.

III. Attempt a study of oxygen isotope thermometry to better constrain metamorphic conditions.

IV. An attempt at studying fluid inclusions in these was made. However, the fine grain size of these rocks made it impossible to extract meaningful data. It would be advantageous to continue with this study, using equipment better suited to the task.

8. WORKS CITED

Archibald, D.A., Schiarizza, P. and Garver, J.I., 1991. $^{40}Ar/^{39}Ar$ Evidence for the Age of Igneous and Metamorphic Events in the Bridge River and Shulaps Complexes, Southwestern, British Columbia. B.C. Ministry of Energy, Mines and Petroleum Resources, Geological Fieldwork 1990, Paper 1991-1: 131-143.

Bradshaw, J.Y., 1978. Petrology and Mineralogy of Interlayered Eclogite and High-Grade Blueschists from the Franciscan Formation, California. unpublished M.Sc Thesis, The University of Calgary, 183 pages

Baltatzis, E., 1996. Blueschist-to-greenschist transition and the P-T path of prasinites from Lavrion area, Greece. Mineralogical Magazine, **60**: 551-561.

Barrientos, X. and Selverstone, J., 1993. Infiltration vs. thermal overprinting of epidote blueschists, Ile de Groix, France. Geology, **21**: 69-72.

Bayliss, P., 1975. Nomenclature of trioctahedral chlorites. Canadian Mineralogist, **13**: 178-180.

Bebout, G.E. and Barton, M.D., 1989. Fluid flow and metasomatism in a subduction zone hydrothermal system: Catalina Schist terrane, California. Geology, **17**: 976-980.

Bebout, G.E. and Barton, M.D., 1993. Metasomatism during subduction: products and possible paths in the Catalina Schist, California. Chemical Geology, **108**: 61-92.

Bence, A.E., and Albee, A.L., 1968. Empirical correction factors for the electron microanalysis of silicates and oxides. Journal of Geology, **76**: 382-403.

Berman, R.G., 1988. Internally-consistent thermodynamic data for stoichiometric minerals in the system Na_2O-K_2O-CaO-MgO-FeO-Fe_2O_3-Al_2O_3-SiO_2-TiO_2-H_2O-CO_2. Journal of Petrology, **29**: 445-522.

Blake, M.C., Irwin, W.P. and Coleman, R.G., 1969. Blueschist-Facies Metamorphism Related to Regional Thrust Faulting. Tectonophysics, **8**: 237-246.

Borg, I.Y. and Smith, D.K., 1969. Calculated X-ray powder patterns for silicate minerals. Geological Society of America Memoir, **122**.

Bowes, D.R., and Park, R.G., 1966. Metamorphic segregation banding in the Loch Kerry basite sheet from the Lewisian of Gairloch, Ross-shire, Scotland. Journal of Petrology, **7**: 306-330.

Brandon, M.T., 1980.Structural geology of Middle Cretaceous thrust faulting on San Juan Island, Washington. M.Sc. thesis, University of Washington, Seattle, 130 p., in Greenwood et al., 1991.

Brothers, R.N. and Blake, M.C., 1987. Comment on blueschists and eclogites. Geology, **15**: 773.

Brown, E.H., Fyfe, W.S. and Turner, F.J., 1962. Aragonite in California glaucophane schists, and the kinetics of the aragonite-calcite transformation. Journal of Petrology, **3**: 566-582.

Brown, E.H., 1967. The greenschist facies in part of eastern Otago, New Zealand. Contributions to Mineralogy and Petrology, **14**: 259-292.

Brown, E.H., 1971. Phase relations of biotite and stilpnomelane in the greenschist facies. Contributions to Mineralogy and Petrology, **31**: 275-299.

Brown, E.H., 1974. Comparison of the mineralogy and phase relations of blueschists from the North Cascades, Washington and blueschists from Otago, New Zealand. Geological Society of America Bulletin, **85**: 333-344.

Brown, T.H., Berman, R.G. and Perkins, E.H., 1989. PTAX-SYSTEM: a Ge0-Calc software package for the calculation of activity-pressure-temperature phase diagrams. American Mineralogist, **74**: 67-83.

Cann, J.R., 1970. Rb, Sr, Y, Zr, Nb in some ocean-floor basaltic rocks. Earth and Planetary Science Letters, **10**: 7-11.

Cawthorn, R.G. and Collerson, K.D., 1974. The recalculation of pyroxene end-member parameters and the estimation of ferrous and ferric iron content from electron microprobe analyses. American Mineralogist, **59**: 1203-1208.

Chatterjee, N.D., 1971. Phase equilibria in the alpine metamorphic rocks of the environs of the Dora-Maira-Massif, Western Italian Alps, Part 1. Neues Jahrbuch fuer Mineralogie, **114**:181-210.

Chatterjee, N.D., 1971. Phase equilibria in the alpine metamorphic rocks of the environs of the Dora-Maira-Massif, Western Italian Alps, Part 2. Neues Jahrbuch fuer Mineralogie, **114**: 211-245.

Chernosky, J.V., Jr., Berman, R.G. and Bryndzia, L.T., 1988. Stability, phase relations and thermodynamic properties of chlorite and serpentine group minerals. *In* Hydrous Phyllosilicates (Exclusive of Micas) (S.W. Bailey, ed.). Reviews in Mineralogy, **19**: 295-346.

Church, B.N. and Pettipas, A.R., 1989. Research and exploration in the Bridge River Mining Camp (92J/15, 16). B.C. Ministry of Energy, Mines and Petroleum Resources, Geological Fieldwork 1988, Paper 1989-1: 105-114.

Cloos, M., 1986. Blueschists in the Franciscan Complex of California: petrotectonic constraints on uplift mechanisms. Geological Society of America Memoir, **164**: 77-94.

Coombs, D.S., 1963. Trends and affinities of basaltic magmas and pyroxenes as illustrated in diopside – olivine – silica diagram. Mineralogical Society of America Special Paper 1, 227-250.

Cordey, F., and Schiarizza, P., 1993. Long-lived Panthalassic remnant: the Bridge River accretionary complex, Canadian Cordillera. Geology, **21**: 263-266.

Cowan, D.S., 1985. Structural Styles in Mesozoic and Cenozoic mélanges in the western Cordillera of North America. Geological Society of America Bulletin, **96**: 451-462.

Cowan, D.S. and Silling, R.M., 1978. A Dynamic, Scaled Model of Accretion at Trenches and Its Implications for the Tectonic Evolution of Subduction Complexes. Journal of Geophysical Research, **83** (B11): 5389-5396.

Deer, W.A., Howie, R.A., Zussman, J., 1992. An Introduction to the Rock-Forming Minerals 2nd ed., John Wiley and Sons, New York.

Dobretsov, N.L., Arnautov, N.V. and Ponomareva, L.G., 1967. Geochemistry of glaucophane metamorphism. Geochemistry International, **4**: 772-782.

Draper, G. and Bone, R., 1980. Denudation rates, thermal evolution and preservations of blueschist terrains. Journal of Geology, **89**: 601-613.

Dungan, M.A., Vance, J.A., and Blanchard, D.P., 1983. Geochemistry of the Shuksan greenschists and blueschists, North Cascades, Washington: variably fractionated and altered metabasalts of oceanic affinity. Contributions to Mineralogy and Petrology, **82**: 131-146.

Ehlers, E.G., and Blatt, H., 1982. Petrology: Igneous, Sedimentary and Metamorphic. San Francisco, W.H. Freeman and Co., 732pp.

El-Shazly, A.D., Coleman, R.G., and Liou, J.G., 1990. Eclogites and blueschists from Northeastern Oman: Petrology and P-T evolution. Journal of Petrology, **31**: 629-666.

Erdmer, P., 1987, Blueschist and eclogite in mylonitic allochthons, Ross River and Watson Lake areas, southeastern Yukon. Canadian Journal of Earth Sciences, **24**, 1439-1449.

Erdmer, P. and Helmstaedt, H., 1983, Eclogite from central Yukon: a record of subduction at the western margin of Ancient North America. Canadian Journal of Earth Sciences, **20**: 1389-1408.

Ernst, W.G., 1965. Mineral parageneses in Franciscan metamorphic rocks, Panoche Pass, California. Geological Society of America Bulletin, **76**: 879-914.

Ernst, W.G., 1988. Tectonic history of subduction zones inferred from retrograde blueschist P-T paths. Geology, **16**: 1081-1084.

Ernst, W.G., 1977. Mineral parageneses and plate tectonic settings of relatively high-pressure metamorphic belts. Fortschr. Miner., **54**: 192-222.

Eskola, P., 1920. The Mineral Facies of Rocks. Norsk Geol. Tidsskr., **6**: 143-194.

Faryad, S.W., 1995. Phase petrology and P-T conditions of mafic blueschists from the Meliata unit, West Carpathians, Slovakia. Journal of Metamorphic Geology, **13**: 701-714.

Gabrielse, H., Monger, J.W.H. Wheeler, J.O. and Yorath, C.J.,1991, Metamorphism, Chapter 16 in Geology of the Cordilleran Orogen in Canada. H. Gabrielse and C.J. Yorath (eds.) Geological Survey of Canada, #4, 533-570.

Garver, J.I., 1989. Basin Evolution and Source Terranes of Albian-Cenomanian Rocks in the Tyaughton Basin, Southern British Columbia: Implications for Mid-Cretaceous Tectonics in the Canadian Cordillera: unpublished Ph.D. thesis, The University of Washington, 227 pages.

Garver, J.I., 1991. Kinematic Analysis and timing of structures in the Bridge River Complex overlying Cretaceous sedimentary rocks, Cinnabar Creek area, southwestern British Columbia. B.C. Ministry of Energy, Mines and Petroleum Resources, Geological Fieldwork 1990, Paper 1990-1: 65-74.

Garver, J.I., Schiarizza, P. and Gaba, R.G., 1989. Stratigraphy and Structure of the Eldorado Mountain area, Chilcotin Ranges, southwestern British Columbia. B.C. Ministry of Energy, Mines and Petroleum Resources, Geological Fieldwork 1988, Paper 1989-1: 131-143.

Ghent, E.D., 1988. A review of chemical zoning in eclogite garnets. In Smith D.C. ed., Eclogites and Eclogite Facies Rocks: New York, Elsevier, 207-236.

Ghent, E.D. and Coleman, R.G., 1973. Eclogites from southwestern Oregon. Geological Society of America Bulletin, **84**: 2471-2488.

Ghent, E.D., Erdmer, P., Archibald, D.A. and Stout, M.Z., 1996. Pressure-temperature and tectonic evolution of Triassic lawsonite-aragonite blueschists from Pinchi Lake, British Columbia. Canadian Journal of Earth Science, **33**: 800-810.

Ghent, E.D., Stout, M.Z. and Erdmer, P., 1990. Howieite in Blueschists, Pinchi Lake, British Columbia. Canadian Mineralogist. **28**: 855-858.

Ghent, E.D., Stout, M.Z. and Erdmer, P., 1993. Pressure-temperature evolution of lawsonite-bearing eclogites, Pinchi Lake, British Columbia. Journal of Metamorphic Geology, **11**, 279-290.

Gordon, T.M., Ghent, E.D. and Stout, M.Z., 1991. Algebraic analysis of the biotite-sillimanite isograd in the File Lake area, Manitoba. Canadian Mineralogist, **29**: 673-686.

Greenwood, H.J., Woodsworth, G.J., Read, P.B., Ghent, E.D., and Evenchick, C.A., 1991, Metamorphism, Chapter 16 in Geology of the Cordilleran Orogen in Canada. H. Gabrielse and C.J. Yorath (eds.) Geological Survey of Canada, #4, 533-570.

Harker, A., 1950. Metamorphism. 3rd ed. Methuen.

Hollister, L.S., 1969. Contact metamorphism in the Kwoiek area of British Columbia: An end member of the metamorphic process. Geological Society of America Bulletin, **80**: 2465-2494.

Irvine, T.N. and Baragar, W.R.A., 1971. A guide to the chemical classification of the common volcanic rocks. Canadian Journal of Earth Sciences, **8**: 523 –548.

Journeay, J.M, Monger J.W.H., Schiarizza, P. and Garver, J.I., 1996. Structure and Crustal Architecture of the Southern Coast Belt Accretionary Complex. Field Guide Book for the Canadian Tectonics Group Meeting, Bowen Island B.C.

Kretz, R., 1983. Symbols for rock-forming minerals. American Mineralogist, **68**: 277-279.

Leake, B.E. and 21 others, (1997). Nomenclature of amphiboles: report of the Subcommittee on Amphiboles of the International Mineralogical Association, Commission on New Minerals and Mineral Names. Canadian Mineralogist, **35**: 219-246.

Le Bas, M.J., Le Maitre, R.W., Streckheisen, A., Zanettin, B., 1986. A chemical classification of volcanic and volcaniclastic rocks based on the total alkali-silica diagram. Journal of Petrology, **27**: 745-750.

Liou J.G., Ho, C.O. and Yen, T.P., 1975. Petrology of some glaucophane schists and related rocks from Taiwan. Journal of Petrology, **16**: 80-109.

Liou, J.G., Maruyama, S., and Cho, M., 1985. Phase equilibria and mineral parageneses of metabasites in low-grade metamorphism. Mineralogical Magazine, **49**: 321-333.

Liu, M. and Yund, R.A., 1993. Transformation kinetics of polycrystalline aragonite-calcite: new experimental data, modeling and implications. Contributions to Mineralogy and Petrology, **114**: 465-478.

Miyashiro, A., 1957. The chemistry, optics and genesis of the alkali amphiboles. J. Fac. Sci. Univ. Tokyo **II**/11: 57-83.

Miyashiro, A.. 1961. Evolution of metamorphic belts. Journal of Petrology, **2**: 277-311.

Moore, J.G., 1966. Rate of Palagonitization of submarine basalt adjacent to Hawaii. U.S. Geological Survey Professional Paper No. 550-D, D163-D171.

Monger, J.W.H., 1975, Upper Paleozoic rocks of the Atlin Terrane, northwestern British Columbia and south-central Yukon. Geological Survey of Canada. Paper 74-7, 63p.

Morimoto, N., 1989. Nomenclature of pyroxenes. Canadian Mineralogist, **27**: 143-156.

Nicholls, J. and Stout, M.Z., 1988. Picritic melts in Kilauea – evidence from the 1967-1968 Halemaumau and Hiiaka eruptions. Journal of Petrology, **29**: 1031-1051.

Nicholls, J., Fiesinger, D., and Ethier, V.G., 1977. FORTRAN IV programs for processing routine electron microprobe data. Computers and Geosciences, **3**: 49-83.

Norrish, K. and Chappell, B.W., 1967. Statistics of X-ray measurement, *in* Zussman, J., ed., Physical methods in determinative mineralogy, Academic Press, London, p. 201-204.

Oxburgh, E.R. and Turcotte, D.L., 1970. Thermal Structure of Island Arcs. Geological Society of America Bulletin, **81**: 1665-1688.

Peacock, S.M., 1993, The importance of the blueschist → eclogite dehydration reactions in subducting oceanic crust. Geological Society of America Bulletin, **105**: 684-694.

Pearce, JA and Cann, J.R., 1973. Tectonic setting of basic volcanic rocks determined using trace element analyses. Earth and Planetary Science Letters, **19**: 290-300.

Platt, J.P., 1986. Dynamics of orogenic wedges and the uplift of high-pressure metamorphic rocks. Geological Society of America Bulletin, **97**: 1037-1053.

Platt, J.P., 1987. The uplift of high-pressure-low-temperature metamorphic rocks. Philosophical Transactions of the Royal Society of London, **321**: 87-103.

Plint, H.E. and Gordon, T.M., 1997. The Slide Mountain Terrane and the structural evolution of the Finlayson Fault Zone, southeastern Yukon. Canadian Journal of Earth Sciences, **34**: 105-126.

Potter, C.J., 1983. Geology of the Bridge River Complex, southern Shulaps Range, British Columbia: a record of Mesozoic convergent tectonics. Ph.D. dissertation, 192 pp. University of Washington, Seattle.

Potter, C.J., 1986. Origin, Accretion and postaccretionary evolution of the Bridge River Terrane, southwest British Columbia. Tectonics, **5**: 1027-1041.

Räheim, A., 1975. Mineral zoning as a record of P,T history of Precambrian eclogites and schists in western Tasmania. Lithos, **8**: 221-236.

Räheim A. and Green, D.H., 1974. Experimental determination of the temperature and pressure dependence of the Fe-Mg partition coefficient of garnet and clinopyroxene. Contribution to Mineralogy and Petrology, **48**: 179-203.

Ramberg, H., 1952. The Origin of Metamorphic and Metasomatic Rocks. Chicago, University of Chicago Press, 317pp.

Reinsch, D., 1979. Glaucophanites and eclogites from Val Chiusella, Sesia-Lanzo zone (Italian Alps). Contributions to Mineralogy and Petrology, **70**: 257-266.

Richard, L.R. and Clarke, D.B., 1990. AMPHIBOL: a program for calculating structural formulae and classifying and plotting chemical analyses of amphiboles. American Mineralogist, **75**: 421-423.

Robin, P.Y.F., 1979. Theory of metamorphic segregation and related processes. Geochimica et Cosmochimica Acta, **43**: 1587-1600.

Robinson P., Spear, F.S., Schumacher, J.C., Laird, J., Klein, C., Evans, B.W. and Doolan, B.L., 1981. Phase relations of metamorphic amphiboles: Natural occurrence and theory. Mineralogical Society of America reviews in Mineralogy, 9B, 1-228.

Schiarizza, P., Gaba, R.G., Glover, J.K. and Garver, J.I., 1989. Geology and Mineral Occurrences of the Tyaughton Creek Area. B.C. Ministry of Energy, Mines and Petroleum Resources, Geological Fieldwork 1988, Paper 1989-1: 115-130.

Schiarizza, P. and Gaba, R.G., 1993. Geology of the Bralorne (north half) and northeastern Dickson Ranges map areas. B.C. Ministry of Energy, Mines and Petroleum Resources, Geoscience Map 1993-7.

Schiarizza, P., Garver, J.I., Journeay, J.W. and Monger, J.W.H., 1995. Geology and Tectonic Evolution of the Southern Coast Belt, Southwestern British Columbia. Field Trip Guide Book, GAC/MAC Annual Meeting, Victoria.

Schliestedt, M., 1986. Eclogite-blueschist relationships as evidenced by mineral equilibria in the high-pressure metabasaltic rocks of Sifnos (Cycladic Islands), Greece. Journal of Petrology, **27**: 1437-1459.

Spear, F.S., 1993. Metamorphic phase equilibria and pressure-temperature-time paths. Mineralogical Society of America Monographs, 799 pp.

Vance, J.A., 1968. Metamorphic aragonite in the prehnite-pumpellyite facies, Northwest Washington. American Journal of Science, **266**: 299-315.

Wicks, F.J., Corbeil, M.C., Back, M.E. and Ramik, R.A., 1995. Microbeam X-ray Diffraction in the analysis of Minerals and Materials. The Canadian Mineralogist, **33**: 313-322.

Yardley, B.W., 1989. An Introduction to Metamorphic Petrology. 248pp. Longman Scientific and Technical., New York.

9. APPENDIX

9.1 STANDARDS USED IN ELECTRON MICROPROBE ANALYSIS *

Mineral	Si	Al	Ti	Fe	Mn	Mg	Ca	Na	K	F
Amphibole	264	48 / 182	249	249 / 22	22 / 84	264	258 / 307	249	299	55
Lawsonite / Epidote	182	182	249	249	22 / 84	264	182	249	299	55
Garnet	258 / 304	258 / 304	249	258 / 304	84	258 / 304	258 / 304	249	-	55
Pyroxene	186 / 307	186 / 307	249	22 / 249	22 / 84	186 / 264	186 / 307	186 / 307	299	55
White mica	299	299		22	22	264	186	249	299	55
Chlorite	22 / 299	22 / 299	249	249	22	264	258	249	299	55
Stilpnomelane	299	299		22	22	264	186	249	299	55
Feldspar	182 / 277	182 / 277	249	22 / 249	22 / 84	186 / 264	277 / 182	113 / 249	90	55
Titanite	182	307	249	249	22	264	182	249	-	55

*Numbers refer to electron microprobe standards (EPS #) held at the Department of Geology and Geophysics, University of Calgary:

EPS #	Description	EPS #	Description
22	Mn-Cummingtonite	249	Aenigmatite
48	Kak. Hornblende	258	Kak. Garnet
55	Flurophlogopite	264	Olsen
84	Rhodonite	277	An_{50} Glass
90	Or-1	299	Muscovite
182	Syn. Anorthite	304	New Garnet
186	Di/Jd Glass	307	Omphacite

9.2 ELECTRON MICROPROBE ANALYSIS OF MINERALS OF KNOWN COMPOSITION

An illustration of the quality of the microprobe data

	Standard 22	Microprobe	Standard 48	Microprobe	Standard 182	Microprobe
SiO_2	55.74	55.24	40.45	41.27	43.2	42.61
TiO_2	0	n.a.	4.9	n.a.	n.a.	0
Al_2O_3	0.23	0.11	14.5	14.46	36.64	35.93
FeO	7.09	7.26	10.96	10.85	0	0.06
MnO	14.73	14.76	0.1	0.08	0	0
MgO	18.55	19.76	12.78	13.14	0	0.01
CaO	1.04	0.51	10.36	9.66	20.16	19.36
Na_2O	0.08	0.03	2.56	2.47	0	0
K_2O	0.02	0	2.04	2.07	0	0
F	0.28	0.22	0	0.19	0	0
Total	97.76	97.89	98.65	94.19	100	97.97

	Standard 299	Microprobe	Standard 277	Microprobe
SiO_2	44.7	44.09	55.59	55.13
TiO_2	0.88	-	n.a.	0
Al_2O_3	31.5	31.61	28.3	26.89
FeO	5.09	5.26	0	0.03
MnO	0.03	0.02	0	0
MgO	0.99	0.9	0	0.05
CaO	0.02	0	10.38	10.04
Na_2O	0.67	0.5	5.73	5.44
K_2O	10.45	10.6	0	0.02
F	0.1	0.16	0	0
Total	94.43	93.14	100	97.6

Abbreviations: n.a. = not analyzed

9.3 DETECTION LIMITS

Detection limits were calculated using the program *SLAVE* of Nicholls et al., (1977), according to the formula:

$$dl = \frac{3(bg \times ct)^{1/2}}{ct} of$$

where bg = background counts per second

ct = counting time (20 seconds in this study)

of = 'oxide' factor, a value obtained from the program *STDS* in the *SLAVE* package.

AVERAGE DETECTION LIMITS FOR MICROPROBE ANALYSES GIVEN IN WEIGHT PER CENT OXIDE

	SiO_2	TiO_2	Al_2O_3	FeO	MnO	MgO	CaO	Na_2O	K_2O	F
Amphibole	0.08	0.02	0.04	0.04	0.03	0.02	0.01	0.04	0.01	0.08
Chlorite	0.11	0.02	0.09	0.04	0.03	0.02	0.00	0.04	0.01	0.09
Epidote	0.09	0.02	0.04	0.04	0.03	0.02	0.01	0.03	0.02	0.07
Feldspar	0.10	-	0.05	0.04	0.03	0.02	0.01	0.03	0.02	0.09
Garnet	0.14	0.03	0.05	0.04	0.04	0.02	0.01	0.04	0.01	0.09
Lawsonite	0.11	-	0.05	0.04	0.03	0.02	0.01	0.04	0.01	0.09
White Mica	0.12	0.02	0.07	0.04	0.03	0.02	0.00	0.04	0.01	0.09
Pyroxene	0.09	0.02	0.04	0.04	0.03	0.02	0.01	0.04	0.02	0.09
Stilpnomelane	0.12	0.02	0.14	0.04	0.03	0.02	0.01	0.04	0.01	0.10
Titanite	0.08	0.02	0.04	0.04	0.03	0.02	0.01	0.05	0.01	0.09

9.4 PRECISION

The precision of the average analysis for each analyzed grain was calculated with the SLAVE program package (Nicholls et al., 1977) according to the method of Norrish and Chappell (1967):

$$P = 3\sqrt{\left(\frac{V_u^2 + V_s^2}{ct}\right) \times (N_p - N_b) \times of}$$

where V_u and V_s refer to the variance for the unknown and standard respectively; N is the total counts in a given counting time, and the subscripts p and b refer to peak and background respectively.

AVERAGE PRECISION FOR MICROPROBE ANALYSES GIVEN IN WEIGHT PER CENT OXIDE

	SiO_2	TiO_2	Al_2O_3	FeO	MnO	MgO	CaO	Na_2O	K_2O	F
Amphibole	0.63	0.01	0.15	0.12	0.02	0.07	0.02	0.10	0.01	0.04
Chlorite	0.59	0.01	0.19	0.15	0.02	0.09	0.47	0.09	0.03	0.05
Epidote	0.44	0.02	0.28	0.10	0.02	0.01	0.11	0.02	0.01	0.03
Feldspar	0.43	-	0.23	0.06	0.02	0.03	0.04	0.04	0.02	0.07
Garnet	0.62	0.02	0.34	0.18	0.07	0.05	0.04	0.02	0.01	0.06
Lawsonite	0.72	-	0.40	0.07	0.02	0.04	0.05	0.04	0.02	0.05
White Mica	0.72	0.02	1.37	0.09	0.02	0.06	0.02	0.02	0.04	0.05
Pyroxene	0.70	0.01	0.20	0.10	0.02	0.05	0.04	0.09	0.02	0.04
Stilpnomelane	0.65	0.02	1.05	0.14	0.03	0.06	0.02	0.03	0.01	0.06
Titanite	0.37	0.16	0.10	0.05	0.02	0.03	0.10	0.12	0.01	0.06